Bjarte Bye Løfaldli

Functional and Morphological Characterization of Central Olfactory Neurons in the Model Insect *Heliothis virescens*

Thesis for the degree of Philosophiae Doctor

Trondheim, June 2012

Norwegian University of Science and Technology
Faculty of Natural Sciences and Technology
Department of Biology

NTNU – Trondheim
Norwegian University of
Science and Technology

NTNU
Norwegian University of Science and Technology

Thesis for the degree of Philosophiae Doctor

Faculty of Natural Sciences and Technology
Department of Biology

ISBN 978-82-471-3633-1 (printed ver.)
ISBN 978-82-471-3634-8 (electronic ver.)
ISSN 1503-8181

Doctoral theses at NTNU, 2012:171

Printed by NTNU-trykk

High resolution figures, reconstructions and files from the standard brain project are available by contact at the following address or email:

http://olfactoryblog.wordpress.com/
olfactoryblog@gmail.com

Affiliate address:
Norwegian University of Science and Technology
The Faculty of Science and technology
Department of Biology, Neuroscience unit
MTFS, Olav Kyrres gate 9
NO-7030 Trondheim
Norway

bjarte.lofaldli@ntnu.no

Preface

All the experimental work underlying this thesis was carried out at the Neuroscience unit, Department of Biology, Norwegian University of Science and Technology (NTNU). The thesis was submitted to the faculty of science and technology at NTNU. My contribution to the three papers included in this thesis, two published and one submitted was substantial. In the first paper of the standard brain atlas Pål Kvello and I shared the experimental work for creating the standard brain including staining, microscopy and reconstructions. I performed the electrophysiological recordings with staining and reconstruction of the olfactory neurons. The generation of the standard brain atlas was carried out together with Jürgen Rybak who was a consultant during the experimental work. The principal responsibility for the writing, in which I contributed substantially, was held by Pål Kvello under supervision of Professor Hanna Mustaparta. Hanna Mustaparta and Professor Randolf Menzel contributed significantly in the planning of the project. In the second paper on the integration of the antennal lobe atlas into the standard brain atlas the planning of the project was carried out together with Pål Kvello and Hanna Mustaparta. I carried out the reconstruction work and the following glomerular identification necessary for transforming the female antetennal lobe atlas into the standard brain atlas. I also carried out the electrophysiological recordings, staining, reconstruction, transformation, identification of innervated glomeruli and the making of figures in this paper. The principal responsibility for the writing was held by me under the supervision of Hanna Mustaparta and Pål Kvello. I planned the studies of the third paper and carried out the electrophysiological recordings, staining, the microscopy work, transformations and making of the figures. Pål Kvello was partly involved in the experimental work. The statistical analyses were done in collaboration with Nicholas Kirkerud. I held the principal responsibility for the writing under supervision of Hanna Mustaparta.

List of content

Papers included in the thesis

This thesis is based on three papers, two published and one submitted. In the continuation they will be refered to by their Roman nummerals.

I. Kvello, P.L., Løfaldli, B.B., Rybak, J.R., Menzel, R., and Mustaparta, H. (2009). Digital, three-dimensional average shaped atlas of the heliothis virescens brain with integrated gustatory and olfactory neurons. *Front. Syst. Neurosci*. 3:14. doi: 10.3389/neuro.06.014.2009.

II. Løfaldli, B.B., Kvello, P., and Mustaparta, H. (2010). Integration of the antennal lobe glomeruli and three projection neurons in the standard brain atlas of the moth Heliothis virescens. *Front. Syst. Neurosci*. 4:5. doi: 10.3389/neuro.06.005.2010.

III. Løfaldli, B.B., Kvello, P., Kirkerud, N., and Mustaparta, H. (2012). A putative neuronal circuit handling information about a ten component plant odor blend in the brain of *H. virescens*. The manuscript is submitted to Frontiers in Systems Neuroscience.

Abbreviations

ACT	**Antenno-cerebral tract**
AL	**Antennal lobe**
APT	**Antenno-protocerebral tract**
GABA	**γ-aminobutyric acid**
ISA	**Iterative shape averaging**
KC	**Kenyon cell**
l-	**lateral**
LH	**Lateral horn**
LP	**Lateral protocerebrum**
m-	**medial**
MB	**Mushroom body**
ml-	**medio lateral**
OA	**Olfactory axis**
ORN	**Olfactory receptor neuron**
PN	**Projection neuron**
SBA	**Standard brain atlas**
SBAGl	**Standard brain atlas with glomeruli**
SP	**Superior protocerebrum**
SOG	**Subesophageal ganglion**
VIB	**Virtual insect brain**

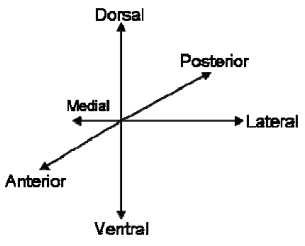

Introduction

Sigmund Freud ones said that the organic sublimation of the sense of smell is a factor of civilization. For ages the sense of smell was considered a primitive and bestial sense which represented a lower cognitive function and the sublimation lifted humans up to a higher cognitive level clearly separated from other animals. In everyday life you may not think so much of this sense unless you are actively using it to decide the condition of a box with expired milk or if it is to feel the rich and wonderful odors from a white rose. An odor plume might also unexpectedly struck you with an indescribable magnitude which catches you're full attention and you suddenly find your self fully engaged in identifying the source so you can get away. Odors also have the power to recall distant memories and make them intimate in a way that fills you with emotions. So, how would life be without the sense of smell? Anosmia or odor blindness can be experienced in various degrees from insensitivity to some odors (hyposmia) to the total lack of sensibility. People that have lost the sense of smell reports reduced appetite, loss of weight, malnutrition, depression and anxiety. A serious problem is also the lack of ability to sense more dangerous odors like smoke and gas. Freud might have been right when he said that social human beings have sublimed this sense but even though we are less aware and dependent on olfaction for survival, it still affects our functioning and quality of life to a great extend. Most other animal species from mammals to insects are highly dependent on this sense which can be seen when a new born pup finds his mothers breast for the first time or when a female moth searches for a suitable plant for laying her eggs. Besides being important, olfaction is also involved in almost all aspects of an animal's life from feeding, navigation, communication, mating and danger avoidance to learning and memory formation.

The olfactory system in mammals and invertebrates

Both mammals and insects have olfactory receptor neurons (ORNs) that are activated upon the binding of air born molecules called odorants. In insects, the ORNs have their dendrites with the membrane receptor proteins placed in sensilla that are usually found on the antennae and on mouth parts. In mammals the ORNs dendrites, which holds cilia with

receptor proteins, are embedded in the mucosa of the olfactory epithelium in the nose cavity (Shepherd, 2006; Sachse and Krieger, 2011). Each ORN expresses only one or exceptionally two to four odorant receptor types (Mombaerts, 2004; Vosshall and Stocker, 2007). The number of expressed receptor types varies in different animal species from around fifty in the fruit fly to about 400 in humans and chimps and up to over a thousand in mouse and dogs. The receptor neurons send information about odor molecules via their axons to glomeruli in the primary olfactory centre, the antennal lobes (AL) in insects and the olfactory bulb in vertebrates. Since each receptor neuron type project axons to only one or two of the numerous glomeruli, the number of glomeruli in the primary olfactory centre is correlated to the number of expressed receptor types. Thus the numbers are species specific, ranging from fifty to several hundreds in insects and up to more than a thousand in some mammals. The primary olfactory centre is a sophisticated processing centre where the multidimensional odor information mediated by the ORN axons is transformed into complex activity patterns among the glomeruli of the neuronal network (Lledo et al., 2005). From the primary olfactory centre the processed information is transferred through parallel pathways to higher brain areas where the olfactory information is further processed and integrated in the neuronal networks (Galizia and Rössler, 2010; Nagayama et al., 2010). In mammals some of the major target areas of the olfactory bulb tracts are the olfactory cortex (including the piriform cortex) and the limbic system (with the hippocampal formation which is important for several types of memories, hypothalamus and amygdala which are closely associated with emotional responses (Greenstein and Greenstein, 2000; Shepherd, 2006). In invertebrates the major target areas of the AL tracts are the Mushroom Bodies (MB) which is important for learning and memory, the superior protocerebrum (SP) proximate to and closely associated with the MB lobes, and the lateral- protocerebrum and horn (LP/LH). The LP also contain a premotoric area (Menzel and Giurfa, 2001; Heisenberg, 2003; Gerber et al., 2004).

A foundation of primary plant odorants

Through the research work in our lab we seek a better understanding on how relevant olfactory information is coded in the neuronal networks of the brain. In achieving this we

have focused our research on a model insect, the American tobacco budworm moth, *Heliothis virescens*. This moth belongs to the sub family Heliothinae consisting of more than 80 species, several of them considered as major pest insects in agriculture causing severe damage for instance in cotton fields (Fitt, 1989; Matthews, 1991). Many insect species, including moths have an excellent sense of smell. Their well developed olfactory system and simple brain with relatively few neurons that are fairly accessible for physiological and morphological studies have made insects important and widely used models for studying the function of the nervous system. Previous studies that were carried out in our lab have provided knowledge about biologically relevant plant odorants detected by the ORNs in three closely related moth species, *H. virescens*, *Helicoverpa armigera* og *Helicoverpa assulta*. In these studies electrophysiological recordings from single receptor neurons linked to gas chromatography and mass spectrometry have revealed a high degree of specificity among these ORNs. Many primary plant odorants was identified, each activating one ORN type. Only one of these odorants, linalool, activated weakly a second ORN type that was primarily activated by geraniol (Stranden et al., 2002; Stranden et al., 2003a; Stranden et al., 2003b; Røstelien et al., 2005). Numerous studies on olfactory receptor neurons of other insect and vertebrates species have been performed by directly testing available odorants. These studies have shown some narrowly tuned but mostly broadly tuned ORNs with a wider molecular receptive range (De Bruyne et al., 1999; Malnic et al., 1999; De Bruyne et al., 2001; Shields and Hildebrand, 2001; Hallem and Carlson, 2006; Nara et al., 2011). The identification of the primary odorants in *H. virescens* laid the foundation for investigations of how the olfactory information is further handled and coded by the neuronal networks in the brain of this moth. By combining sharp in vivo electrophysiological recordings with staining and visualization techniques of neurons in the primary olfactory centre and higher olfactory areas of the brain, the neuronal networks involved in the sense of smell in this model insect could be elucidated (paper I, II and III).

Standard brain atlases

The relatively small sized brain of *H. virescens* and other insect species is advantageous when studying connectivity between different brain regions, because the projections

between the neuropils can be kept intact. Resolving the functional connectivity in the neuronal networks is crucial for understanding how the system operates. One challenging aspect in using intracellular recording and staining techniques for this purpose is to spatially relate and visualize morphological data acquired from different brain preparations. To meet this challenge, digital brain atlases (SBAs) have been made for several insects species (fruit fly (*Drosophila melanogaster*), Rein et al., 2002; honeybee (*Apis melifera*), Brandt et al., 2005; locust (*Schistocerca gregaria*), Kurylas et al., 2008) including two moth species, *H. virescens* (paper I) and the hawk moth (*Manduca sexta*, Jundi et al., 2009). Two different methods have been used, the iterative shape averaging (ISA) procedure originally developed for studies on the honeybee (Rohlfing et al., 2001; Brandt et al., 2005) and the virtual insect brain (VIB) procedure developed for the fruit fly (Jenett et al., 2006). One principal difference between these two procedures is that ISA reduces anatomical variability, whereas VIB preserves it (Jundi et al., 2009). Various neuropils have been included in the different SBAs according to requirements in the projects and the visibility of the different brain structures. The SBA with its neuropils serves as a common framework where physiologically and morphological characterized neurons from different preparations can be integrated in order to visualize neuronal projections and possible functional connectivity. Intensity based transformation techniques based on raw data images have also been developed (Rohlfing et al., 2004; Jefferis et al., 2007). Separate atlases of sub-brain compartments like the ALs has been made in several insect species, including *H. virescens* (Rospars and Chambille, 1981; Flanagan and Mercer, 1989; Stocker et al., 1990; Galizia et al., 1999a; Laissue et al., 1999; Rospars and Hildebrand, 2000; Chiang et al., 2001; Berg et al., 2002; Smid et al., 2003; Greiner et al., 2004; Huetteroth and Schachtner, 2005; Masante-Roca et al., 2005; Skiri et al., 2005; Staudacher et al., 2009; Varela et al., 2009; paper II). Because these atlases often are based on confocal microscopy scans of higher resolution than the SBAs, they contain more precise and detailed spatial information about the selected neuropile architecture.

The sharp intracellular recordings in the olfactory and the gustatory system in of *H. virescens* generated physiologically and morphologically characterized neurons (Kvello

et al., 2010; paper I, II and III) as illustrated in **Figure 1**. In order to understand how the processed information in these neurons were integrated and distributed through the networks of the brain, it was important to develop the SBA of *H. virescens*. Integration of all glomeruli from the high resolution antennal lobe atlas into the SBA, resulted in the SBAGl, in which both glomerular arborisation and protocerebral projections of projection neurons (PNs) of the AL could be visualized.

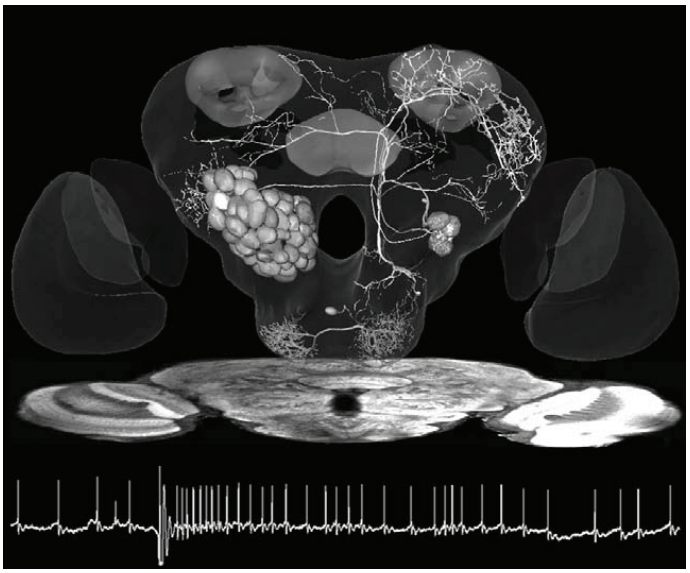

Figure 1: Illustration photo of data acquired from the intracellular recordings and staining experiments. Three olfactory and two gustatory neurons have been transformed into the SBAGl. Photo: Bjarte Bye Løfaldli/Pål Kvello.

The primary olfactory centre

Mainly three types of neurons make connections in and among the numerous glomeruli in the insect AL, the receptor neurons, local inhibitory neurons which connect most or all glomeruli of the AL and uni and multiglomerular PNs (Stocker et al., 1990; Sun et al., 1993a; Sun et al., 1997; Ng et al., 2002). In the AL of the fruit fly also excitatory local interneurons have been described (Olsen et al., 2007; Shang et al., 2007). The local

interneurons have been shown to constitute two systems which contribute to odor processing among the glomeruli in the networks of the AL of the honeybee and the fruit fly. One is a global inhibitory system which receives input and gives output in most if not all glomeruli. This system may either constitute a gain control system or it may participate in the synchronization of the network activity. The second is a more local inhibitory system (and an excitatory system in the fruit fly) involved in glomerulus specific regulation, which de-correlates the activity between individual glomeruli and increase the coding capacity of the AL network (Sachse and Galizia, 2002; Silbering and Galizia, 2007; Silbering et al., 2008). In addition to these main types of neurons, modulatory centrifugal neurons have also been found to make widely distributed connections among the glomeruli of the AL. One example is the octopaminergic WUM mx1 neuron identified by Hammer (1993) in the honeybee. Another example is the serotoninergic neurons described in different moth species, including one of the heliothines, *H. assulta* (Sun et al., 1993b; Kloppenburg et al., 1999; Zhao and Berg, 2009). The atlases of the ALs in the various insect species demonstrate the different glomerular numbers, counting about 50 in the fruit fly (Stocker et al., 1990; Laissue et al., 1999), around 60-67 in different moth species (Rospars and Hildebrand, 2000; Berg et al., 2002; Skiri et al., 2005; Varela et al., 2009; paper II), 180 in the honeybee (Flanagan and Mercer, 1989; Galizia et al., 1999a) and between 250 to 630 in ants (Zube and Rössler, 2008; Kelber et al., 2009). These atlases have supported the early finding that the number and position of glomeruli in the AL is highly constant between individuals and gender of the same species (Rospars and Chambille, 1981; Rospars, 1983).

The AL of moths is clearly separated in two parallel sub systems, the macroglomerular complex (MGC) which is devoted to processing of pheromone information and the numerous ordinary glomeruli constituting the plant odor system. Much is known about information processing of the pheromone system in the AL (Christensen et al., 1991 and 1995; Berg et al., 1998; Vickers et al., 1998; Anton and Hansson, 1999; Galizia et al., 2000; Kanzaki et al., 2003; Vickers and Christensen, 2003) compared to the more complex plant odor system. Studies of the AL in different insect species have indicated different coding mechanisms based on the presence of highly specific as well as broader

information channels. Two examples of highly specific systems comes from electrophysiological studies in hawk moth, where one glomerulus, the LPOG is shown to mediate information about carbon dioxide (Guerenstein et al., 2004) and two other identified glomeruli about one specific plant odorant (Roche King et al., 2000; Reisenman et al., 2004; Reisenman et al., 2005). In contrast to these findings other electrophysiological and calcium imaging studies have reported that odor information is coded and processed in a more integrative manner among the networks of the AL. For instance, by intracellular recordings of PNs in the moth *Spodoptera littoralis* both odor specific and more broadly responding PNs have been identified (Anton and Hansson, 1994; Sadek et al., 2002). In calcium imaging studies of the AL in *H. virescens* some of the primary odorants were each specifically represented in single glomeruli, whereas others were represented by activity in two or three glomeruli (Galizia et al., 2000; Skiri et al., 2004). Based on the findings that different odorants elicit specific activity patterns both among the olfactory receptor neurons and the glomeruli in the primary olfactory centre, a combinatorial type of odor processing have been proposed both in insects and vertebrates (Honeybee: Joerges et al., 1997; Sachse et al., 1999; Galizia and Szyszka, 2008). Moths: Vickers et al., 1998; Lei et al., 2004. OB in vertebrates: Friedrich and Korsching, 1997 and 1998; Spors and Grinvald, 2002; Leon and Johnson, 2003; Nara et al., 2011). This implies that information about some odorant might be encoded specifically in certain neurons and in a combinatorial manner in other neurons of the network (Keene and Waddell, 2007).

Other questions raised concerns how odor blends and the single constituents are represented in the AL. For instance, calcium imaging in the AL of the honeybee have demonstrated that single odorants and their blends are differently represented in ORNs and PNs. In contrast to the PNs showing less elemental mixture effects (more inhibition), the responses of the ORNs to antennal stimulation with odor blends could be predicted by the responses elicited by the constituting single odorants (more elemental, Deisig et al., 2006; Deisig et al., 2010). Studies in the same insect species have also shown that mixtures are differently processed in two of the antenno-protocerebral tracts (APTs), PNs of the medial-APT processing mixtures elementally and the lateral-APT PNs

synthetically. These conclusions was based on the findings that most medial-APT PNs responded with hypoaditivity to some of the single odorants and their mixtures whereas the lateral-APT PNs showed more suppressive responses to the mixtures compared to the constituents (Krofczik et al., 2009; Yamagata et al., 2009). Multiunit recording in the AL of the hawk moth has supported the findings reported in the honeybee regarding dissimilar representations of single odorants and their blends. In the moth the mixtures and the single constituents evoked specific spatio-temporal activity patterns among the neurons of the AL (Riffell et al., 2009a; Riffell et al., 2009b). A spatial independent mechanism for odor quality coding has been proposed in the locust. Here, odors are represented by the synchronous temporal activity patterns of several multiglomerular PNs (Laurent et al., 1996; Perez-Orive et al., 2004).

The antenno-protocerebral tracts

The processed odor information is conveyed from the AL to higher brain areas mainly by the three parallel antenno-protocerebral tracts (APTs), a term proposed as a common nomenclature by Galizia and Rössler (2010). This term replaces the previous term, antenno-cerebral tracts (ACTs) used in *H. virescens* (Rø et al., 2007; paper I and II). Thus, the inner-, the medial and the outer ACT is accordingly termed the medial-, the medio-lateral- and the lateral APT (m-APT, ml-APT and l-APT), respectively. The PNs of the three APTs projects to three higher brain areas associated with the olfactory system in insects (for rev: Galizia and Rössler 2010). The m-APT, which house PNs that innervates one or a few glomeruli, runs medio-posteriorly to the calyces of the MB, giving off three to five axonal branches before turning anterior-laterally and projecting into the LP/LH (Homberg et al., 1988; Stocker et al., 1990; Malun et al., 1993; Abel et al., 2001; Müller et al., 2002; Kirschner et al., 2006; Jefferis et al., 2007; Rø et al., 2007; paper I and II). In the LP of *H. virescens* the projections of the m-APT PNs form a dorso-ventral axis, termed the olfactory axis (OA). Neurons innervating the same glomerulus show similar projection patterns, whereas those from different glomeruli project to partly overlapping areas (paper I and II). Similar patterns have also been reported in other moth species and in the fruit fly (Marin et al., 2002; Wong et al., 2002; Jefferis et al., 2007; Namiki and Kanzaki, 2011). PNs of the l-APT run more laterally from the AL to the

LP/LH, before projecting dorso-posteriorly into the calyces of the MB (Homberg et al., 1988; Müller et al., 2002; Kirschner et al., 2006; Rø et al., 2007). In *H. virescens* the l-APT PNs enters the LP in the ventral part of the OA, extending in a ventro-dorsal direction (Rø et al., 2007; paper III). Similar projection patterns have been shown by mass staining in the honeybee (Kirschner et al., 2006). The multiglomerular PNs of the ml-APT have axonal projections directly to the LP/LH, with some axons branching off and turning dorso-medially into the superior protocerebrum (SP), located proximate to and dorsally of the MB lobes, extending from the anterior to the posterior part of the lobes (Homberg et al., 1988; Abel et al., 2001; Kirschner et al., 2006; Rø et al., 2007; paper III). Several if not all of the PN fibers of the ml-APT have been shown to contain γ-aminobutyric acid (GABA, Hoskins et al., 1986; Schäfer and Bicker, 1986; Berg et al., 2009). In *H. virescens* the PNs of the ml-APT enters the LP in the medial parts of the OA where they project both in a dorsal and ventral direction and thereby showing overlapping projections with PNs both in the m- and the l-APT (paper III).

Odor processing in higher brain areas

In the MB the kenyon cells (KCs) receive the processed odor information via PNs in two of the APTs. The KC constitute the major type of intrinsic neurons of the MB, each making synaptic contact with multiple PNs, and each PN giving input to multiple KCs (for rev: Menzel and Muller, 1996; Heisenberg, 2003; Keene and Waddell, 2007). In addition to the excitatory synapses formed by the PN and the KC in the calyces inhibitory neurons have been found to project to the calyces (Ganeshina and Menzel, 2001).Typical for the KCs are sparse response patterns to olfactory stimulation (Perez-Orive et al., 2002; Stopfer et al., 2003; Szyszka et al., 2005; Szyszka et al., 2008). The MB system is closely connected to other brain areas through several types of efferent and afferent MB extrinsic neurons, as shown in several insect species (Homberg, 1984; Mauelshagen, 1993; Li and Strausfeld, 1997; Ito et al., 1998; Rybak and Menzel, 1998; Strausfeld, 2002; Tanaka et al., 2008). Afferent neurons projecting from brain areas like the LP/LH and SP to the MB calyces and lobes have been shown. Efferent MB extrinsic neurons receives input from KC and projects from the MB lobes and the pedunculus to different brain areas, like the inferior medial protocerebrum, the SP, the LP/LH and to other parts

of the MB complex. Connections are made both on the ipsi and the contra-lateral side of the brain. The central role of the MB complex in olfactory learning and memory, and the ability of efferent MB extrinsic neurons, like the PE1 in the honeybee, to change response activity after conditioning, show that these neurons convey learned information from the MB complex to other parts of the brain, like the SP and the LP (Mauelshagen, 1993; Rybak and Menzel, 1998; Okada et al., 2007). Here they might be in position to influence and change the activity of postsynaptic neurons (Okada et al., 2007). This indirect olfactory pathway via the MB complex is likely to constitute an associative or experience dependent route for olfactory information from the AL to the premotoric area of the LP (Heisenberg, 2003; Keene and Waddell, 2007; Okada et al., 2007).

A parallel and more direct route for olfactory information from the AL leads directly to the LP/LH through all three APTs. In the fruit fly three types of third order LH neurons have been identified. All three types have most of their dendritic arborisations in the LH and axonal projections in different parts of the brain, including the SP and the more ventral areas of the LP (Tanaka et al., 2004; Jefferis et al., 2007). These third order neurons receive input from projections originating in several other brain areas, including the AL. It has been suggested that the direct AL-LH/LP pathway might represents a more naïve and experience independent processing stream for olfactory information (for rev: Heisenberg, 2003; Keene and Waddell, 2007). In addition to the LP/LH and the MB complex, the SP is another higher olfactory area that receives input both from the AL, the MB complex and the LP (Li and Strausfeld, 1997; Ito et al., 1998; Abel et al., 2001; Tanaka et al., 2008; Kirschner et al., 2006; Rø et al., 2007; paper III). In spite of the substantial olfactory input to the SP as shown in several insect species we have scares knowledge about the handling of the olfactory information in this area.

In trying to elucidate how odour information is represented in the brain of the model insect *H. virescens*, sharp in vivo electrophysiological recordings and staining was performed in order to physiologically and morphologically characterise olfactory neurons. In the studies underlying this thesis, the initial recordings was carried out in the AL, from were characterized PNs was transformed into the developed SBA (paper I, II).

This work laid the foundation for the subsequent recordings in the protocerebrum (paper III). A highly detailed and accurate map of the APT projections in the LP and the SP was produced through the transformation of reconstructed AL PNs into the SBA. This map was used to guide the localisation of the olfactory areas of the LP and SP during the recordings. The change of recording sites from the AL to the LP and the SP was based on the following reasons: Recordings from the AL is technically challenging, probably because of its loose structure. Therefore, the more compact protocerebrum was considered to yield more stable and long lasting recordings. In addition, recordings in the LP and the SP would provide insight about processing of relevant plant odour information in higher olfactory neurons in *H. virescens*. This would elucidate how the olfactory information is dispread and integrated in these higher olfactory areas by identifying functional connections between the neuropiles.

Aim of the thesis

The aims of this thesis were:

- To create an average standard brain atlas of the female moth *H. virescens* into which physiologically and morphologically characterized neurons could be transformed. This in order to elucidate possible connectivity in the networks of the brain (paper I).
- To integrate the antennal lobe atlas with all glomeruli into the *H. virescens* standard brain atlas in order to identify glomerular innervation and map the axonal projections of AL PNs in higher brain areas (paper II).
- To physiologically and morphologically characterize neurons processing information about primary plant odorants in the protocerebrum of *H. virescens.* This, in order to elucidate possible functional connectivity between higher olfactory areas (paper III).

Survey of the papers

Paper I

The aim of the study of paper one was to create an average standard brain atlas (SBA) of the female *H. virescens* that could serve as a common framework into which intracellular recorded and stained neurons of different brain preparations could be transformed. This was important since intracellular recordings and staining result in single identified neurons in each brain preparation. Since individual brains varies in size and shape integration of neurons from different preparation require an SBA.

The SBA of *H. virescens* was created using the iterative shape averaging (ISA) protocol originally developed in the standard brain atlas project of the honeybee brain. In *H. virescens* 72 female brain preparations were stained using the monoclonal antibody against the synaptic protein synapsin (SYNORF1) and the secondary antibody CY5. Based on the staining quality eleven brain preparations were chosen for manually labeling of the following selected neuropiles; the glomerular layer of the ALs, the MB system (calyces, peduncle and lobes), the central complex, the anterior optical tubercle, the mid brain region consisting of the protocerebrum (with the protocerebral lobes, the lateral horn, the lateral accessory lobes and the protocerebral bridge), parts of the deutocerebrum (the antenno-mechanosensory and motor centre and a small structure located ventrally to the glomerular layer), the tritocerebrum and the subesophageal ganglion (SOG) and the eye lobes (constituting the lobula, lobula plate and the medulla). Two olfactory and two gustatory neurons, in addition to axonal projections from gustatory receptor neurons were transformed into the SBA to demonstrate the application of the atlas. The transformation of two m-APT PNs and the gustatory neurons showed that neurons innervating both highly compartmentalized neuropiles (AL and MB) and a more uniform structure without landmarks (LP and SOG) could be transformed into the SBA. The m-APT PNs innervating the same glomerulus in the AL showed similar and overlapping projection patterns in the LP. Some of the axonal projection from one of the gustatory neurons, which responded to quinine, was identified in an area ventro-anteriorly in the LP, with one branch extending dorsally towards and proximate to the

projections from the olfactory PNs. These results indicated that olfactory and gustatory information might be integrated in third or higher order neurons in the LP of *H. virescens*.

Paper II

The aim of the study of paper two was to integrate into the SBA of the female *H. virescens* the antennal lobe atlas with all individual glomeruli identified and numbered according to a common numbering system used in heliothine moths. This allowed visualization of both glomerular arborisation in the AL and protocerebral projection patterns of the transformed neurons. The SBA with the glomeruli (SBAGl) could in addition aid the identification of the innervated glomeruli. Since the AL of the SBA of *H. virescens* included the glomerular layer exclusively, the antennal lobe atlas could with success be integrated into the SBA. To demonstrate the application of the SBAGl three m-APT PNs with different glomerular innervation was transformed. Two of the PNs were uniglomerular and one innervated three glomeruli, one glomerulus extensively and the two others more weakly. The axons of these neurons ran posteriorly in the brain, giving off three to five branches to the calyces of the MB before projecting anterior-laterally, and entered the dorsal parts of the LP. Here, the projections partly overlapped, following the dorso-ventral olfactory axis. The new antennal lobe atlas was made after the first AL model by Berg et al. (2002) in order to identify and number the glomeruli according to the numbering system developed for the two closely related heliothine species, *Helicoverpa armigera* and *Helicoverpa assulta* (Skiri et al., 2005). The identification of female specific glomeruli required comparison with the atlas of the male antennal lobe which also was made using the same numbering system. The results confirmed the findings in Berg et al. (2002), about the position and identity of the four male specific glomeruli in the MGC. In addition, in the present study four female specific glomeruli were identified, which showed consistency between individuals. The ordinary glomeruli also showed consistency both within and between individuals and genders. One exception was an ordinary glomerulus (G63) only present in the male AL of *H. virescens*. In the comparison between the three species larger differences were seen in the gender specific glomeruli with the typical four glomeruli units in *H. virescens* in contrast to the three

units in the helicoverpa species. In contrast, the ordinary glomeruli were constant in number and positions between species.

Paper III

The aim of the study of paper three was to identify a putative circuit in the brain of *H. virescens* involved in handling information about single odorants and blends. Primary odorants and blends ranging from a binary two component mixture to a complex twelve component mixture were used as stimuli. In vivo sharp recordings were performed from neurons in two higher olfactory areas of the brain, the LP and the SP. The strength of the odor elicited responses of 28 neurons was analyzed by dividing the response window into excitatory and inhibitory phases. Three response modes were identified, excitation only, inhibition only and complex responses composed of both excitatory and inhibitory phases. The analysis revealed that some neurons responded specifically to a few odorants and mixtures, however most neurons responded to a broader range of the odor stimuli, but with different response strengths. This implied that the neurons might integrate olfactory information from several input channels and that the odors are processed in a combinatorial manner in the higher brain areas. The staining and transformation of six neurons, two multiglomerular PNs of the ml-APT, two efferent MB extrinsic neurons, one LP-SP neuron and a LP-descending neuron revealed partly morphological overlap in two higher brain areas, the LP and the SP. All, except one ml-APT PN responded to stimulation with a ten component mixture. This implies that these neurons might be involved in a putative circuit connecting the three higher olfactory areas, the LP, the MB complex and the SP with the input from the AL. The results also suggest that olfactory information conveyed from the AL is being processed in parallel in the three protocerebral areas. An undefined area located anterior-ventrally of the OA in the LP was found to house the dendrites of a descending neuron with axonal projections running into the ipsi-lateral connective. This neuron responded with inhibition to antennal stimulation with the ten component blend.

Discussion

Odor representation in higher brain areas

Knowledge about the function of the olfactory system is growing and much research has been carried out in invertebrate and vertebrates, which has broaden our understanding of this fascinating sense. Odor processing in the primary olfactory centre, the AL in insects has been the centre of attention in many electrophysiological and imaging studies. In several species, the olfactory pathways to higher brain areas like the MB, the LP/LH and the SP have been identified (for review: Galizia and Rössler, 2010). How the processed odor information from the AL is integrated and coded in the networks of these higher brain areas are important question for the understanding how odors influence and guide relevant behaviors. Important questions also concerns how olfactory information is learned and stored in the insect brain, which particularly have involved studies of the MB complex. A wide range of techniques have been applied including electrophysiological recordings, imaging and labeling techniques in several insect species and important mechanisms and principles underlying learning and memory formation have been revealed (for review: Menzel and Muller, 1996; Heisenberg, 2003; Keene and Waddell, 2007; Strausfeld et al., 2009). Although some studies have focused on the networks in the LP/LH and the SP, the knowledge is scarce on how odor information is processed and distributed in these protocerebral areas, including the premotoric areas of the LP.

The previous and unique identification of many primary plant odorants in *H. virescens* laid the foundation for the studies on the function of the central networks of the olfactory system. Stimulation with the identified odorants and their blends during electrophysiological recordings combined with staining techniques has elucidated parts of the central olfactory networks dealing with relevant plant odor information. A custom made blend of ten primary plant odorants (PB10), which specifically activated a multiglomerular PN of the ml-APT proved to be important in this work. Particularly in the recordings from neurons in the LP and SP, the two target areas of the PNs of the ml-APT, the PB10 was found to be particularly effective in eliciting responses. Thus, this potent and relevant stimulus was important for the identification of possible functional

connections between the different neuropiles of the olfactory network. The reconstruction and transformation of the physiologically characterized neurons from different preparations into the standard brain atlas ensured that the suggested functional connectivity could be supported by the identification of morphological overlap (paper III).

Previous electrophysiological and imaging studies, both in the AL and in the higher brain areas of different insect species have addressed the question on how odor quality is represented in the activity of neurons in the olfactory networks of the brain. Several different processing mechanisms have been proposed (Laurent et al., 1996; Müller et al., 2002; Perez-Orive et al., 2002; Stopfer et al., 2003; Lei et al., 2004; Szyszka et al., 2005; Galizia and Szyszka, 2008; Yamagata et al., 2009). In the present study of *H. virescens* the intracellular recordings from the two higher brain areas, the LP and the SP, revealed a few neurons with a relatively high specificity to stimulation with single odorants and blends, as well as many neurons responding to stimulation with several odorants (paper III). This observed response pattern points to a combinatorial coding mechanism where information about different odorants is coded specifically in some neurons and in concert with others in other neurons (Keene and Waddell, 2007). A similar strategy has previously been shown in the primary olfactory centre of other insect and vertebrate species. The knowledge about the processing of plant odor information in the AL of *H. virescens* is scarce, the results from the recordings obtained so far seem to reflect the observed representation of the primary plant odorants in the higher olfactory areas of protocerebrum, presented in paper III.

In general, results obtained in electrophysiological studies of various insect species have suggested that different odor qualities are separately represented not only in the spatial but also in the temporal firing patterns among neurons of the olfactory network (MacLeod and Laurent, 1996; Perez-Orive et al., 2002; Stopfer et al., 2003; Riffell et al., 2009a; Riffell et al., 2009b). The odor responses obtained from the recorded neurons in *H. virescens* partly supports this by the fact that most neurons differed in response strength to various single odorants and blends (paper III). Different from this are findings

in the honeybee, showing that MB extrinsic neurons display unspecific responses to different odor stimuli (Homberg, 1984; Mauelshagen, 1993; Rybak and Menzel, 1998; Okada et al., 2007). This suggests that the MB neurons in the honeybee in contrast to the moth do not differentiate between odor qualities through response strength or temporal patterns. The different findings across species may either be ascribed to inter species differences or to multiple coding mechanisms co-existing in the complex networks of the olfactory system within a species. Based on the sophisticated behaviors expressed by insects to different odor qualities one might expect that odor information is integrated and processed in a manner that conserves odor quality throughout the networks of the olfactory system, from the binding at the receptors to descending neurons in the brain.

Morphological overlap and functional connectivity

To resolve the central questions regarding olfactory coding mechanisms, the functionality and the connectivity of the neurons in the network must be clarified. One challenging task is to integrate and coordinate results obtained from multiple experimental trials, resulting in identification of single neurons in different individual brains. A solution to this problem was offered by the creation of SBAs. These atlases serving as common frameworks for integration and visualization of physiologically and morphologically characterized neurons proved to be valuable (paper I, II and III). The ISA procedure, reducing the variability between preparations and constraining the degree of allowed deformation of registered neurons is considered as an advantage. This secures that the traced neurons keep their original shape during the transformation from the experimental preparations to the SBA. Compared to manual transformation techniques the registration of neurons by the use of transformation algorithms offer a more objective and comprehensive solution where references to multiple factors are taken into consideration. Although advantageously, the use of SBAs as common frameworks for transforming neurons have one clearly limitary factor, which is the relatively slow and time consuming process of manually labeling innervated neuropiles and stained neurons. Following the progression and availability of different labeling techniques such as genetic labeling and the progression of electrophysiological recordings and staining experiment, the amount of accessible morphological data is rapidly growing. This has generated the need of

additional procedures which minimize or avoids the process of manually labeling. One such transformation procedure was applied in a study of Jefferies et al. (2007) on the fruit fly. Instead of manually labeling the new method relay on an intensity 3D- imaging registration algorithm combined with genetic single cell labeling were high resolution confocal images were linearly transformed before different brain structures were deformed in a nonrigid way. A high degree of precision was reported were transformation accuracy was calculated down to a few micrometers. Another advantage of this method is that the registration procedure can be applied in any study generating two channel confocal images, one channel with stained neurons and the other a background staining of the neuropiles. However, this method used in genetically labeling might not be as suitable for studies using intracellular recordings and staining because of the mechanical damage that may occur during penetration of the electrode.

In the ongoing search for the neuronal networks underlying the sense of smell it is important to remember that morphologically identified overlap of neuritis does not automatically mean functional connections. Transformation of stained neurons into a common framework might only indicate functional connections. Therefore, the combination of morphological and physiological studies is desired. This was elegantly approached in the paper by Ruta et al. (2010) where a circuit for pheromone processing was identified from the receptor neurons on the antenna to descending neurons in the dimorphic lateral triangle and the superior-medial tract (SMP) in the LP of the fruit fly. By neuronal staining (genetically photoactivation and electroporation) morphological overlap was identified between upstream and downstream neurons in three areas of the brain, the AL, the LH and the LP. Functional connections were indicated by electrophysiological and calcium imaging recordings where both electro-chemical (iontophoresing of acetycholin into glomeruli) and pheromone stimulation elicited activity in the downstream neurons of the AL. Similar labeling techniques as used in the fruit fly have not been available in the present studies of *H. virescens*. However the SBA in *H. virescens* represent a good tool for linking electrophysiological and morphological data in which functional connections of the neuronal network can be indicated and visualized, as shown in paper III.

The lateral protocerebrum and the olfactory axis

Relatively little is known about the function and the connectivity of the networks of the LP/LH even though this area receives major olfactory input from the AL through multiple APTs in several insect species studied (Homberg et al., 1988; Stocker et al., 1990; Kirschner et al., 2006; Rø et al., 2007; Galizia and Rössler, 2010; paper I, II and III)). In addition to olfactory input, the LP receives input from multiple modalities and is also considered as a premotoric area. It has been proposed that the LP might be involved in more naive or direct odor processing, whereas the MB complex is primarily important for learning and memory (for review: Menzel and Muller, 1996; Heisenberg, 2003; Keene and Waddell, 2007). A deeper understanding of the role of LP/LH in integration of odor information might bring us closer to the understanding of how this information influence and guide animal behavior. A challenging property of the LP/LH is its undefined and loose structure with very little landmark neuropiles. In the process of understanding the integrative properties of neurons in the LP as well as other brain areas with similar loose structural appearance the use of standard brain atlases or other common frameworks is of great advantage.

In *H. virescens* the work of mapping the neuronal connections in the LP started with the making of the SBA and the SBAGl (paper I and II and III). By integrating reconstructed PNs into the SBAGl both the glomerular innervation in the AL and axonal projections in the LP could be visualized. Here, it became evident that m-APT PNs innervating different glomeruli projected to partly overlapping areas of the LP along the dorso-ventral olfactory axis (paper II). PNs innervating the same glomerulus showed more intermingled and similar projection patterns (paper I). Such a stereotypic projection pattern among PNs has also been shown in the fruit fly by genetically labeling methods (Marin et al., 2002; Wong et al., 2002; Jefferis et al., 2007) and more recently by staining techniques in the hawk moth (Namiki and Kanzaki, 2011). A compartmentalization of the LH into several zones (three) has earlier been proposed for the fruit fly (Tanaka et al., 2004). However other studies have contradicted the findings of zones. In the more recent study of the LH in the fruit fly by Jefferies et al. (2007), a stratified and more complex projection patterns were identified instead of zones. The present studies of *H. virescens* supported the

findings by Jefferies et al., showing no indication of zones. The transformation of m- and ml-APT PNs into the SBA and the mass staining of the APTs in *H. virescens* showed a high degree of overlap between the PNs in the three APTs (paper II and III). Similar patterns have been shown in the honeybee (Kirschner et al., 2006). Taken together this suggests that the information carried by the three AL-LP channels might be integrated on third order LP neurons.

Parallel pathways to the higher brain areas

The multiple tracts mediating processed information from the AL to higher order olfactory areas in protocerebrum have raised the question about their differential functions (Müller et al., 2002; Rø et al., 2007; Krofczik et al., 2009; Galizia and Rössler, 2010; paper III). Although knowledge is growing, much is still unclear about the processing and the function of these parallel pathways in the olfactory system of insects. Recent studies in the honeybee have suggested a differential processing of mixtures in the m- and the l-APT, the m-APT processes mixture information in an elemental way and the l-APT PNs in a more synthetic manner (Krofczik et al., 2009). However, the system may differ in *H. virescens*. So far the recordings from m-APT PNs have indicated specific responses to primary odorants, which seems to reflect the high specificity and only minor overlap of the molecular receptive ranges of the plant odor receptor neurons compared to what is known in honeybees. Although two or three major tracts are found in all insect species, some inter-species variations exist. Compared to the attention in many studies of the m- and the l-APT PNs, relatively few studies have been performed on the ml-APT PNs. In the present study of *H. virescens* one of the topics concerned the function and the morphology of the ml-APT PNs (paper III). The existence of morphologically different types of ml-APT PNs have previously been shown in the honeybee as well as in *H. virescens* (Kirschner et al., 2006; Rø et al., 2007) and is in *H. virescens* further described in paper III. Interestingly, the electrophysiological recordings from two of the ml-APT PNs in *H. virescens* revealed a sparse response pattern, one of them responding exclusively to stimulation with the complex blend B10 and not to single odorants. This response property could be related to the loose innervation of numerous glomruli in the AL by this ml-APT neuron (paper III). However, recordings from multiglomerular ml-

APT PNs in the AL of the honeybee revealed responses to single odorants (Abel et al., 2001). This difference might be related to the more broadly tuned receptor neurons in the honeybee, if not to different types of ml-APT PNs within a species. Concerning the general function of the ml-APT PNs, it has been suggested that because of their multiglomerular connections in the AL, single ml-APT PNs may be in position to read out specific odor evoked activity patterns among the glomeruli in the AL (Kirschner et al., 2006; Galizia and Rössler, 2010). In *H. virescens* the blend B10 may define one of the activity patterns.

Further information about the ml-APT PNs comes from immunoreactivity studies. Thus, using immuno-staining of the ml-APT in moths, including *H. virescens* and honeybees, most if not all PN fibers in this tract showed GABA immunoreactivity (Hoskins et al., 1986; Schäfer and Bicker, 1986; Berg et al., 2009). This implies that the ml-APT PNs represent an inhibitory processing channel in parallel to the two other presumably excitatory pathways to the LP. Thus, the m- and the l-APT PNs may carry differentiated excitatory information about mixtures and single odorants, whereas the ml-APT exhibit inhibitory information about the combinatorial activity patterns in the AL. The extensive overlap between the projections of these parallel pathways in the LP/LH in *H. virescens* and the honeybee, make third order LP/LH neurons in position to integrate both the inhibitory and the excitatory information from the AL.

Several functional implications of inhibitory signals have been proposed for different brain areas. How these relate to the odor evoked inhibitory signal in the ml-APT PN, one can only be speculate about. One possibility is that these signals are involved in the regulation and synchronization of the odor evoked activity in third order LP neurons, in a similar manner as have been suggested for other inhibitory protocerebral neurons (Grünewald, 1999; Ganeshina and Menzel, 2001; Perez-Orive et al., 2004; Szyszka et al., 2005). Another possible function could be to reset the odor activated third order integrative neurons in the LP and thereby making them receptive to the continuous flow of incoming signals either from the AL-LP pathway or from other indirect pathways like the efferent extrinsic neurons from the MB complex.

Parallel olfactory processing in higher brain areas

How processed odor information from the primary olfactory centre is represented, dispersed and integrated in the higher olfactory processing areas of the brain are one of the ultimate questions regarding the function of the olfactory system. Clarification of this question might lay in tracing the odor signal information through all processing stages of the olfactory system, from the olfactory receptor neurons on the antennae to descending neurons in the premotoric areas of the brain. Since no methods exist for achieving this in one and the same individual, another attempt used in this study is to collect physiological and morphological data from neurons of different individuals and bring them together in a common framework. Similar to the study by Ruta et al., (2010) showing a circuit for handling pheromone information in the fruit fly, the present thesis presents a putative circuit that handles information about a ten component plant odor mixture in the brain of the *H. virescens* (paper III). The electrophysiological recordings from the neurons in *H. virescens* revealed that the information about this blend is parallel processed and mediated to three higher brain areas, the LP, the MB complex and the SP (**Figure 2**).

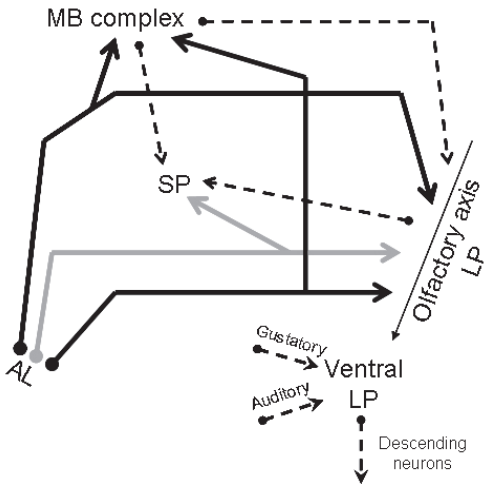

Figure 2: Illustration of the identified putative circuitry in *H. virescens*.

As previously mentioned, third order LP/LH neurons in insects might receive processed olfactory information directly from the AL via PNs of the three APTs. In addition to this direct olfactory pathway from the AL, several types of MB extrinsic neurons have been shown to project from the MB complex to the LP/LH in several insect species, in *H. virescens* shown in paper III. The extrinsic MB neurons represent the output of the MB complex and some of these neuron have been related to learning and memory processes in the MB (Mauelshagen, 1993; Rybak and Menzel, 1998; Okada et al., 2007). Therefore this indirect pathway to the LP is considered to convey odor information in an associative and experience dependent context. Three types of third order LH neurons have been identified by genetically labeling in the fruit fly in which all types are believed to receive input in the LH and sending axonal projections to different areas of the brain, like the superior medial and superior lateral protocerebrum, the ventro-lateral and ventro-medial protocerebrum and the deutocerebrum (including the antennal mechanosensory and motor centre. Tanaka et al., 2004; Jefferis et al., 2007). In *H. virescens,* one third order LP neuron that responded to stimulation with the PB10 is characterized in paper III. This neuron, with dendrites in the OA of the LP and axonal projections in the SP is in position to integrate olfactory information from the different channels in the LP and convey this information to the SP (**Figure 2**). Two medial lobe efferent MB extrinsic neurons that responded to stimulation with the PB10 were also identified in *H. virescens* (paper III). These neurons showed axonal projections in different areas, one in the SP and the other in the OA of the LP. These results suggest that information about the PB10 is conveyed from the associative networks of the MB complex to two higher olfactory areas, the LP and the SP (**Figure 2**). The SP receives olfactory information from multiple areas of the insect brain. A close connections between the MB complex and the SP have previously been suggested, based on the massive neuronal projections found between these two areas (Ito et al., 1998; Tanaka et al., 2008). The results obtained in the *H. virescens* suggest that neurons in the SP may integrate olfactory information from at least three parallel processing channels, from the MB complex, the LP and the AL (**Figure 2**).

Descending neurons in the LP

In order to understand how the processed olfactory information in the multiple relay areas of the olfactory system is transformed into relevant behavior, it is important to know how this information is integrated and represented in the descending neurons of the brain. Although descending neurons have been previously identified in moths (Kanzaki and Shibuya, 1986; Kanzaki et al., 1991; Kanzaki et al., 1994), relatively little is known about the physiology and morphology of LP descending neurons in moths. In this study of *H. virescens* an undefined neuropile area located in the LP, anterior-ventrally of the OA, was found to house the dendrites of a descending neuron. The axon of this neuron projected out of the brain via the ipsi-lateral connective ventrally in the SOG (paper III, **Figure 2**). Dual mass staining from the pro-thoracic ganglion and the AL in *H. virescens* indicates that there might be only some overlap between the most ventral ml- and l-APT projections and some of the dendrites of the descending neurons (Siri Børø, master thesis NTNU). This is in accordance with the findings that only close projections and no direct overlap was found between the axons of the ml-APT PNs and the dendrites of the descending neuron after transformation into the SBA (paper III). It was suggested in this study that there might be overlap by other APT PN projections and descending neurons. This anterior-ventral area of the LP is clearly separated from the areas more medially in the protocerebrum, which houses the dendrites of pheromone responding descending neurons, as shown in the silkworm moth and in the hawk moth (Kanzaki and Shibuya, 1986; Kanzaki et al., 1991; Kanzaki et al., 1994). This suggests that information about pheromones and plant odorants are kept separated also in the descending pathways of the moth brain. However, since the present study of H. virescens concerns the brain of the female moth, the two descending systems should be studied in the male moth before conclusions can be made.

In addition to olfactory input the anterior-ventral area of the LP in *H. virescens* has been shown to receive input from other modalities. For instance, transformation into the SBA of the descending neuron and a taste neuron responding to quinine (paper I) indicated morphological overlap between the axons of the quinine neuron and the dendrites of the descending neuron (data not shown). In addition axonal projections of auditory neurons

have been found in this anterior-ventral area of the LP (Pfhül et al., personal communication). Integration of multimodal information has previously been proposed for areas in the ventro-lateral parts of the protocerebrum and in the deutocerebrum in flies, including the fruit fly based on projections both from olfactory, mechanosensory and visual areas have been described (Strausfeld, 1976; Strausfeld et al., 1984; Tanaka et al., 2004). In flies including the fruit fly, the ventro-lateral deutocerebrum have been shown to house descending neurons (Strausfeld et al., 1984). The characterized descending neuron recorded in *H. virescens,* showing long lasting inhibitory responses to stimulation with the complex mixture PB10, made it particularly interesting to look for overlap of its dendrites with axonal projections of the ml-APT PN specifically responding to B10. However, no direct overlap could be found. This implies that the odor information is being relayed to this neuron by other PNs in the ml- or l-APT. Another possibility is an indirect pathway, either from third order LP neurons or from efferent MB extrinsic neurons, like the PE1 in the honeybee as discussed by Okada et al. (2007). The MB extrinsic neurons might connect with the descending neurons either through direct synapses or indirectly through other protocerebral neurons like the third order LP neurons. Through these connections the MB complex is in position to influence and possibly change the inhibitory response profile of descending neurons in response to learning and experience. One can further speculate that activity in this network is partly responsible for some changes in odor driven behavior following learning.

An interesting question regarding the connection between odor evoked neuronal activity and odor driven behaviors concerns which odors may evoke relevant behaviors. The importance of mixtures in eliciting behavior is well known from pheromone attraction and sexual behavior in many insect species, including heliothine moths. In *H. virescens*, the behavioral effect of one primary odorant, germacrene D, on attraction and oviposition, was shown by adding the odorant to host plants releasing volatiles except germacrene D (Mozuraitis et al., 2002). Electrophysiological multi unit recordings combined with behavioral studies in the hawk moth suggests that feeding behavior is not initiated by the single components constituting a nine or a six component mixture derived from natural odor mixtures released by host plants (Riffell et al., 2009a; Riffell et al.,

2009b). In line with these behavioral findings, the descending neuron in H. virescens responded specifically to the complex mixture PB10 and not or only weakly to the single primary odorants (paper III). Taken together these results imply that activity in multiple channels must coincide in order to elicit relevant odor behaviors or response in descending neurons, activity in multiple channels must coincide. This might either be achieved through the activity of multiple olfactory channels or by other simultaneously activated pathways, for instance from the MB system through associative learning and memory.

Concluding remarks

This thesis has provided new insight into how olfactory information is coded, integrated and dispread in the networks of the higher brain areas, the MB, the LP and the SP in the model insect *H. virescens*. The electrophysiological recordings and the following staining, reconstruction and transformation of the neurons into the standard brain atlas revealed both the projection pattern of AL PNs in the OA of the LP and of higher order neurons. The characterization of these higher order neurons suggests that relevant plant odor information are integrated and processed in parallel in the three higher brain areas, the MB complex, the LP and the SP. The SP was shown to receive odor information from three different processing channels, the AL, the MB and the LP. In addition, an undefined area anterior-ventrally of the OA in the LP was found to house the dendrites of an olfactory responding descending neuron. Together with the results from mass staining experiments these results suggests that there are little or no morphological overlap between dendrites of descending neurons and axons of PNs from the AL in the LP. This further suggests that the output region with dendrites of descending neurons is a defined and separate area of the LP in *H. virescens*.

Although knowledge has been achieved, much more work still needs to be carried out in order to understand the complexity of odor coding in the central networks of *H. virescens* and other insects. Among other methods, electrophysiological recordings, staining and

transformation of single neurons into common frameworks as SBAs are important techniques which should be intensified in the continuation of this work. Particularly more effort should be invested in revealing the functionality and the connectivity of the networks in the LP and the SP. One particularly interesting and important task would be to characterize third order LP neurons in order to elucidate how odor information is integrated, coded and conveyed to other brain areas by these neurons. Another focus should be on the descending neurons in the LP in order to broaden our knowledge on how plant odor processing might lead to relevant behavioral responses.

Acknowledgement

The principal financial support for this PhD project was granted from the "Kongelige Norske videnskapers selskap" (DKNVS, the Royal Norwegian Society of Sciences and Letters). Additional financial support was provided from the Department of Biology, NTNU.

I would like to express my deepest gratitude to my supervisor Professor Hanna Mustaparta who introduced me to the fascinating world of science and "olfaction". Dear Hanna, thank you for having believed in me and for all the time and energy you have invested in me and my work. I will never forget our discussions and shared thoughts. I would also like to thank Professor Randolf Menzel for our discussions and collaborations during you're visits in Trondheim and for helping with the standard brain project. I'm also thankful for the help provided by Dr. Jürgen Rybak in the standard brain project and to Dr. Robert Brandt for his help and advices during the work with Amira. I'm also grateful to Professor Giovanni Galizia, his family and his colleagues and student at the University of Konstanz for receiving me and for all the help you gave during my stay. A special thank also goes to Aneke Meyer for our collaboration.

In the Neuroscience unit I'm deeply grateful for the close collaboration with Pål Kvello, thank you for all the great times both inside and outside the lab and for sharing you're

insight and wisdom with me. I'm also especially thankful for the close collaboration with MSc Nicholas Kirkerud. Thanks to all colleagues and students, current and former of the Neuroscience unit including Bente Berg, Dr. Xin-Cheng Zhao, Marit Stranden, Kari Jørgensen, Hanne Therese Skiri, Helge Rø, Gerit Pfül, Stig Ullan, Øystein Roten, Tor Jørgen Almaas, Øyvind Høydahl, Bente Jacobsen, Siri Børø, Erik Nilssen, Siri Lillevoll, Helene Mørk, Ingrid Dahl, Maria Herzog, Anja Fredriksen, Hilde Fjærli og Jens Halvorsen.

I would also like to thank for all technical assistance at NTNU and the Department of Biology and a special thanks goes to Lisbeth Aune, Per Harald Olsen and Astrid Bjørkøy.

Last I want to direct my deepest gratefulness to my fiancée Caroline Kvistnes for your incredible patience and support during the work of my PhD project.

Refrences

Abel, R., Rybak, J., and Menzel, R. (2001). Structure and response patterns of olfactory interneurons in the honeybee, Apis mellifera *J. Comp. Neurol.* 437**,** 363-383.

Anton, S., and Hansson, B.S. (1994). Central processing of sex pheromone, host odour, and oviposition deterrent information by interneurons in the antennal lobe of female Spodoptera littoralis (Lepidoptera: Noctuidae). *J. Comp. Neurol.* 350**,** 199-214.

Anton, S., and Hansson, B.S. (1999). Physiological mismatching between neurons innervating olfactory glomeruli in a moth. *Proc. Roy. Soc. Lond. B.* 266**,** 1813-1820.

Berg, B.G., Almaas, T.J., Bjaalie, J.G., and Mustaparta, H. (1998). The macroglomerular complex of the antennal lobe in the tobacco budworm moth *Heliothis virescens*: specified subdivision in four compartments according to information about biologically significant compounds. *J. Comp. Physiol. A.* 183**,** 669-682.

Berg, B.G., Galizia, C.G., Brandt, R., and Mustaparta, H. (2002). Digital atlases of the antennal lobe in two species of tobacco budworm moths, the oriental *Helicoverpa assulta (*male) and the American *Heliothis virescens* (male and female). *J. Comp. Neurol.* 446**,** 123-134.

Berg, B.G., Schachtner, J., and Homberg, U. (2009). γ-Aminobutyric acid immunostaining in the antennal lobe of the moth *Heliothis virescens* and its colocalization with neuropeptides. *Cell Tissue Res.* 335**,** 593-605

Brandt, R., Rohlfing, T., Rybak, J., Krofczik, S., Maye, A., Westerhoff, M., Hege, H.-C., and Menzel, R. (2005). Three-dimensional average-shape atlas of the honeybee brain and its applications. *J. Comp. Neurol.* 492**,** 1-19.

Chiang, A.S., Liu, Y.C., Chiu, S.L., Hu, S.H., Huang, C.Y., and Hsieh, C.H. (2001). Three-dimensional mapping of brain neuropils in the cockroach, *Diploptera punctata J. Comp. Neurol.* 440**,** 1-11.

Christensen, T.A., Mustaparta, H., and Hildebrand, J.G. (1991). Chemical communication in heliothine moths. II. Central processing of intra- and interspecific olfactory messages in the male corn earworm moth *Helicoverpa zea*. *J. Comp. Physiol. A.* 169**,** 259-274.

Christensen, T.A., Mustaparta, H., and Hildebrand, J.G. (1995). Chemical communication in heliothine moths VI. Parallel pathways for information processing in the macroglomerular complex of the male tobacco budworm moth *Heliothis virescens*. *J. Comp. Physiol. A*. 177**,** 545-557.

De Bruyne, M., Clyne, P.J., and Carlson, J.R. (1999). Odor coding in a model olfactory organ: the *Drosophila* maxillary palp. *J. Neurosci.* 19**,** 4520-5432.

De Bruyne, M., Foster, K., and Carlson, J.R. (2001). Odor coding in the *drosophila* antenna. *Neuron* 30**,** 537-552.

Deisig, N., Giurfa, M., Lachnit, H., and Sandoz, J.-C. (2006). Neural representation of olfactory mixtures in the honeybee antennal lobe. *EJN.* 24**,** 1161-1174.

Deisig, N., Giurfa, M., and Sandoz, J.C. (2010). Antennal Lobe Processing Increases Separability of Odor Mixture Representations in the Honeybee. *J. Neurophysiol.* 103**,** 2185-2194.

Fitt, G.P. (1989). The ecology of Heliothis species in relation to agroecosystems. *Ann. Rev. Entomol.* 34**,** 17-52.

Flanagan, D., and Mercer, A.R. (1989). An atlas and 3-D reconstruction of the antennal lobes in the worker honey bee, *Apis mellifera* L. (Hymenoptera: Apidae). *Int. J. Insect. Morphol. Embryol.* 18**,** 145-159.

Friedrich, R.W., and Korsching, S.I. (1997). Combinatorial and Chemotopic Odorant Coding in the Zebrafish Olfactory Bulb Visualized by Optical Imaging. *Neuron* 18**,** 737-752.

Friedrich, R.W., and Korsching, S.I. (1998). Chemotopic, Combinatorial, and Noncombinatorial Odorant Representations in the Olfactory Bulb Revealed Using a Voltage-Sensitive Axon Tracer. *J. Neurosci.* 18**,** 9977-9988.

Galizia, C.G., Mcilwrath, S.L., and Menzel, R. (1999a). A digital three-dimensional atlas of the honeybee antennal lobe based on optical sections acquired by confocal microscopy. *Cell Tissue Res.* 295**,** 383-394.

Galizia, C.G., and Rössler, W. (2010). Parallel Olfactory Systems in Insects: Anatomy and Function. *Annu. Rev. Entomol.* 55**,** 399-420.

Galizia, C.G., Sachse, S., and Mustaparta, H. (2000). Calcium responses to pheromones and plant odours in the antennal lobe of the male and female moth *Heliothis virescens*. *J. Comp. Physiol. A.* 186**,** 1049-1063.
Galizia, C.G., and Szyszka, P. (2008). Olfactory coding in the insect brain: molecular receptive ranges, spatial and temporal coding. *Entomol. Exp. Appl.*
Ganeshina, O., and Menzel, R. (2001). GABA-immunoreactive neurons in the mushroom bodies of the honeybee: An electron microscopic study. *J. Comp. Neurol.* 437**,** 335-349.
Gerber, B., Tanimoto, H., and Heisenberg, M. (2004). An engram found? Evaluating the evidence from fruit flies. *Nat. Neurosci.* 14**,** 737-744.
Greenstein, B., and Greenstein A. (2000). Color atlas of neuroscience: neuroanatomy and neurophysiology. *Georg Thieme Verlag, Stuttgart/New York*.
Greiner, B., Gadenne, C., and Anton, S. (2004). Three-dimensional antennal lobe atlas of the male moth, *Agrotis ipsilon*: A tool to study structure-function correlation. *J. Comp. Neurol.* 475**,** 202-210.
Grünewald, B. (1999). Physiological properties and response modulations of mushroom body feedback neurons during olfactory learning in the honeybee, *Apis mellifera*. *J. Comp. Physiol. A.* 185**,** 565-576.
Guerenstein, P.G., Christensen, T.A., and Hildebrand, J.G. (2004). Sensory processing of ambient CO 2 information in the brain of the moth *Manduca sexta*. *J. Comp. Physiol. A.* 190**,** 707-725.
Hallem, E.A., and Carlson, J.R. (2006). Coding of Odors by a Receptor Repertoire. *Cell* 125**,** 143-160.
Hammer, M. (1993). An identified neuron mediates the unconditioned stimulus in associative olfactory learning in honeybees. *Nature* 366**,** 59-63.
Heisenberg, M. (2003). Mushroom body memoir: from maps to models. *Nat. Rev. Neurosci.* 4**,** 266-275.
Homberg, U. (1984). Processing of antennal information in extrinsic mushroom body neurons of the bee brain. *J. Comp. Physiol. A.* 154**,** 825-836.
Homberg, U., Montague, R.A., and Hildebrand, J.G. (1988). Anatomy of antenno-cerebral pathways in the brain of the sphinx moth *Manduca sexta*. *Cell Tissue Res.* 254**,** 255-281.
Hoskins, S.G., Homberg, U., Kingan, T.G., Christensen, T.A., and Hildebrand, J.G. (1986). Immunocytochemistry of GABA in the antennal lobes of the sphinx moth *Manduca sexta*. *Cell Tissue Res.* 244**,** 243-252.
Huetteroth, W., and Schachtner, J. (2005). Standard three-dimensional glomeruli of the *Manduca sexta* antennal lobe: a tool to study both developmental and adult neuronal plasticity. *Cell Tissue Res.* 319**,** 513-524.
Ito, K., Suzuki, K., Estes, P., Ramaswami, M., Yamamoto, D., and Strausfeld, N.J. (1998). The Organization of Extrinsic Neurons and Their Implications in the Functional Roles of the Mushroom Bodies in *Drosophila melanogaster* Meigen. *Learn & Mem.* 5**,** 52-77.
Jefferis, G.S.X.E., Potter, C.J., Chan, A.I., Marin, E.C., Rohlfing, T., Maurer, C.R., and Luo, L.Q. (2007). Comprehensive maps of *Drosophila* higher offactory centers: Spatially segregated fruit and pheromone representation. *Cell* 128**,** 1187-1203.
Jenett, A., Schindelin, J.E., and Heisenberg, M. (2006). The Virtual Insect Brain protocol: creating and comparing standardized neuroanatomy. *Bmc Bioinformatics* 7. 544.
Joerges, J., Kuttner, A., Galizia, C.G., and Menzel, R. (1997). Representations of odours and odour mixtures visualized in the honeybee brain. *Nature* 387**,** 285-288.
Jundi, B.E., Huetteroth, W., Kurylas, A.E., and Schachtner, J. (2009). Anisometric Brain Dimorphism Revisited: Implementation of a Volumetric 3D Standard Brain in Manduca sexta. *J. Comp. Neurol.* 517**,** 210-225.
Kanzaki, R., Arbas, E.A., and Hildebrand, J.G. (1991). Physiology and morphology of descending neurons in pheromone-processing olfactory pathways in the male moth *Manduca sexta*. *J. Comp. Physiol. A.* 169**,** 1-14.
Kanzaki, R., Ikeda, A., and Shibuya, T. (1994). Morphological and physiological properties of pheromone-triggered flipflopping descending interneurons of the male silkworm moth Bombyx mori. *J. Comp. Physiol. A.* 175**,** 1-14.
Kanzaki, R., and Shibuya, T. (1986). Descending protocerebral neurons related to the mating dance of the male silkworm moth. *Brain Research* 377**,** 378-382.
Kanzaki, R., Soo, K., Seki, Y., and Wada, S. (2003). Projections to Higher Olfactory Centers from Subdivisions of the Antennal Lobe Macroglomerular Complex of the Male Silkmoth. *Chem Senses* 28**,** 113-130.

Keene, A.C., and Waddell, S. (2007). *Drosophila* olfactory memory: single genes to complex neural circuits. *Nat. Rev. Neurosci.* 8**,** 341-354.
Kelber, C., Rössler, W., Roces, F., and Kleineidam, C.J. (2009). The Antennal Lobes of Fungus-Growing Ants (Attini): Neuroanatomical Traits and Evolutionary Trends. *Brain Behav. Evol.* 73**,** 273-284.
Kirschner, S., Kleineidam, C.J., Zube, C., Rybak, J., Grünewald, B., and Rössler, W. (2006). Dual olfactory pathway in the honeybee, *Apis mellifera*. *J. Comp. Neurol.* 499**,** 933-952.
Kloppenburg, P., Ferns, D., and Mercer, A.R. (1999). Serotonin enhances central olfactory neuron responses to female sex pheromone in the male sphinx moth *Manduca sexta*. *J. Neurosci.* 19**,** 8172-8181.
Krofczik, S., Menzel, R., and Nawrot, M.P. (2009). Rapid odor processing in the honeybee antennal lobe network. *Front. Comput. Neurosci*. 2:9. doi: 10.3389/neuro.10.009.2008.
Kurylas, A.E., Rohlfing, T., Krofczik, S., Jenett, A., and Homberg, U. (2008). Standardized atlas of the brain of the desert locust, *Schistocerca gregaria*. *Cell Tissue Res.* 333**,** 125-145.
Kvello, P., Jørgensen, K., and Mustaparta, H. (2010). Central Gustatory Neurons Integrate Taste Quality Information From Four Appendages in the Moth *Heliothis virescens*. *J. Neurophysiol.* 103**,** 2965-2981.
Laissue, P.P., Reiter, C., Hiesinger, P.R., Halter, S., Fischbach, K.F., and Stocker, R.F. (1999). Three-dimensional reconstruction of the antennal lobe in *Drosophila melanogaster*. *J. Comp. Neurol.* 405**,** 543-552.
Laurent, G., Wehr, M., and Davidowitz, H. (1996). Temporal Representations of Odors in an Olfactory Network. *J. Neurosci.* 16**,** 3837-3847.
Lei, H., Christensen, T.A., and Hildebrand, J.G. (2004). Spatial and Temporal Organization of Ensemble Representations for Different Odor Classes in the Moth Antennal Lobe. *J. Neurosci.* 24**,** 11108-11119.
Leon, M., and Johnson, B.A. (2003). Olfactory coding in the mammalian olfactory bulb. *Brain Research Rev.* 42**,** 23-32.
Li, Y., and Strausfeld, N.J. (1997). Morphology and sensory modality of mushroom body extrinsic neurons in the brain of the cockroach, *Periplaneta americana*. *J. Comp. Neurol.* 387**,** 631-650.
Lledo, P.M., Gheusi, G., and Vincent, J.D. (2005). Information Processing in the Mammalian Olfactory System. *Physiol. Rev.* 85**,** 281-317.
Macleod, K., and Laurent, G. (1996). Distinct mechanisms for synchronization and temporal patterning of odor-encoding neural assemblies. *Science* 274**,** 976-979.
Malnic, B., Hirono, J., Sato, T., and Buck, L.B. (1999). Combinatorial receptor codes for odors. *Cell* 96**,** 713-723.
Malun, D., Waldow, U., Kraus, D., and Boeckh, J. (1993). Connections between the deutocerebrum and the protocerebrum, and neuroanatomy of several classes of deutocerebral projection neurons in the brain of male *Periplaneta americana*. *J. Comp. Neurol.* 329**,** 143-162.
Marin, E.C., Jefferis, G.S.X.E., Komiyama, T., Zhu, H., and Luo, L. (2002). Representation of the Glomerular Olfactory Map in the *Drosophila* Brain. *Cell* 109**,** 243-255.
Masante-Roca, I., Gadenne, C., and Anton, S. (2005). Three-dimensional antennal lobe atlas of male and female moths, *Lobesia botrana* (Lepidoptera : Tortricidae) and glomerular representation of plant volatiles in females. *J. Exp. Biol.* 208**,** 1147-1159.
Matthews, M. (1991). Classification of the Heliothinae. *Natural Resources Institute Bulletin* 40**,** 1-198
Mauelshagen, J. (1993). Neural correlates of olfactory learning paradigms in an identified neuron in the honeybee brain. *J. Neurophysiol.* 69**,** 609-625.
Menzel, R., and Giurfa, M. (2001). Cognitive architecture of a mini-brain: the honeybee. *TRENDS Cogn. Sci.* 5**,** 62-71.
Menzel, R., and Muller, U. (1996). Learning and Memory in Honeybees: From Behavior to Neural Substrates. *Annu. Rev. Neurosci.* 19**,** 379-404.
Mombaerts, P. (2004). Odorant receptor gene choice in olfactory sensory neurons: the one receptor-one neuron hypothesis revisited. *Curr. Opin. Neurobiol.* 14**,** 31-36.
Mozuraitis, R., Stranden, M., Ramirez, M.I., Borg-Karlson, A.K., and Mustaparta, H. (2002). (-)-Germacrene D Increases Attraction and Oviposition by the Tobacco Budworm Moth *Heliothis virescens*. *Chem. Senses* 27**,** 505-509.

Müller, D.M., Abel, R.A., Brandt, R.B., Zöckler, M.Z., and Menzel, R.M. (2002). Differential parallel processing of olfactory information in the honeybee, *Apis mellifera* L. *J. Comp. Physiol. A.* 188**,** 359-370.

Nagayama, S., Enerva, A., Fletcher, M.L., Masurkar, A.V., Igarashi, K.M., Mori, K., and Chen, W.R. (2010). Differential Axonal Projection of Mitral and Tufted Cells in the Mouse Main Olfactory System. *Front Neural Circuits* 4:120. doi: 10.3389/fncir.2010.00120.

Namiki, S., and Kanzaki, R. (2011). Heterogeneity in dendritic morphology of moth antennal lobe projection neurons. *J. Comp. Neurol.* 519**,** 3367-3386.

Nara, K., Saraiva, L.R., Ye, X., and Buck, L.B. (2011). A Large-Scale Analysis of Odor Coding in the Olfactory Epithelium. *J. Neurosci.* 31**,** 9179-9191.

Ng, M., Roorda, R.D., Lima, S.Q., Zemelman, B.V., Morcillo, P., and Miesenböck, G. (2002). Transmission of Olfactory Information between Three Populations of Neurons in the Antennal Lobe of the Fly. *Neuron* 36**,** 463-474.

Okada, R., Rybak, J., Manz, G., and Menzel, R. (2007). Learning-Related Plasticity in PE1 and Other Mushroom Body-Extrinsic Neurons in the Honeybee Brain. *J. Neurosci.* 27**,** 11736-11747.

Olsen, S., Bhandawat, V., and Wilson, R. (2007). Excitatory Interactions between Olfactory Processing Channels in the *Drosophila* Antennal Lobe. *Neuron* 54**,** 89-103.

Perez-Orive, J., Bazhenov, M., and Laurent, G. (2004). Intrinsic and Circuit Properties Favor Coincidence Detection for Decoding Oscillatory Input. *J. Neurosci.* 24**,** 6037-6047.

Perez-Orive, J., Mazor, O., Turner, G.C., Cassenaer, S., Wilson, R.I., and Laurent, G. (2002). Oscillations and sparsening of odor representations in the mushroom body. *Science* 297**,** 359-365.

Rein, K., Zöckler, M., Mader, M.T., Gr Bel, C., and Heisenberg, M. (2002). The *Drosophila* standard brain. *Curr. Biol.* 12**,** 227-231.

Reisenman, C.E., Christensen, T.A., Francke, W., and Hildebrand, J.G. (2004). Enantioselectivity of projection neurons innervating identified olfactory glomeruli. *J. Neurosci.* 24**,** 2602-2611.

Reisenman, C.E., Christensen, T.A., and Hildebrand, J.G. (2005). Chemosensory Selectivity of Output Neurons Innervating an Identified, Sexually Isomorphic Olfactory Glomerulus. *J. Neurosci.* 25**,** 8017-8026.

Riffell, J.A., Lei, H., Christensen, T.A., and Hildebrand, J.G. (2009a). Characterization and Coding of Behaviorally Significant Odor Mixtures. *Curr. Biol.* 19**,** 335-340.

Riffell, J.A., Lei, H., and Hildebrand, J.G. (2009b). Neural correlates of behavior in the moth *Manduca sexta* in response to complex odors. *PNAS.* 106**,** 19219-19226.

Roche King, J., Christensen, T.A., and Hildebrand, J.G. (2000). Response characteristics of an identified, sexually dimorphic olfactory glomerulus. *J. Neurosci.* 20**,** 2391-2399.

Rohlfing, T., Brandt, R., Maurer, C.R., Jr., and Menzel, R. (2001). Bee Brains, B-splines and Computational Democracy: Generating an Average Shape Atlas. *Proceedings of IEEE Workshop on Mathematical Methods in Biomedical Image Analysis, MMBIA, Kauai, Hawaii***,** 187-194.

Rohlfing, T., Brandt, R., Menzel, R., and Maurer Jr, C.R. (2004). Evaluation of atlas selection strategies for atlas-based image segmentation with application to confocal microscopy images of bee brains. *Neuroimage* 21**,** 1428-1442.

Rospars, J.P. (1983). Invariance and sex-specific variations of the glomerular organization in the antennal lobes of a moth, *Mamestra brassicae* and a butterfly *Pieris brassicae J. Comp. Neurol.* 220**,** 80-96.

Rospars, J.P., and Chambille, I. (1981). Deutocerebrum of the cockroach *Blaberus craniifer burm*. Quantitative study and automated identification of the glomeruli. *J. Neurobiol.* 12**,** 221-247.

Rospars, J.P., and Hildebrand, J.G. (2000). Sexually Dimorphic and Isomorphic Glomeruli in the Antennal Lobes of the Sphinx Moth *Manduca sexta*. *Chem Senses* 25**,** 119-129.

Ruta, V., Datta, S.R., Vasconcelos, M.L., Freeland, J., Looger, L.L., and Axel, R. (2010). A dimorphic pheromone circuit in *Drosophila* from sensory input to descending output. *Nature* 468**,** 686-690.

Rybak, J., and Menzel, R. (1998). Integrative Properties of the Pe1 Neuron, a Unique Mushroom Body Output Neuron. *Learn & Mem* 5**,** 133-145.

Rø, H., Muller, D., and Mustaparta, H. (2007). Anatomical organization of antennal lobe projection neurons in the moth *Heliothis virescens*. *J. Comp. Neurol.* 500**,** 658-675.

Røstelien, T., Stranden, M., Borg-Karlson, A.K., and Mustaparta, H. (2005). Olfactory receptor neurones in two heliothine moth species responding selectively to aliphatic green leaf volatiles, aromatics, monoterpenes and sesquiterpenes of plant origin. *Chem. Senses* 30**,** 443-461.

Sachse, S., and Galizia, C.G. (2002). Role of inhibition for temporal and spatial odor representation in olfactory output neurons: A calcium imaging study. *J. Neurophysiol.* 87**,** 1106-1117.
Sachse, S., and Krieger, J. (2011). Olfaction in insects. *e-Neuroforum* 2**,** 49-60.
Sachse, S., Rappert, A., and Galizia, C.G. (1999). The spatial representation of chemical structures in the antennal lobe of honeybees: steps towards the olfactory code. *EJN.* 11**,** 3970-3982.
Sadek, M.M., Hansson, B.S., Rospars, J.P., and Anton, S. (2002). Glomerular representation of plant volatiles and sex pheromone components in the antennal lobe of the female *Spodoptera littoralis*. *J. Exp. Biology* 205**,** 1363-1376.
Schäfer, S., and Bicker, G. (1986). Distribution of GABA-like immunoreactivity in the brain of the honeybee. *J. Comp. Neurol.* 246**,** 287-300.
Shang, Y., Claridge-Chang, A., Sjulson, L., Pypaert, M., and Miesenböck, G. (2007). Excitatory Local Circuits and Their Implications for Olfactory Processing in the Fly Antennal Lobe. *Cell* 128**,** 601-612.
Shepherd, G.M. (2006). Smell images and the flavour system in the human brain. *Nature* 444**,** 316-321.
Shields, V.D.C., and Hildebrand, J.G. (2001). Responses of a population of antennal olfactory receptor cells in the female moth *Manduca sexta* to plant-associated volatile organic compounds. *J. Comp. Physiol. A.* 186**,** 1135-1151.
Silbering, A.F., and Galizia, C.G. (2007). Processing of Odor Mixtures in the *Drosophila* Antennal Lobe Reveals both Global Inhibition and Glomerulus-Specific Interactions. *J. Neurosci.* 27**,** 11966-11977.
Silbering, A.F., Okada, R., Ito, K., and Galizia, C.G. (2008). Olfactory Information Processing in the *Drosophila* Antennal Lobe: Anything Goes? *J. Neurosci.* 28**,** 13075-13087.
Skiri, H.T., Galizia, C.G., and Mustaparta, H. (2004). Representation of primary plant odorants in the antennal lobe of the moth *Heliothis virescens*, using calcium imaging. *Chem. Senses* 29**,** 253 -267.
Skiri, H.T., Rø, H., Berg, B.G., and Mustaparta, H. (2005). Consistent organization of glomeruli in the antennal lobes of related species of heliothine moths. *J. Comp. Neurol*. 491**,** 367-380.
Smid, H.M., Bleeker, M.A., Van Loon, J.J.A., and Vet, L.E. (2003). Three-dimensional organization of the glomeruli in the antennal lobe of the parasitoid wasps *Cotesia glomerata* and *C. rubecula. Cell Tissue Res.* 312**,** 237-248.
Spors, H., and Grinvald, A. (2002). Spatio-Temporal Dynamics of Odor Representations in the Mammalian Olfactory Bulb. *Neuron* 34**,** 301-315.
Staudacher, E.M., Huetteroth, W., Schachtner, J., and Daly, K.C. (2009). A 4-dimensional representation of antennal lobe output based on an ensemble of characterized projection neurons. *J. Neurosci. Methods* 180**,** 208-223.
Stocker, R.F., Lienhard, M.C., Borst, A., and Fischbach, K.F. (1990). Neuronal architecture of the antennal lobe in *Drosophila melanogaster*. *Cell Tissue Res.* 262**,** 9-34.
Stopfer, M., Jayaraman, V., and Laurent, G. (2003). Intensity versus identitiy coding in an olfactory system. *Neuron* 39**,** 991-1004.
Stranden, M., Borg-Karlson, A.K., and Mustaparta, H. (2002). Receptor neuron discrimination of the germacrene D enantiomers in the moth *Helicoverpa armigera*. *Chem. Senses* 27**,** 143-152.
Stranden, M., Liblikas, I., König, W.A., Almaas, T.J., Borg-Karlson, A.K., and Mustaparta, H. (2003a). (-)-Germacrene D receptor neurones in three species of heliothine moths: structure-activity relationships. *J. Comp. Physiol. A.* 189, 563-577.
Stranden, M., Røstelien, T., Liblikas, I., Almaas, T.J., Borg-Karlson, A.K., and Mustaparta, H. (2003b). Receptor neurones in three heliothine moths responding to floral and inducible plant volatiles. *Chemoecology* 13**,** 143-154.
Strausfeld, N.J. (1976). *Atlas of an Insect Brain.* New York: Springer-Verlag.
Strausfeld, N.J. (2002). Organization of the honey bee mushroom body: Representation of the calyx within the vertical and gamma lobes. *J. Comp. Neurol.* 450**,** 4-33.
Strausfeld, N.J., Bassemir, U., Singh, R.N., and Bacon, J.P. (1984). Organizational principles of outputs from dipteran brains. J. Insect. Physiol. 30:1, 73-93.
Strausfeld, N.J., Sinakevitch, I., Brown, S.M., and Farris, S.M. (2009). Ground plan of the insect mushroom body: Functional and evolutionary implications. *J. Comp. Neurol.* 513**,** 265-291.
Sun, X.J., Fonta, C., and Masson, C. (1993a). Odour quality processing by bee antennal lobe interneurones. *Chem. Senses* 18**,** 355-377.

Sun, X.J., Tolbert, L.P., and Hildebrand, J.G. (1993b). Ramification pattern and ultrastructrural characteristics of the serotonin-immunoreactive neuron in the antennal lobe of the moth *Manduca sexta*: A laser scanning confocal and electron microscopic study. *J. Comp. Neurol.* 338**,** 5-16.
Sun, X.J., Tolbert, L.P., and Hildebrand, J.G. (1997). Synaptic organization of the uniglomerular projection neurons of the antennal lobe of the moth *Manduca sexta*: a laser scanning confocal and electron microscopic study. *J. Comp. Neurol.* 379**,** 2-20.
Szyszka, P., Ditzen, M., Galkin, A., Galizia, C.G., and Menzel, R. (2005). Sparsening and temporal sharpening of olfactory representations in the honeybee mushroom bodies. *J. Neurophysiol.* 94**,** 3303-3313.
Szyszka, P., Galkin, A., and Menzel, R. (2008). Associative and non-associative plasticity in Kenyon cells of the honeybee mushroom body. *Front. Syst. Neurosci.* 2:3. doi: 10.3389/neuro.06.003.2008.
Tanaka, N.K., Awasaki, T., Shimada, T., and Ito, K. (2004). Integration of chemosensory pathways in the *Drosophila* second-order olfactory centers. *Curr. Biol.* 14**,** 449-457.
Tanaka, N.K., Tanimoto, H., and Ito, K. (2008). Neuronal assemblies of the *Drosophila* mushroom body. *J. Comp. Neurol.* 508**,** 711-755.
Varela, N., Couton, L., Gemeno, C., Avilla, J., Rospars, J.-P., and Anton, S. (2009). Three-dimensional antennal lobe atlas of the oriental fruit moth, *Cydia molesta* (Busck) (Lepidoptera: Tortricidae): comparison of male and female glomerular organization. *Cell and Tissue Res.* 337**,** 513-526.
Vickers, N., Christensen, T., and Hildebrand, J. (1998). Combinatorial odor discrimination in the brain: Attractive and antagonist odor blends are represented in distinct combinations of uniquely identifiable glomeruli. *J. Comp. Neurol.* 400**,** 35-56.
Vickers, N.J., and Christensen, T.A. (2003). Functional divergence of spatially conserved olfactory glomeruli in two related moth species. *Chem. Senses* 28**,** 325-338.
Vosshall, L.B., and Stocker, R.F. (2007). Molecular Architecture of Smell and Taste in *Drosophila*. *Annu. Rev. Neurosci.* 30**,** 505-533.
Wong, A.M., Wang, J.W., and Axel, R. (2002). Spatial representation of the glomerular map in the *Drosophila* protocerebrum. *Cell* 109**,** 229-241.
Yamagata, N., Schmuker, M., Szyszka, P., Mizunami, M., and Menzel, R. (2009). Differential odor processing in two olfactory pathways in the honeybee. *Front. Syst. Neurosci.* 3:16.doi: 10.3389/neuro.06.016.2009.
Zhao, X.C., and Berg, B.G. (2009). Morphological and Physiological Characteristics of the Serotonin-Immunoreactive Neuron in the Antennal Lobe of the Male Oriental Tobacco Budworm, *Helicoverpa assulta*. *Chem. Senses* 34**,** 363-372.
Zube, C., and Rössler, W. (2008). Caste- and sex-specific adaptations within the olfactory pathway in the brain of the ant *Camponotus floridanus*. *Arthropod Struct Dev.* 37**,** 469-479.

Individual papers

Paper I

frontiers in
SYSTEMS NEUROSCIENCE

ORIGINAL RESEARCH ARTICLE
published: 26 October 2009
doi: 10.3389/neuro.06.014.2009

Digital, three-dimensional average shaped atlas of the *Heliothis virescens* brain with integrated gustatory and olfactory neurons

Pål Kvello[1], Bjarte Bye Løfaldli[1], Jürgen Rybak[2], Randolf Menzel[2] and Hanna Mustaparta[1]*

[1] *Department of Biology, Norwegian University of Science and Technology, Trondheim, Norway*
[2] *Institut für Biologie-Neurobiologie, Freie Universität Berlin, Berlin, Germany*

Edited by:
Raphael Pinaud,
Rochester University, USA

Reviewed by:
Sylvia Anton,
Institut National de la Recherche Agronomique, France
Kevin Daly,
West Virginia University, USA
C. G. Galizia,
Universität Konstanz, Germany

***Correspondence:**
Hanna Mustaparta,
Department of Biology, Norwegian University of Science and Technology, Neuroscience Unit, MTFS, Olav Kyrres gt. 9, 7489 Trondheim, Norway.
e-mail: hanna.mustaparta@bio.ntnu.no

We use the moth *Heliothis virescens* as model organism for studying the neural network involved in chemosensory coding and learning. The constituent neurons are characterised by intracellular recordings combined with staining, resulting in a single neuron identified in each brain preparation. In order to spatially relate the neurons of different preparations a common brain framework was required. We here present an average shaped atlas of the moth brain. It is based on 11 female brain preparations, each stained with a fluorescent synaptic marker and scanned in confocal laser-scanning microscope. Brain neuropils of each preparation were manually reconstructed in the computer software Amira, followed by generating the atlas using the Iterative Shape Average Procedure. To demonstrate the application of the atlas we have registered two olfactory and two gustatory interneurons, as well as the axonal projections of gustatory receptor neurons into the atlas, visualising their spatial relationships. The olfactory interneurons, showing the typical morphology of inner-tract antennal lobe projection neurons, projected in the calyces of the mushroom body and laterally in the protocerebral lobe. The two gustatory interneurons, responding to sucrose and quinine respectively, projected in different areas of the brain. The wide projections of the quinine responding neuron included a lateral area adjacent to the projections of the olfactory interneurons. The sucrose responding neuron was confined to the suboesophageal ganglion with dendritic arborisations overlapping the axonal projections of the gustatory receptor neurons on the proboscis. By serving as a tool for the integration of neurons, the atlas offers visual access to the spatial relationship between the neurons in three dimensions, and thus facilitates the study of neuronal networks in the *Heliothis virescens* brain. The moth standard brain is accessible at http://www.ntnu.no/biolog/english/neuroscience/brain

Keywords: insect, taste, olfaction, neuron, three-dimensional reconstruction

INTRODUCTION

Challenged by the need to integrate the rapidly growing data in neuroscience, digital brain atlases have become an important tool serving as a database for neural structures with their three dimensional spatial information. The intention is to provide common frameworks into which data from different brain preparations can be registered and spatially related. As the scientific record includes data from many animal species, digital brain atlases of several vertebrates and invertebrates have been made (Toga and Thompson, 2001; Rein et al., 2002; Toga, 2002; Van Essen, 2002; Brandt et al., 2005; Kurylas et al., 2008; Jundi et al., 2009). In insects, three dimensional digital brain atlases have been generated for four species; the population-based quantitative atlas of the fruit fly *Drosophila melanogaster* (Rein et al., 2002), the average shaped standard atlas of the honeybee *Apis mellifera* (Brandt et al., 2005) and the locust *Schistocerca gregaria* (Kurylas et al., 2008), and the recently made standard brain atlas of the hawkmoth *Manduca sexta* (Jundi et al., 2009). In creating the locust brain atlas two procedures were used for comparison, the Virtual Insect Brain (VIB) procedure initially developed for standardisation of the fruit fly neuroanatomy (Jenett et al., 2006) and the Iterative Shape Averaging (ISA) procedure developed to generate the honeybee standard brain (Rohlfing et al., 2001; Brandt et al., 2005). This study concluded that the VIB procedure using a global and a local rigid transformation followed by a local nonrigid transformation preserves anatomical variability, whereas the ISA procedure using an affine transformation followed by iterative nonrigid registrations reduces the variability.

The digital brain atlases of these four insects are based on common neuropil substrates like the protocerebrum including the optic lobes, the central body and the mushroom bodies, the deutocerebrum with the antennal lobes, and the tritocerebrum. Additional structures included in two or three of the atlases are the protocerebral bridge, anterior optic tubercles, lateral horns and the suboesophageal ganglion, the latter fused with the brain in the fly, the honeybee and the moth. These structures are involved in visual, olfactory and gustatory information processing as well as associative learning and memory formation. They are linked by neurons mediating information from one structure to the next where the information is further processed, thus forming networks within and between the different brain structures. In order to

understand how the neuronal networks operate, it is critical to clarify the connectivity between physiologically and morphologically characterised neurons in the circuits. Revealing such details is a very elaborate process requiring a preparation accessible for *in vivo* recordings of identifiable neurons. Particularly suited for these examinations are the insects. Their nervous system is easily accessible for intracellular electrophysiological recordings. Combined with staining the entire morphology of the neurons can be precisely determined and three dimensionally visualised in the individual brain. In addition the brain is small enough to be studied as a whole, avoiding the problem of cutting neurons projecting out of a section. The number of identified neurons is large and growing, like neurons of the visual system in the fly *Calliphora vicina* and the locust *Schistocerca gragaria* (Borst and Haag, 2002; Heinze and Homberg, 2007), the olfactory system in a number of species (Kanzaki et al., 1989; Heinbockel et al., 1999; Lei et al., 2001; Müller et al., 2002; Reisenman et al., 2005; Rø et al., 2007; Yamagata et al., 2007) auditory system of the crickets (Poulet and Hedwig, 2006) the mushroom bodies in the honeybee (Mauelshagen, 1993; Rybak and Menzel, 1998) as well as neuromodulatory neurons and descending neurons (Kanzaki et al., 1991; Hammer, 1993; Bräunig and Pflüger, 2001). Consequently the need for a standardized brain model as a tool for organizing and analyzing data has been substantial in many species. In addition to the three dimentional digital standard atlases providing common frames for integrating neurons in the entire brain, separate atlases of the antennal lobes have been made in a number of species, including heliothine moths (Rospars and Chambille, 1981; Flanagan and Mercer, 1989; Stocker et al., 1990; Galizia et al., 1999; Laissue et al., 1999; Rospars and Hildebrand, 2000; Chiang et al., 2001; Berg et al., 2002; Sadek et al., 2002; Reischig and Stengl, 2002; Smid et al., 2003; Greiner et al., 2004; Huetteroth and Schachtner, 2005; Masante-Roca et al., 2005; Skiri et al., 2005a; Iyengar et al., 2006; Jefferis et al., 2007). These atlases are valuable tools for studying the neuronal network involved in processing olfactory information (Namiki and Kanzaki, 2008; Staudacher et al., 2009).

The moth, *Heliothis virescens*, is a major pest insect in agriculture and an object for extensive research in many areas, including chemosensory coding, learning and memory (Hartlieb, 1996; Mustaparta, 2002; Skiri et al., 2005b; Jørgensen et al., 2006, 2007a,b; Kvello et al., 2006). The generation of a standard brain atlas of *H. virescens* is particularly motivated by the already large amount of data on the olfactory and the gustatory system. Tuning of olfactory receptor neurons according to biologically relevant odorants, pheromones as well as plant odorants have been described (Berg et al., 1998; Mustaparta and Stranden, 2005; Røstelien et al., 2005). Projections of the primary axons in particular glomeruli of the antennal lobe are shown for the pheromone system by functional tracing (Berg et al., 1998). Antennal lobe projection neurons have been anatomically described according to glomerular innervation and axonal tracts (Rø et al., 2007), studies that are being followed up in ongoing investigations focusing on the physiology of morphologically characterised neurons.

Whereas the central olfactory pathways have been described in this as well as in many insect species, only scarce knowledge exists about the central gustatory pathways in two insect species, the fly *Sarcophaga bullata* (Mitchell and Itagaki, 1992) and in the locust *Locusta migratoria* (Rogers and Newland, 2003). *H. virescens* is emerging as one of few model insects in elucidating the gustatory pathways. The axonal projections of the gustatory receptor neurons have been traced to defined areas of the suboesophageal ganglion and tritocerebrum (Jørgensen et al., 2006; Kvello et al., 2006), and intracellular recordings combined with staining of individual gustatory neurons in the CNS have been made from a large number of neurons (unpublished). Particularly interesting is the connection between the gustatory and the olfactory systems which forms the neuronal basis for associative learning of odorants and tastants. In order to integrate the existing and future data, as well as to spatially relate neurons of any brain compartment, a common framework of the entire *H. virescens* brain is needed. Using standard brain atlases to integrate identified neurons of different preparations offers easy visual access to the relative position of the neurons in three dimensions and thus promotes an understanding of their functional relationship. Therefore, in the search for neuronal networks in any animal species, a standard brain atlas is a valuable tool.

In this paper we present a digital standard brain atlas of the moth *Heliothis virescens*. Since the purpose is to relate spatial information between different preparations it is important to minimize individual variability. We therefore chose to generate the standard brain using the ISA procedure. To demonstrate its application we have registered two olfactory and two gustatory interneurons, as well as the axonal projections of the gustatory receptor neurons on the antennae and proboscis into the model using the procedure described by Brandt et al. (2005). The presented average standard brain atlas of this moth will be used as a tool for investigating and visualising the neural networks underlying gustatory and olfactory coding as well as appetitive and aversive learning and memory formation. The moth standard brain is accessible at http://www.ntnu.no/biolog/english/neuroscience/brain

MATERIALS AND METHODS

INSECTS

The moths, *Heliothis virescens* (Heliothinae; Lepidoptera; Noctuidae) were imported as pupae from a laboratory culture at Novartis Crop Protection, Basel, Switzerland. Before emerging the pupae were separated according to sex and placed in a glass container (height: 18 cm, width: 12 cm, depth: 17 cm) covered by a perforated plexiglass. The container with pupae was kept in a Refritherm 6 E incubator (Struers) at a reversed photoperiod (14-h light and 10-h dark) and at a temperature of 22–23°C. When emerged, the adults were placed into a plexiglass cylinder (height: 20 cm, diameter: 10 cm) covered by a perforated lid. The moths were fed *ad. lib.* on a 0.15 M sucrose solution. Experiments were performed on adult female moths 3- to 5-days after emerging.

THE STANDARD BRAIN

Preparations

Female moths were mounted in plastic tubes with the head immobilized by dental wax (Kerr Corporation, Romulus, MI, USA). After removing cephalic scales and mouthparts, the moths were decapitated. The brains were dissected in Ringer solution and fixed in 4% paraformaldehyde in a phosphate-buffered saline (PBS: 684 mM NaCl, 13 mM KCl, 50.7 mM Na2HPO4 and 5 mM

KH2PO4, pH 7.2) over night at 4°C. After a 10-min rinse in PBS, preparations were dehydrated in an increasing ethanol series (50%, 70%, 90%, 96%, 100%, 10 min each), degreased in xylol for 5 min, and rehydrated in a decreasing ethanol series (100%, 96%, 90%, 70%, 50%, 10 min each). The brains were then washed for 10 min in PBS, and incubated for 30 min in 1 mg/ml collagenase solution (Collagenase Type I, Invitrogen Norge AS) at 36°C. Subsequently the brains were preincubated in 10% normal goat serum (NGS; Sigma, St. Louis, MO, USA) in a PBS solution containing 0.1% Triton X (PBSX) for 30 min at room temperature. The brains were further incubated with a monoclonal antibody against the synaptic protein synapsin (SYNORF 1, kindly provided by Dr. E. Buchner, Würzburg, Germany), diluted 1:10 in PBSX and 10% NGS for 48 h at 4°C. After the preparations had been rinsed five times each for 20 min in PBS, they were incubated for 24 h with a Cy5-conjungated goat anti-mouse secondary antibody (Jackson Immunoresearch; dilution 1:500 in PBSX) at 4°C. The incubation was followed by rinsing in PBS, five times for 20 min, before the brains were dehydrated in increasing ethanol series. Finally the brains were cleared in methyl salicylate and mounted as whole mounts in double-sided aluminium slides.

Visualization of brain preparations

The stained whole-mount brain preparations were visualized with a laser-scanning confocal microscope (LSM 510 META Zeiss, Jena, Germany) using a C-Apochromat 10×/0.45NA water objective. The fluorescent dye (Cy5) was exited by a 633 nm line of argon laser. Due to the large size of the brain, each preparation was scanned in two partially overlapping tiles with a resolution of 1024 × 1024 pixels in the xy-plane and an interslice distance of 3 μm (voxel size of 0.75 μm × 0.75 μm × 3 μm). The resulting two stacks of optical sections per brain were resampled in order to make the size of the files manageable for the computer, then merged and filtered by the computer software Amira 4.1 (Mercury Computer Systems, San Diego, CA, USA). To compensate for the refraction indexes of the mountant and that of the water objective, the *z*-axis dimension was multiplied by a factor of 1.3. The final voxel size of each stack consequently increased to 1.1 μm × 1.1 μm × 3.9 μm.

Reconstruction of brain structures

The gray value image stacks acquired from the confocal microscope were elaborately examined section by section and brain structures of interest were manually labelled using the segmentation editor in Amira (**Table 1**). In this process any group of voxels belonging to a particular brain structure was given a unique label resulting in a stack of label images corresponding to the underlying confocal images. As a prerequisite to the subsequent registration and averaging process corresponding structures of the different brain preparations were given the same label. These label images were subsequently used to perform conventional volumetric analyzes, to reconstruct polygonal surface models and to generate the average standard brain atlas. The volume of each labelled structure was calculated by the "TissueStatistics" tool in Amira 4.1. Other conventional volumetric analyses, like mean volume, relative volume, standard deviations and relative standard deviation, were performed using Microsoft office Excel (2003).

Averaging brain structures

Creating the average standard brain followed the ISA method according to the description for the honeybee *Apis mellifera* and the locust *Schistocerca gregaria* (Rohlfing et al., 2001; Brandt et al., 2005; Kurylas et al., 2008). One brain was first selected as a template. Then the label images of the other brain preparations were affine registered to the label images of the template brain followed by making an average. Then the affine registered brain preparations and the template were elastically registered to the average followed by the generation of a second average. This was repeated by a second elastic registration of the previous elastic registered preparations to the

Table 1 | Volumetric analysis of the 16 reconstructed brain structures included in the standard brain atlas. Calculations for the medulla, lobula and lobula plate are based on 10 brains, whereas the remaining structures are based on 11. Mean volume (Mean V), relative volume (Rel. V), standard deviation (SD) and relative standard deviation (Rel. SD).

Structure	Mean V (μm³)	Rel. V (%)	SD (μm³)	Rel. SD (%)
Right antennal lobe	4.34×10^6	2.95	4.95×10^5	11.37
Left antennal lobe	4.31×10^6	2.92	5.15×10^5	11.96
Central body	1.69×10^6	1.14	3.05×10^5	18.07
Right calyx	2.38×10^6	1.61	3.15×10^5	13.22
Left calyx	2.38×10^6	1.61	3.24×10^5	13.61
Right peduncle and lobe	1.41×10^6	0.96	4.34×10^5	30.76
Left peduncle and lobe	1.34×10^6	0.91	3.89×10^5	28.93
Right anterior optic tubercle	4.98×10^5	0.34	1.26×10^5	25.37
Left anterior optic tubercle	5.00×10^5	0.34	1.24×10^5	24.77
Midbrain region	9.31×10^7	63.12	1.52×10^7	16.32
Right medulla	1.30×10^7	8.79	1.07×10^6	8.24
Left medulla	1.27×10^7	8.63	1.05×10^6	8.26
Right lobula	3.61×10^6	2.44	2.52×10^5	6.98
Left lobula	3.40×10^6	2.30	3.34×10^5	9.82
Right lobula plate	1.47×10^6	1.00	2.83×10^5	19.23
Left lobula plate	1.38×10^6	0.94	3.22×10^5	23.33

second average brain. Thus, the affine registration compensating for position, rotation and global size differences was performed only once whereas the elastic registration compensating for local differences in shape was performed twice. To verify the average shape property of the ISA-generated standard brain atlas, three dimentional polygonal surface models of the standard brain and each individual brain were made. They were subsequently aligned with respect to position, orientation and size before the shape differences between them were calculated. The calculations were performed using the surface distance tool in Amira 4.1 which measured the average distance between corresponding points on the surface of the different brain preparations.

INTERNEURONS

Preparation

The insects were mounted in a plastic tube with the head exposed. Wax was used to immobilize the head and the mouthparts. For recording from the olfactory neurons, the antennae were fastened to the wax with tungsten cramps. The cuticle between the eyes was removed, exposing the antennal lobes and the protocerebrum. Large trachea, intracranial- and antennal muscles were removed to eliminate brain movements. When recording from gustatory interneurons the antenna and the uncoiled proboscis were fastened to the wax with tungsten cramps. The labium was cut off and the underlying trachea removed. Subsequently the left eye was cut off and the preparation tilted in order to expose the left side of the SOG and tritocerebrum. To facilitate insertion of the microelectrode the neurolemma was removed with a tungsten hook and the preparation was superfused with ringer solution.

Stimulation, recordings and staining

The taste stimuli used in the experiments were sucrose (1 M, Sigma-Aldrich), quinine hydrochloride (0.1 M, VWR), distilled water, and tactile touch, previously found to elicit responses in separate receptor neurons (Jørgensen et al., 2007a). The stimuli were applied to the sensilla as droplets on a glass rod. The olfactory stimuli were applied as air puffs (0.8 ml/500 ms) through glass cartridges, each containing the odorants applied to a filter paper. The two neurons included were tested for 100 µg of each of 12 primary plant odorants (Hexanol, (3Z)-Hexen-1-ol, (3Z)-Hexenyl acetate, Ocimene, racemic- Linalool, Geraniol, (+)-3-Carene, trans-Verbenol, Methyl benzoate, 2-Phenylethanol, (-)-Germacrene D, Farnesene) (Røstelien et al., 2005). Neuronal activity in the antennal lobe and the SOG was recorded intracellularly with a glass microelectrode containing 0.2 M K^+-acetate solution with 4% dye (Micro-Ruby or Micro-Emerald, Invitrogen). After stimulation with tastants and odorants the neurons were stained by passing a 1–3 nA depolarizing current of 2 Hz with 0.2 s duration. Complete labelling of the neurons required dye injection for 5–10 min. After current injection, the dye was allowed to diffuse over night at 4°C. The brains were dissected in Ringer solution. The "olfactory" preparation was fixed in 4% paraformaldehyde in PBS similar to the standard brain preparations. The two "gustatory" preparations were also fixed in a solution of 4% paraformaldehyde in PBS, but additionally added 0.5% glutaraldehyde as an alternative and less time consuming way of visualizing neuropile structures. All three preparations were left over night at 4°C. To amplify the staining of the labelled neurons the brains were incubated in Streptavidin-Cy3 (Micro-Ruby stained preparations) and Streptavidin-Cy2 (Micro-Emerald stained preparations) (Jackson immunoresearch, West Grove, PA, USA; diluted 1:200 in PBS) over night at 4°C. After 10 min rinse in PBS the "olfactory" preparation went through the same protocol as the preparations used for the standard brain, starting with preincubation in 10% normal goat serum (NGS; Sigma, St. Louis, MO, USA) in a PBS solution containing 0.1% Triton X (PBSX) for 30 min at room temperature. Finally, all preparations were dehydrated in increasing ethanol series and cleared in methyl salicylate.

Visualization

The brains were mounted as whole mounts on double-sided aluminium slides and the stained neurons were examined with a confocal laser-scanning microscope (LSM 510 META, Zeiss, Jena, Germany) using a C-Apochromat 10×/0.45NA water objective, a C-Achroplan 40×/0.8NA water objective and a Plan-Neofluar 20×/0.5 dry lens objective. The two fluorescent dyes were exited by different lasers. Micro-emerald was excited by a Titanium Sapphire laser of 780 nm and a 488 nm argon laser, both filtered through a bandpass filter BP 500–550 IR. Micro-ruby was excited by a 543 nm Helium Neon laser and filtered through a bandpass filter BP 565–615 IR. The Titanium Sapphire laser was used for two-photon microscopy increasing the resolution in the *z*-axis which enabled us to better distinguish among overlapping neurites. The brains were scanned frontally with an interslice distance of 0.5–3 µm and an optical resolution in the *y*- and *x*-axis of 1024 × 1024 pixels. The neurons were scanned in several tiles and the tiles were manually merged in Amira. To compensate for the refraction indexes of the mountant and that of the water and dry lens objective, the *z*-axis dimension was multiplied by a factor of 1.3 and 1.6, respectively.

Reconstruction and registration of neurons into the average standard brain atlas

The gray value image stacks acquired from the confocal microscope were examined section by section and the neurons were semi-automatically reconstructed using the skeleton tool (Evers et al., 2004; Schmitt et al., 2004), which was implemented as a custom module in Amira 3.1. Registration of the neurons into the standard brain atlas followed the same procedure as described by Brandt et al. (2005). Selected brain structures in the "neuron-preparations" were reconstructed as label images. The selection only included brain structures corresponding to the structures in the standard brain atlas. Then, the label images in the "neuron-preparations" were affine- and elastically registered to the label images of the standard brain. The resulting transformation parameters for the brain structures were subsequently applied to the reconstructed neurons. The same procedure was followed for integrating the previously described gustatory receptor neurons (Jørgensen et al., 2006; Kvello et al., 2006).

RESULTS

RECONSTRUCTION

For creating the standard brain of the moth *Heliothis virescens* we selected the 11 best out of 72 female brain preparations. The selection was mainly based on the staining quality and the preservation

of brain structures. Brain neuropils with high synaptic density were clearly stained with the antibody SYNORF 1 against synapsin, as visualized in the confocal microscope images (**Figure 1**).

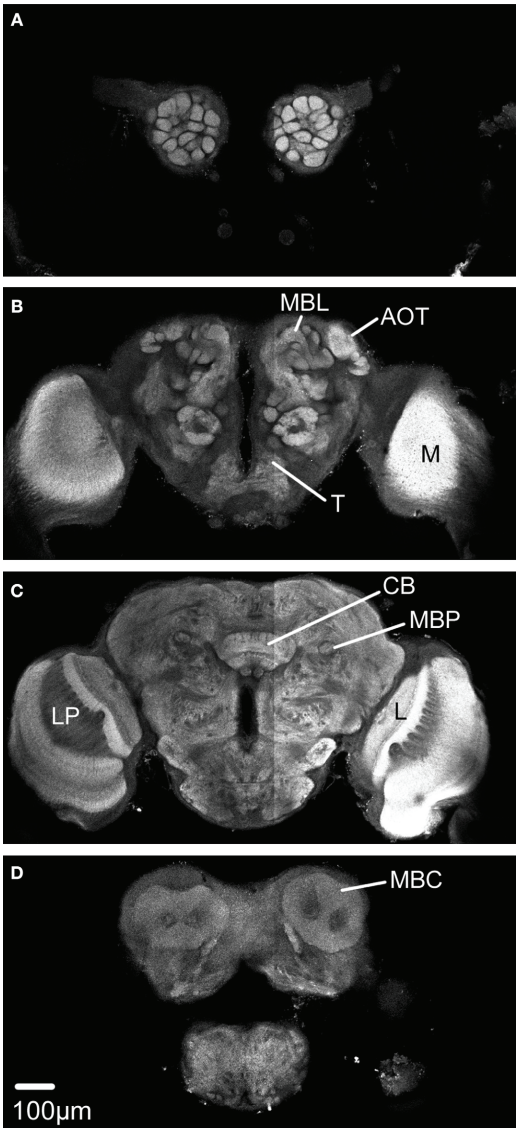

FIGURE 1 | Confocal images of the *Heliothis virescens* brain immunostained with the synaptic marker SYNORF 1. Sections from anterior to posterior at depths 30 µm, 100 µm, 162 µm and 246 µm. **(A)** Right and left antennal lobes with olfactory glomeruli. **(B–D)** Anterior optic tubercle (AOT), mushroom body lobes (MBL), tritocerebrum (T), central body (CB), medulla (M), lobula (L), Lobula plate (LP), mushroom body peduncle (MBP) and mushroom body calyces (MBC). Light intensity difference is due to merging of two image stacks with different light intensities.

Based on distinguishable structures, each of the 11 brain preparations was divided into 16 anatomical regions that were separately labelled (**Table 1**).

In one of the 11 preparations the optic lobes were excluded because of mechanical damage. However, the medial part of this brain was included because of its high staining quality. Because some neuropil structures could not be clearly distinguished in these whole mount preparations, they were included in a larger region. Thus, the region termed "Midbrain region" includes the protocerebral lobes with the lateral horns, the lateral accessory lobes, the protocerebral bridge and a small, previously not described structure located posterior to the antennal lobe glomeruli and merging into the protocerebrum. The midbrain region also includes the antennal mechanosensory and motor centre of the deutocerebrum, the tritocerebrum and the suboesophageal ganglion (SOG) (**Figures 2A,B**).

The calyces of the mushroom bodies could be clearly distinguished from the surrounding protocerebrum and labelled as one distinct structure (**Figures 2C,D**). The pedunculus and the lobe system of the mushroom bodies were difficult to completely separate and were therefore included as a single labelled region (**Figures 2E,F**). The central body and the anterior optic tubercles could be distinguished and were assigned to separate labels (**Figures 2G–J**). Among the lateral protocerebral structures comprising the optic lobes we included the medulla, the lobula and the lobula plate as separate labels (**Figures 2K,L**). Among the deutocerebral structures we have collectively assigned the antennal lobe glomeruli as one labelled region (**Figures 2M,N**). As a prerequisite to the subsequent registration process corresponding structures of the different preparations were given the same label. From the constructed label files a complete three dimensional surface reconstruction of one brain was made, shown in **Figure 3**.

Conventional volumetric analyzes including means and standard deviations of the absolute and relative volumes were performed on the label images of each anatomical region in all 11 brain preparations (**Table 1**).

AVERAGING

After constructing the label images of all 11 brain preparations one brain was selected as a template into which the other were registered and subsequently averaged. The selection of the template brain was based on staining quality and shape. Before starting the ISA procedure the label images were divided into three major compartments, the right optic lobe, the left optic lobe and the remaining medial brain structures. The registration and averaging procedures were subsequently performed separately on each compartment. The procedures were repeated according to the ISA method. The three average label image stacks resulting from the second elastic registration were selected as the standard brain. A three dimentional polygonal surface model of each major compartment was created (**Figure 4**).

To verify the average shape property of the standard brain which we defined as the brain shape being most similar to the 11 individual brains, we calculated the shape difference between them. The calculations were performed using the surface distance tool in Amira 4.1 which measured the mean distance between corresponding points on the surface of the different brain preparations.

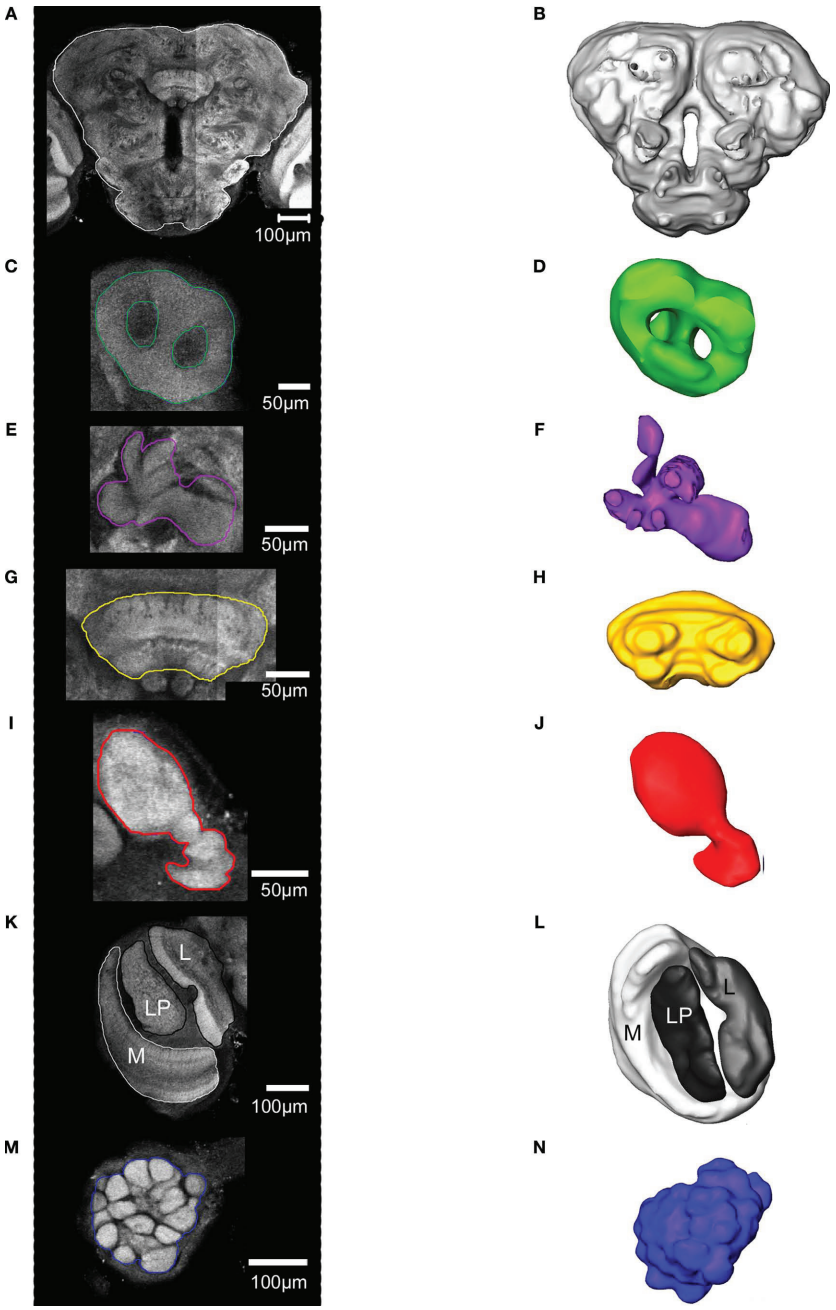

FIGURE 2 | The structures included in the *Heliothis virescens* standard brain atlas visualized by confocal images including their labelled outline (left) and surface reconstructions (right). The images are from a single brain preparation. **(A,B)** Midbrain region. **(C,D)** Mushroom body calyx. **(E,F)** Mushroom body peduncle and lobes. **(G,H)** Central body. **(I,J)** Anterior optic tubercle. **(K,L)** Optic lobe neuropils including the medulla (M), lobula plate (LP) and lobula (L). **(M,N)** Antennal lobe glomeruli. Light intensity difference is due to merging of two image stacks with different light intensities.

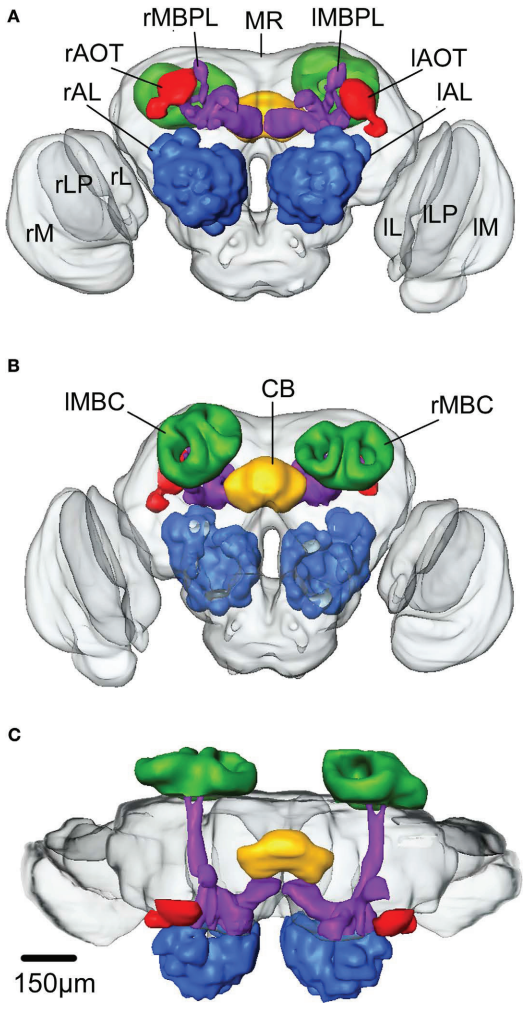

FIGURE 3 | Surface reconstruction of an individual brain of *Heliothis virescens*. (A) Anterior view. **(B)** Posterior view. **(C)** Dorsal view. Midbrain region (MR), right mushroom body calyces (rMBC), right mushroom body peduncle and lobes (rMBPL), central body (CB), right anterior optic tubercle (rAOT), right antennal lobe (rAL), right medulla (rM), right lobula plate (rLP), right lobula (rL), left mushroom body calyces (lMBC), left mushroom body peduncle and lobes (lMBPL), left anterior optic tubercle (lAOT), left antennal lobe (lAL), left medulla (lM), left lobula plate (lLP), left lobula (lL).

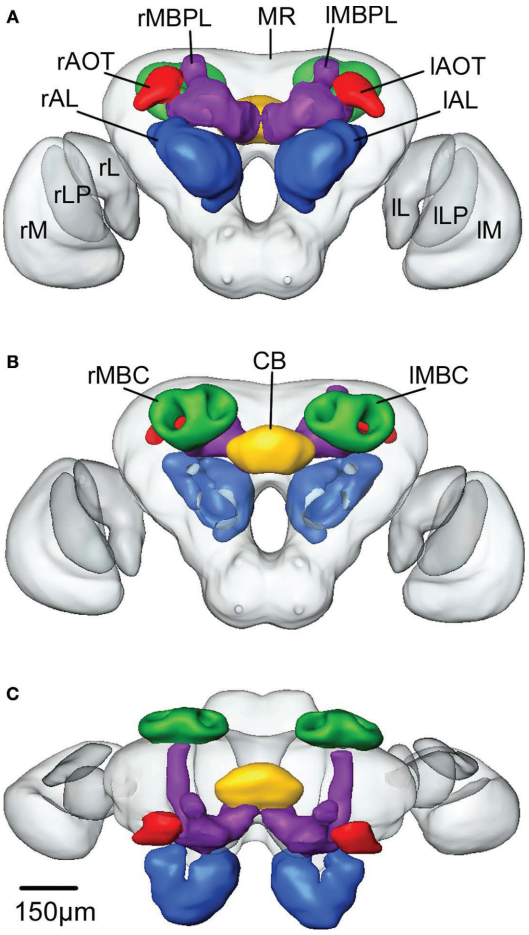

FIGURE 4 | The average standard brain of *Heliothis virescens*. (A) Anterior view. **(B)** Posterior view. **(C)** Dorsal view. Midbrain region (MR), right mushroom body calyces (rMBC), right mushroom body peduncle and lobes (rMBPL), central body (CB), right anterior optic tubercle (rAOT), right antennal lobe (rAL), right medulla (rM), right lobula plate (rLP), right lobula (rL), left mushroom body calyces (lMBC), left mushroom body peduncle and lobes (lMBPL), left anterior optic tubercle (lAOT), left antennal lobe (lAL), left medulla (lM), left lobula plate (lLP), left lobula (lL).

All the brains were compared with each other and with the standard after they had been aligned with respect to position, rotation and global size (rigid and iso-scaling transformations). The calculations were performed separately on each of the three major compartments (**Figure 5**).

As shown in **Figure 5**, on average the standard brain is a true average brain, fulfilling the average shape requirements for the standard brain atlas.

FITTING SINGLE NEURONS INTO THE STANDARD BRAIN ATLAS

To demonstrate the application of the average standard brain atlas we have registered four intracellularly recorded and stained interneurons into the model, two olfactory and two gustatory neurons. To visualize the gustatory input region we have also registered the previously described axonal projections of the antennal and the proboscis gustatory receptor neurons (Jørgensen et al., 2006; Kvello et al., 2006). The two olfactory interneurons were stained simultaneously during one recording, a phenomenon often observed for antennal lobe projection neurons. The olfactory function was manifested as exitation to several of the tested odorants in repeated

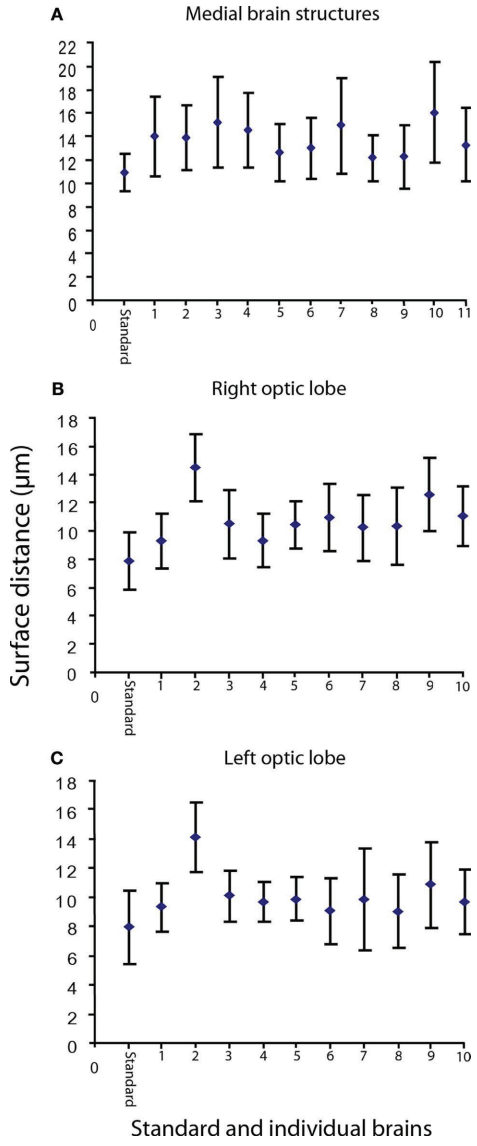

FIGURE 5 | The mean surface distance between the standard brain and the individual brains, as well as between each individual brain and the other brains. (A) The mean distance between the standard (the medial brain structures) and the 11 individual brains is 11.0 µm, whereas the mean distance between the individual brains range from 12.2 to 16.1 µm. **(B)** The right optic lobe. The mean distance between the standard and the 10 individual brains is 8.0 µm, whereas the mean distance between the individual brains range from 9.3 to 14.5 µm **(C)** The left optic lobe. The mean distance between the standard and the 10 individual brains is 8.0 µm, whereas the mean distance between the individual brains range from 9.1 to 14.2 µm. On average the standard brain is more similar to each individual brain than the individual brains are to each other. The vertical bars show the standard deviation.

stimulation. The axons closely followed each other all the way from the left antennal lobe to the calyces of the ipsilateral mushroom body and laterally in the protocerebral lobe (**Figure 6**).

The two neurons densely innervated the same glomerulus (**Figure 6A**), but no connections to the somata were identified. The axons followed the inner antenno-cerebral tract, each giving off four branches projecting in partially overlapping areas of the mushroom body calyces (**Figures 6B–D**). They continued anterior laterally in the protocerebral lobe, extending several branches into an area posterior dorsally of the lateral horn. One branch of both axons extended into the lateral horn (**Figures 6C,D**). The lateral area of the protocerebral lobes also received gustatory information, as shown by one neuron (**Figure 7A**).

This neuron was excited by quinine and tactile stimulation of the right antenna. The excitation was strongest to quinine appearing as two bursts, similar to the quinine responses of the receptor neurons (Jørgensen et al., 2007a). The response to sucrose stimulation did not exceed the mechanosensory response. The dendrites arborised in the dorsal SOG/tritocerebrum and the axon projected in wide areas of the protocerebral lobes. To elucidate whether the axonal projections of the gustatory- and the olfactory interneurons laterally in the protocerebral lobes are overlapping or separated, they were registered into the standard brain atlas (**Figures 7B–D**). The registration revealed two closely, but separated projection areas (smallest distance 34 µm); the gustatory area located anterior-ventrally to the olfactory area.

The other gustatory interneuron, with excitatory responses to repeated application of sucrose to the proboscis (latency: 47 ms), was confined to the SOG (**Figure 8**), the terminal area of the gustatory receptor neurons on the antennae and the proboscis.

The interneuron showed no response to sucrose stimulation of the antennae. The dendrites arborized extensively in the left, lateral SOG with branches extending from the anterior surface of the neuropil to the most posterior part (**Figures 8A–D**). The axon ran contra laterally in a medial commissure before bifurcating in one lateral and one ventral branch. Both branches turn in posterior direction ramifying extensively throughout the right, ventro lateral SOG, each ramification ending in a large beaded terminal. The soma was located dorso medially, close to the oesophagus (**Figure 8C**). To indicate possible connections between the gustatory receptor neurons and the interneuron, the antennal and the proboscis gustatory receptor neurons were registered into the standard brain atlas together with the interneuron. Overlap with the dendritic arborisations of the interneuron only occurred with the proboscis receptor neuron projections, as shown in **Figures 8C,D** by the single axon of category two described in Kvello et al. (2006). In fact, direct contact occurred between a few of the neurites. No overlap with the antennal gustatory receptor neurons was found.

DISCUSSION

The results present a digital, three dimensional average standard brain atlas of *Heliothis virescens*, based on brain preparations of 3- to 5-days-old females. Since the aim is to use this atlas as a common framework into which identified neurons of different brain preparations will be transformed, the important feature is a minimized difference between the standard model and any individual brain. Both from nature and experimental procedures, the individual brain

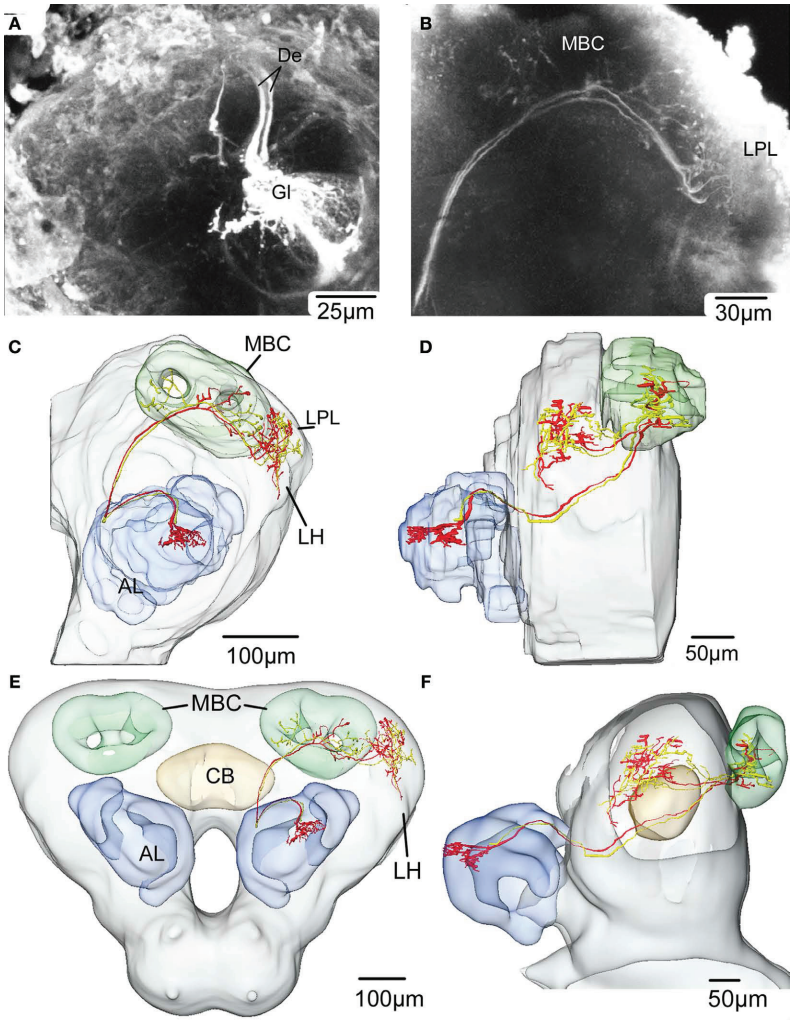

FIGURE 6 | Confocal images and registration of two antennal lobe projection neurons (simultaneously stained) into the average standard brain atlas of *Heliothis virescens*. (A) Confocal image of a section showing Micro-Ruby stained dendrites (De) of two antennal lobe projection neurons innervating a single glomerulus (Gl). Their branching pattern within the glomerulus could not be distinguished. **(B)** Confocal image showing the projections of the two neurons in the mushroom body calyces and in the lateral part of the protocerebral lobe. **(C,D)** Reconstruction of the left protocerebral lobe with the two neurons innervating one glomerulus (Gl) of the antennal lobe (AL), the mushroom bodies calyces (MBC) and the lateral protocerebral lobe (LPL) in a frontal view **(C)** and lateral view **(D)**. One branch of both axons extends into the lateral horn (LH). **(E,F)** The two neurons registered into the standard brain atlas in a frontal view **(E)** and lateral view **(F)**. Central body (CB).

preparations differ slightly, not only in size and orientation, but also in shape of the whole brain as well as brain structures exemplified by the 11 individual preparations in this study (**Table 1**, **Figure 5**). The ISA procedure takes this variability into account in the rigid and the elastic registrations as well as in the averaging procedures, resulting in a brain model with minimized differences to the individual brains (**Figure 5**), as previously demonstrated for the honeybee and the locust brain models (Brandt et al., 2005; Kurylas et al., 2008).

The procedure used and the structures selected for making the moth standard brain atlas are in general the same as for the honeybee brain, with a few modifications. The division of the moth brain into three compartments compensated for individual differences of the optic lobe orientations. The segregation allowed the use of 11 specimen for the midbrain region and 10 for the optic lobes because of mechanical damage. The selection of structures was based on staining quality, significance as landmarks and relevance

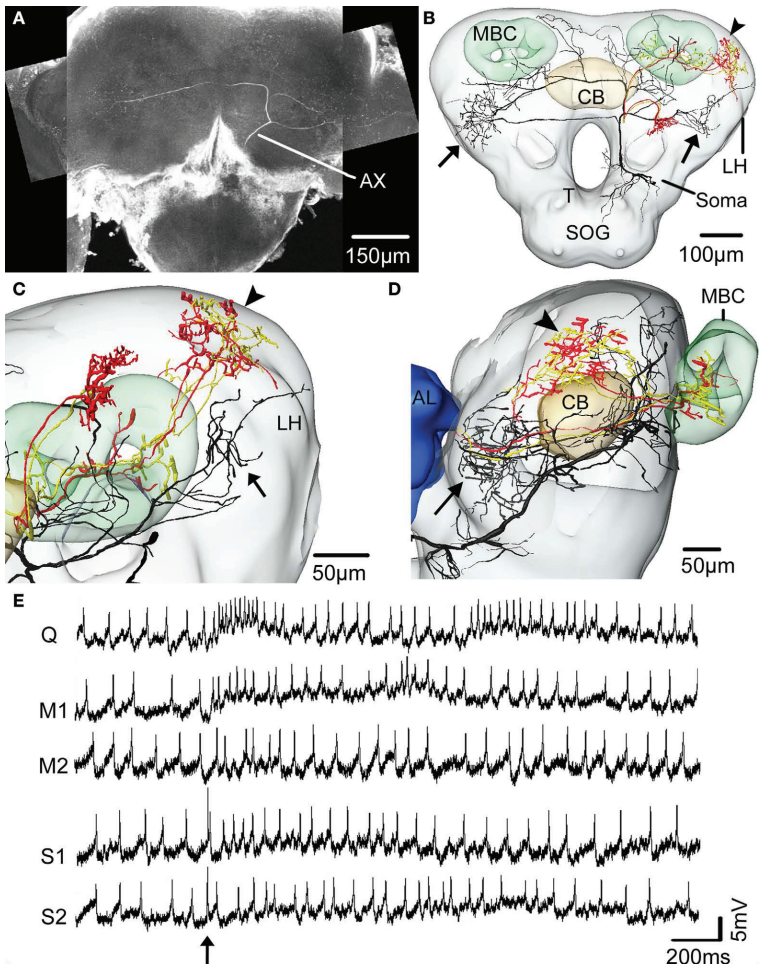

FIGURE 7 | The spatial relationship between a single gustatory interneuron and the two antennal lobe projection neurons visualised in the standard brain atlas of *Heliothis virescens*. **(A)** Confocal image of a brain section showing the gustatory interneuron stained with Micro-Emerald. Axon (Ax). **(B)** Reconstruction of the gustatory interneuron (black) and the two antennal lobe projection neurons (yellow and red) registered into the standard brain atlas (frontal view with selected brain structures). Mushroom body calyces (MBC), Central body (CB), Lateral horn (LH), Suboesophageal ganglion (SOG), Tritocerebrum (T). **(C,D)** Magnified sections of the lateral parts of the left protocerebral lobe in a frontal view **(C)** and a lateral view **(D)**. The segregated axonal projections of the gustatory interneuron and the antennal lobe projection neurons appear. Arrows point to the axonal projections of the gustatory interneuron and the arrowheads to the axonal projections of the antennal lobe projection neurons. Antennal lobe (AL). **(E)** Electrophysiological recordings from the interneuron during stimulation of the right antenna with quinine (Q), mechanosensory stimuli (M1, M2) and sucrose (S1, S2). Arrow points to the stimulus onset.

with respect to chemosensory coding and learning. Structures of the optic lobes like the medulla, lobula and lobula plate were well stained and also necessary to make the brain model complete. The well stained central body and the anterior optic tubercles are important landmarks in the midbrain. The antennal lobe glomeruli, the mushroom bodies, and the lateral parts of the protocerebral lobes are involved in processing olfactory information (Rø et al., 2007), and the SOG/tritocerebrum in processing gustatory information (Jørgensen et al., 2006; Kvello et al., 2006). However, the staining quality of these structures varied, either because of how well the antibody penetrated the tissue or because of different synaptic density. As a result the weakly stained structures were collectively assigned to one large label (Midbrain region) whereas the well stained structures were given a unique label.

The antennal lobe glomeruli with high synaptic density appeared as distinct stained structures, easily distinguished from the dark surroundings. They were collectively assigned as one label, separate from the remaining antennal lobe. This differs from the standard brain of the fruit fly, honeybee and the locust where the whole antennal lobe was assigned as one label (Rein et al., 2002; Brandt et al.,

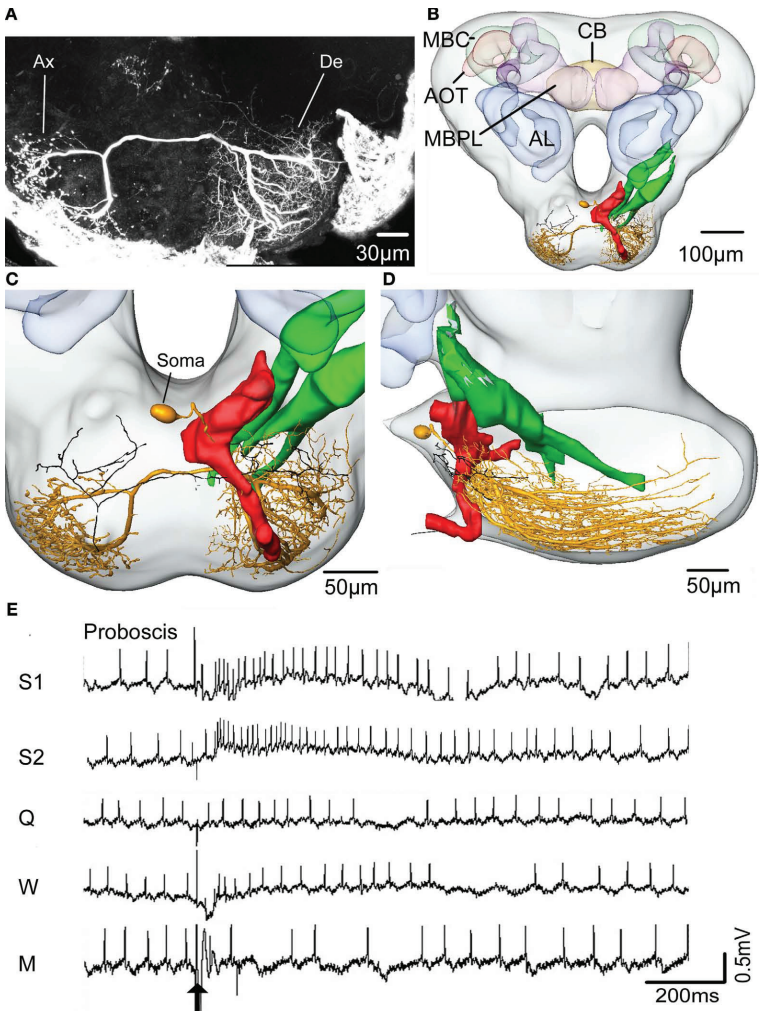

FIGURE 8 | The spatial relationship between a single gustatory interneuron and the axonal projections of the antennal and proboscis gustatory receptor neurons visualized in the standard brain atlas of the *Heliothis virescens*. (A) Confocal image of a section of the suboesophageal ganglion with a Micro-Ruby stained gustatory interneuron. Axon (Ax), Dendrite (De). **(B)** The gustatory interneuron (yellow) and the axonal projections of the antennal (green) and proboscis (red and black) gustatory receptor neurons registered into the standard brain atlas (frontal view with a few selected structures) Mushroom body calyces (MBC), Anterior optic tubercle (AOT), Mushroom body peduncle and lobes (MBPL), Antennal lobe (AL), Central body (CB). **(C,D)** Magnified section of the suboesophageal ganglion in a frontal view **(C)** and a lateral view **(D)**. The axon terminals of the proboscis gustatory receptor neuron (black) overlap the dendritic arborisations of the gustatory interneuron with direct contact between a few of the neurites. **(E)** Electrophysiological recordings from the interneuron during stimulation of the proboscis with sucrose (S1, S2), quinine (Q), water (W) and a mechanosensory stimulus (M). Arrow points to the stimulus onset.

2005; Kurylas et al., 2008). One reason for the separate glomerular labelling in the moth brain atlas was the difficulties in determining the borderline between the antennal lobe and the protocerebrum. In addition, the antennal lobe glomeruli have a larger surface relative to the volume as compared to the whole antennal lobe, which is an advantage when registering neurons into the atlas. The particular registration algorithm developed for label images use information that lies in the borderline of the label images (Rohlfing et al., 2001). A larger surface gives the algorithm more information and consequently improves the precision when registering neurons into the brain atlas. Finally, we also want to emphasize the glomeruli, being of particular interest since they relay information from olfactory sensory neurons to the second order neurons. We did not find it practical to include each of the 66 glomeruli as separate labels because

we have already made three dimensional atlases of the antennal lobe glomeruli of this species (Berg et al., 2002; Skiri et al., 2005a). At present, the separate antennal lobe atlas seems necessary for identifying the glomeruli innervated by a neuron, since this needs a detailed analysis of the relative position of the glomeruli. If practical and technically possible the atlas of the antennal lobe glomeruli may be registered into the standard brain atlas in the future.

The mushroom bodies were divided into the calyces and the peduncle/lobe system. These two compartments were easily distinguished, but a further division into their sub-compartments proved unreliable. Consistent with previous studies of *H. virescens* (Rø et al., 2007) and *Spodoptera littoralis* (Sjöholm et al., 2005) we could not distinguish any accessory calyx from the primary calyces. Such a division of the calyces, described in the moth *Manduca sexta*, may reflect a functional difference between the species (Homberg et al., 1988; Nighorn et al., 2001). Because of the difficulties of separating the mushroom body peduncle and the lobe system in the *H. virescens* brain these structures were included in the same label like in the other insect brain atlases (Rein et al., 2002; Brandt et al., 2005; Kurylas et al., 2008; Jundi et al., 2009). As shown in *Heliothis virescens* and *Spodoptera littoralis* the peduncle fuses anteriorly with the lobe system dividing into a dorsal α lobe and a medial β lobe, both intimately associated with the γ lobe (Sjööholm et al., 2005; Rø et al., 2007). Specific to Lepidoptera is the Y lobe which was vaguely observed in a few preparations and therefore was not included in the standard atlas.

The SOG, tritocerebrum and protocerebral lobes, including the lateral accessory lobes, the protocerebral bridge and the lateral horns did not appear distinct and therefore were collectively included into the midbrain region label. In the same label we also included the particular structure located posterior to the antennal lobe glomeruli merging into the protocerebral lobes without a distinct borderline. The SOG, tritocerebrum and protocerebral lobes are also included in the same label in the honeybee and the fruit fly brain atlases. In these species as in the moth, the three structures are highly interconnected and seem to lack an area with high synaptic density where a reliable distinction can be made (Rein et al., 2002; Brandt et al., 2005). This differs from the locust where the SOG (not included in the standard locust brain atlas) is a distinct ganglion connected to the brain by the circumoesophageal connectives (Burrows, 1996). The lateral horn is another structure treated differently among the five insect brain atlases. In *H. virescens*, they were weakly stained and therefore included in the same label as the SOG, tritocerebrum and protocerebral lobes like in the honeybee and M. sexta (Brandt et al., 2005; Jundi et al., 2009). This differs from the fruit fly and the locust where the lateral horns were given a unique label (Rein et al., 2002; Kurylas et al., 2008). The midbrain region is by far the largest structure in the standard moth brain atlas. Its shape results in a relative small surface which is disadvantageous when registering neurons into the structure. Therefore, the central body and the anterior optic tubercles, located within the midbrain region, serve as important landmarks. These two structures appeared quite distinct in all 11 preparations. Especially the central body is a stable landmark because its location in the middle of the brain keeps it protected from distortion by external factors.

The application of the average standard brain atlas is demonstrated by the four registered interneurons, as well as the axonal projections of the gustatory receptor neurons shown in **Figures 7 and 8**. The olfactory interneurons showed the typical morphology of inner-tract antennal lobe projection neurons (Rø et al., 2007), with dendrites innervating a single glomerulus of the antennal lobe, and axons projecting via the inner antenno-cerebral tract to the calyces of the mushroom body involved in olfactory learning and memory (Menzel, 2001; Heisenberg, 2003), and to the lateral parts of the median protocerebrum considered to be a premotoric area (**Figure 6**). Interestingly, axonal projections of the quinine responding neuron were identified in a separate, but closely located area of the olfactory projections. Because of the absence of distinct landmarks in this brain region the standard brain atlas proved particularly valuable in visualizing and distinguishing these target areas of the gustatory- and olfactory projections (**Figures 7B–D**). However, registration of more neurons into the standard brain atlas combined with electrophysiology is needed to verify whether the projection areas of the two chemosensory modalities are completely separated or partly overlapping in this area of the brain. The atlas also proved valuable in visualising possible connections between the sucrose responding interneuron and the receptor neurons in the SOG (**Figure 8**). The direct contact between the intermingled dendritic branches of one gustatory interneuron and the projections of the proboscis gustatory receptor neuron suggest input from the proboscis. In contrast the non overlapping projections of the antennal gustatory receptor neuron indicate no antennal input. This was in fact shown physiologically by the excitatory responses of the interneuron to sucrose stimulation of the proboscis, but not of the antennae. Furthermore, the short and constant latency of the response indicate monosynaptic connections (Burrows and Newland, 1994; Newland, 1999). The axon projected contra laterally relative to the dendritic arborizations, terminating in the ventro lateral SOG where motorneurons of the mouthparts presumably are located. Thus, this neuron may receive direct synaptic input from the sucrose receptor neurons on the proboscis and feed into motor neurons involved in feeding.

The standard brain atlas is a valuable tool for visualising the spatial relationship between neurons from different brain preparations, detecting regions of overlap among the neurites, and thus to make predictions about neuronal connectivity. The procedure of rigid and elastic registration is particularly suited as an objective way to integrate neurons from different preparations into the digital standard brain atlas. The average property of the atlas ensures that the neurons undergo a minimal deformation in the registration procedure. In combination with physiological data the atlas provides an important tool for investigating and visualising the neural networks underlying gustatory and olfactory coding as well as appetitive and aversive learning and memory formation.

ACKNOWLEDGMENTS

The project was financed by the Norwegian University of Science and Technology and the Royal Norwegian Society of Sciences and Letters. We thank Prof. Erich Buchner (Universität Würzburg, Würzburg, Germany) for providing antibodies, Dr. Robert Brandt (Mercury Computer Systems, Berlin, Germany) and Anja Kuss (Zuse-Institute Berlin) for help with Amira, Dr. Sabine Krofczik (Freie Universität Berlin) for staining protocols and Gisela Manz (Freie Universität Berlin) for advices during the intracellular recordings.

REFERENCES

Berg, B. G., Almaas, T. J., Bjaalie, J. G., and Mustaparta, H. (1998). The macroglomerular complex of the antennal lobe in the tobacco budworm moth *Heliothis virescens*: specified subdivision in four compartments according to information about biologically significant compounds. *J. Comp. Physiol. A* 183, 669–682.

Berg, B. G., Galizia, C. G., Brandt, R., and Mustaparta, H. (2002). Digital atlases of the antennal lobe in two species of tobacco budworm moths, the oriental Helicoverpa assulta (male) and the American *Heliothis virescens* (male and female). *J. Comp. Neurol.* 446, 123–134.

Borst, A., and Haag, J. (2002). Neural networks in the cockpit of the fly. *J. Comp. Physiol. A* 188, 419–437.

Brandt, R., Rohlfing, T., Rybak, J., Krofczik, S., Maye, A., Westerhoff, M., Hege, H. C., and Menzel, R. (2005). Tree-dimensional average-shape atlas of the honeybee brain and its applications. *J. Comp. Neurol.* 492, 1–19.

Bräunig, P., and Pflüger, H.-J. (2001). The unpaired median neurons of insects. *Adv. In Insect Phys.* 28, 185–266.

Burrows, M. (1996). The Neurobiology of an Insect Brain. New York, Oxford University Press.

Burrows, M., and Newland, P. L. (1994). Convergence of mechanosensory afferents from different classes of exteroceptors onto spiking local interneurons in the locust. *J. Neurosci.* 14, 3341–3350.

Chiang, A.-S., Liu, Y.-C., Chiu, S. L., Hu, S. H., Huang, C.-Y., and Hsieh, C.-H. (2001). Three-dimensional mapping of brain neuropils in the cockroach, *Diploptera punctata*. *J. Comp. Neurol.* 440, 1–11.

Evers, J. F., Schmitt, S., Sibila, M., and Duch, C. (2004). Progress in functional neuroanatomy: precise automatic geometric reconstruction of neuronal morphology from confocal image stacks. *J. Neurophysiol.* 93, 2331–2342.

Flanagan, D., and Mercer, A. R. (1989). An atlas and 3-D reconstruction of the antennal lobes in the worker honey bee, *Apis mellifera* L. (*Hymenoptera: Apidae*). *Int. J. Insect Morphol. Embryol.* 18, 145–159.

Galizia, C. G., McIlwrath, S. L., and Menzel, R. (1999). A digital three-dimensional atlas of the honeybee antennal lobe based on optical sections acquired by confocal microscopy. *Cell Tissue Res.* 295, 383–394.

Greiner, B., Gadenne, C., and Anton, S. (2004). Three-dimensional antennal lobe atlas of the male moth, *Agrotis ipsilon*: a tool to study structure-function correlation. *J. Comp. Neurol.* 475, 202–210.

Hammer, M. (1993). An identified neuron mediates the unconditioned stimulus in associative olfactory learning in honeybees. *Nature* 366, 59–63.

Hartlieb, E. (1996). Olfactory conditioning in the moth *Heliothis virescens*. *Naturwissenschaften* 83, 87–88.

Heinbockel, T., Christensen, T. A., and Hildebrand, J. G. (1999). Temporal tuning of odor responses in pheromone-responsive projection neurons in the brain of the sphinx moth *Manduca sexta*. *J. Comp. Neurol.* 409, 1–12.

Heinze, S., and Homberg, U. (2007). Maplike representation of celestial E-vector orientations in the brain of an insect. *Science* 315, 995–997.

Heisenberg, M. (2003). Mushroom body memoir: from maps to models. *Nat. Rev. Neurosci.* 4, 266–275.

Homberg, U., Montague, R. A., and Hildebrand. J. G. (1988). Anatomy of antenno-cerebral pathways in the brain of the sphinx moth *Manduca sexta*. *Cell Tissue Res.* 254, 255–281.

Huetteroth, W., and Schachtner, J. (2005). Standard three-dimensional glomeruli of the *Manduca sexta* antennal lobe: a tool to study both developmental and adult neuronal plasticity. *Cell Tissue Res.* 319, 513–524.

Iyengar, B. G., Chou, C. J., Sharma, A., and Atwood, H. L. (2006). Modular neuropile organization in the Drosophila larval brain facilitates identification and mapping of central neurons. *J. Comp. Neurol.* 499, 583–602.

Jefferis, G. S. X. E., Potter, C. J., Chan, A. I., Marin, E. C., Rohlfing, T., Maurer, C. R., and Luo, L. Q. (2007). Comprehensive maps of Drosophila higher olfactory centers: Spatially segregated fruit and pheromone representation. *Cell* 128, 1187–1203.

Jenett, A., Schindelin, J. E., and Heisenberg, M. (2006). The Virtual Insect Brain protocol: creating and comparing standardized neuroanatomy. *BMC Bioinformatics* 7, 544.

Jørgensen, K., Almaas, T. J., Marion-Poll, F., and Mustaparta, H. (2007a). Electrophysiological characterization of responses from gustatory receptor neurons of sensilla chaetica in the Moth *Heliothis virescens*. *Chem. Senses* 32, 863–879.

Jørgensen, K., Stranden, M., Sandoz, J. C., Menzel, R., and Mustaparta, H. (2007b). Effects of two bitter substances on olfactory conditioning in the moth *Heliothis virescens*. *J. Exp. Biol.* 210, 2563–2573.

Jørgensen, K., Kvello, P., Almaas, T. J., and Mustaparta, H. (2006). Two closely located areas in the suboesophageal ganglion and the tritocerebrum receive projections of gustatory receptor neurones located on the antennae and the proboscis in the moth *Heliothis virescens*. *J. Comp. Neurol.* 496, 121–134.

Jundi, B. E., Huetteroth, W., Kurylas, A. E., and Schachtner, J. (2009). Anisometric brain dimorphism revisited: implementation of a volumetric 3D standard brain in *Manduca sexta*. *J. Comp. Neurol.* 517, 210–225.

Kanzaki, R., Arbas, E. A., and Hildebrand, J. G. (1991). Physiology and morphology of descending neurons in pheromone-processing olfactory pathways in the male moth *Manduca sexta*. *J. Comp. Physiol. A* 169, 1–14.

Kanzaki, R., Arbas, E. A., Strausfeld, N. J., and Hildebrand, J. G. (1989). Physiology and morphology of projection neurons in the antennal lobe of the male moth *Manduca sexta*. *J. Comp. Physiol. A* 165, 427–453.

Kurylas, A. E., Rohlfing, T., Krofczik, S., Jenett, A., and Homberg, U. (2008). Standardized atlas of the brain of the desert locust, *Schistocerca gregaria*. *Cell Tissue Res.* 333, 125–145.

Kvello, P., Almaas, T. J., and Mustaparta, H. (2006). A confined taste area in a lepidopteran brain. *Arthropod Struct. Dev.* 35, 35–45.

Laissue, P. P., Reiter, C., Hiesinger, P. R., Halter, S., Fischbach, K. F., and Stocker, R. F. (1999). Three-dimensional reconstruction of the antennal lobe in *Drosophila melanogaster*. *J. Comp. Neurol.* 405, 543–552.

Lei, H., Anton, S., and Hansson, B. S. (2001). Olfactory protocerebral pathways processing sex pheromone and plant odor information in the male moth *Agrotis segetum*. *J. Comp. Neurol.* 432, 356–370.

Masante-Roca, I., Gadenne, C., and Anton, S. (2005). Three-dimensional antennal lobe atlas of male and female moths, *Lobesia botrana* (Lepidoptera : Tortricidae) and glomerular representation of plant volatiles in females. *J. Exp. Biol.* 208, 1147–1159.

Mauelshagen, J. (1993). Neural correlates of olfactory learning paradigms in an identified neuron in the honeybee brain. *J. Neurophysiol.* 69, 609–625.

Menzel, R. (2001). Searching for the memory trace in a mini-brain, the honeybee. *Learn. Mem.* 8, 53–62.

Mitchell, B. K., and Itagaki, H. (1992). Interneurons of the subesophageal ganglion of *Sarcophaga bullata* responding to gustatory and mechanosensory stimuli. *J. Comp. Physiol. A* 171, 213–230.

Müller, D., Abel, R., Brandt, R., Zöckler, M., and Menzel, R. (2002). Differential parallel processing of olfactory information in the honeybee, *Apis mellifera* L. *J. Comp. Physiol. A* 188, 359–370.

Mustaparta, H. (2002). Encoding of plant odour information in insects: peripheral and central mechanisms. *Entomol. Exp. Appl.* 104, 1–13.

Mustaparta, H., and Stranden, M. (2005). Olfaction and learning in moths and weevils living on angiosperm and gymnosperm hosts. *Recent Adv. Phytochem.* 39, 269–292.

Namiki, S., and Kanzaki, R. (2008). Reconstructing the population activity of olfactory output neurons that innervate identifiable processing units. *Front. Neural Circuits* 2, 1. doi: 10.3389/neuro.01.028.2009.

Newland, P. L. (1999). Processing of gustatory information by spiking local interneurons in the locust. *J. Neurophysiol.* 82, 3149–3159.

Nighorn, A., Simpson, P. J., and Morton, D. B. (2001). The novel guanylyl cyclase MsGC-I is strongly expressed in higher-order neuropils in the brain of *Manduca sexta*. *J. Exp. Biol.* 204, 305–314.

Poulet, J. F. A., and Hedwig, B. (2006). The cellular basis of a corollary discharge. *Science* 311, 518–522.

Rein, K., Zöckler, M., Mader, M. T., Grübel, C., and Heisenberg, M. (2002). The Drosophila standard brain. *Curr. Biol.* 12, 227–231.

Reischig, T., and Stengl, M. (2002). Optic lobe commissures in a three-dimensional brain model of the cockroach *Leucophaea maderae*: a search for the circadian coupling pathways. *J. Comp. Neurol.* 443, 388–400.

Reisenman, C. E., Christensen, T. A., and Hildebrand, J. G. (2005). Chemosensory selectivity of output neurons innervating an identified, sexually isomorphic olfactory glomerulus. *J. Neurosci.* 25, 8017–8026.

Rø, H., Müller, D., and Mustaparta, H. (2007). Anatomical organization of antennal lobe projection neurons in the moth *Heliothis virescens*. *J. Comp. Neurol.* 500, 658–675.

Rogers, S. M., and Newland, P. L. (2003). The neurobiology of taste in insects. *Adv. In Insect Phys.* 141–204.

Rohlfing, T., Brandt, R., Maurer, C. R. Jr., and Menzel, R. (2001). Bee Brains, B-splines and Computational Democracy: Generating an Average Shape Atlas. In Proceedings of IEEE Workshop on Mathematical Methods in Biomedical Image Analysis, MMBIA, Kauai, Hawaii. pp. 187–194.

Rospars, J. P., and Chambille, I. (1981). Deutocerebrum of the cockroach *Blaberus craniifer* burm. Quantitative study and automated identification of the glomeruli. *J. Neurobiol.* 12, 221–247.

Rospars, J. P., and Hildebrand, J. G. (2000). Sexually dimorphic and isomorphic

glomeruli in the antennal lobes of the sphinx moth *Manduca sexta*. *Chem. Senses* 25, 119–129.

Røstelien, T., Stranden, M., Borg-Karlson, A.-K., and Mustaparta, H. (2005). Olfactory receptor neurones in two heliothine moth species responding selectively to aliphatic green leaf volatiles, aromatics, monoterpenes and sesquiterpenes of plant origin. *Chem. Senses* 30, 443–461.

Rybak, J., and Menzel, R. (1998). Integrative properties of the pe1 neuron, a unique mushroom body output neuron. *Learn. Mem.* 5, 133–145.

Sadek, M. M., Hansson, B. S., Rospars, J. P., and Anton, S. (2002). Glomerular representation of plant volatiles and sex pheromone components in the antennal lobe of the female *Spodoptera littoralis*. *J. Exp. Biology* 205, 1363–1376.

Schmitt, S., Evers, J. F., Duch, C., Scholz, M., and Obermayer, K. (2004). New methods for the computer-assisted 3-D reconstruction of neurons from confocal image stacks. *Neuroimage* 23, 1283–1298.

Sjöholm, M., Sinakevitch, I., Ignell, R., Strausfeld, N. J,, and Hansson, B. S. (2005). Organization of Kenyon cells in subdivisions of the mushroom bodies of a lepidopteran insect. *J. Comp. Neurol.* 491, 290–304.

Skiri, H. T., Rø, H., Berg, B. G., and Mustaparta, H. (2005a). Consistent organization of glomeruli in the antennal lobes of related species of heliothine moths. *J. Comp. Neurol.* 491, 367–380.

Skiri, H. T., Stranden, M., Sandoz, J. C., Menzel, R., and Mustaparta, H. (2005b). Associative learning of plant odorants activating the same or different receptor neurones in the moth *Heliothis virescens*. *J. Exp. Biol.* 208, 787–796.

Smid, H. M., Bleeker, M. A., Van Loon, J. J. A., and Vet, L. E. (2003). Three-dimensional organization of the glomeruli in the antennal lobe of the parasitoid wasps *Cotesia glomerata* and *C. rubecula*. *Cell Tissue Res.* 312, 237–248.

Staudacher, E. M., Huetteroth, W., Schachtner, J., and Daly, K. C. (2009). A 4-dimensional representation of antennal lobe output based on an ensemble of characterized projection neurons. *J. Neurosci. Methods* 180, 208–223.

Stocker, R. F., Lienhard, M. C., Borst, A., and Fischbach, K. F. (1990). Neuronal architecture of the antennal lobe in *Drosophila melanogaster*. *Cell Tissue Res.* 262, 9–34.

Toga, A. W. (2002). Neuroimage databases: the good, the bad and the ugly. *Nat. Rev. Neurosci.* 3, 302–309.

Toga, A. W., and Thompson, P. M. (2001). Maps of the brain. *Anat. Rec.* 265, 37–53.

Van Essen D. C. (2002). Windows on the brain: the emerging role of atlases and databases in neuroscience. *Curr. Opin. Neurobiol.* 12, 574–579.

Yamagata, N., Nishino, H., and Mizunami, M. (2007). Neural pathways for the processing of alarm pheromone in the ant brain. *J. Comp. Neurol.* 505, 424–442.

Conflict of Interest Statement: The authors declare that the research was conducted in the absence of any commercial or financial relationships that could be construed as a potential conflict of interest.

Received: 04 August 2009; paper pending published: 20 August 2009; accepted: 02 October 2009; published online: 26 October 2009.

Citation: Kvello P̊, Løfaldli BB, Rybak J, Menzel R and Mustaparta H (2009) Digital, three-dimensional average shaped atlas of the Heliothis virescens brain with integrated gustatory and olfactory neurons. Front. Syst. Neurosci. ***3****:14. doi: 10.3389/neuro.06.014.2009*

Paper II

frontiers in
SYSTEMS NEUROSCIENCE

ORIGINAL RESEARCH ARTICLE
published: 12 February 2010
doi: 10.3389/neuro.06.005.2010

Integration of the antennal lobe glomeruli and three projection neurons in the standard brain atlas of the moth *Heliothis virescens*

Bjarte Bye Løfaldli, Pål Kvello and Hanna Mustaparta*

Neuroscience Unit, Department of Biology, Norwegian University of Science and Technology, Trondheim, Norway

Edited by:
Randolf Menzel, Freie Universitat Berlin, Germany

Reviewed by:
Joachim Schachtner, Philipps-Universitat Marburg, Germany
Uwe Homberg, Philipps-Universitat Marburg, Germany

Correspondence:
Hanna Mustaparta, Neuroscience Unit, MTFS, Department of Biology, Norwegian University of Science and Technology, Olav Kyrres gt. 9, 7489 Trondheim, Norway.
e-mail: hanna.mustaparta@bio.ntnu.no

Digital three dimensional standard brain atlases (SBAs) are valuable tools for integrating neuroimaging data of different preparations. In insects, SBAs of five species are available, including the atlas of the female *Heliothis virescens* moth brain. Like for the other species, the antennal lobes (ALs) of the moth brain atlas were integrated as one material identity without internal structures. Different from the others, the *H. virescens* SBA exclusively included the glomerular layer of the AL. This was an advantage in the present study for performing a direct registration of the glomerular layer of individual preparations into the standard brain. We here present the *H. virescens* female SBA with a new model of the AL glomeruli integrated into the atlas, i.e. with each of the 66 glomeruli identified and labelled with a specific number. The new model differs from the previous *H. virescens* AL model both in respect to the number of glomeruli and the numbering system; the latter according to the system used for the AL atlases of two other heliothine species. For identifying female specific glomeruli comparison with the male AL was necessary. This required a new male AL atlas, included in this paper. As demonstrated by the integration of three AL projection neurons of different preparations, the new SBA with the integrated glomruli is a helpful tool for determining the glomeruli innervated as well as the relative position of the axonal projections in the protocerebrum.

Keywords: insect, olfaction, three dimensional reconstruction, mushroom body calyces, lateral protocerebrum

INTRODUCTION

Digital three dimensional standard brain atlases (SBAs) have been made of several vertebrate and insect species in order to integrate neuroimaging data of different preparations (Toga and Thompson, 2001; Rein et al., 2002; Toga, 2002; Van Essen, 2002; Brandt et al., 2005; Kurylas et al., 2008; el Jundi et al., 2009; Kvello et al., 2009). In insects, whole brain atlases of five species are available as suitable tools for studying the three dimensional spatial relationship between neurons innervating different brain structures (Rein et al., 2002; Brandt et al., 2005; Kurylas et al., 2008; el Jundi et al., 2009; Kvello et al., 2009). Based on confocal scans with higher resolution, separate atlases of specific brain compartments like the primary olfactory centre, the antennal lobe (AL), and the central complex involved in processing visual information, have also been made (Rospars and Chambille, 1981; Flanagan and Mercer, 1989; Stocker et al., 1990; Galizia et al., 1999; Laissue et al., 1999; Rospars and Hildebrand, 2000; Chiang et al., 2001; Berg et al., 2002; Reischig and Stengl, 2002; Sadek et al., 2002; Smid et al., 2003; Greiner et al., 2004; Huetteroth and Schachtner, 2005; Masante-Roca et al., 2005; Skiri et al., 2005; Iyengar et al., 2006; Jefferis et al., 2007; Kazawa et al., 2009; Varela et al., 2009; el Jundi et al., 2010). Thus, the neurons can be registered into these particular structures with higher precision, suitable for studying the network within the brain compartments. Recently, we have made a SBA of *Heliothis virescens* based on the iterative shape average (ISA) procedure, with the aim to spatially relate identified neurons forming the networks underlying chemosensory coding and learning in this moth species (Kvello et al., 2009). Like for all five insect brain atlases, the ALs are included as a single brain compartment without internal structures. Different from the other atlases, the AL of the *H. virescens* brain atlas includes exclusively the glomerular layer as a single labelled identity, an advantage for registering the AL glomeruli as separate units into the atlas.

Numerous studies have been devoted to the neuronal network of the primary olfactory centres, the olfactory bulb in vertebrates and the AL in insects, in trying to elucidate how olfactory information is processed and coded (Laurent et al., 1996; Hildebrand and Shepherd, 1997; Galizia and Menzel, 2000; Lledo et al., 2005; Wilson and Mainen, 2006; Stopfer, 2007; Kloppenburg and Mercer, 2008). Common for the two systems are the input elements of sensory neurons, the output elements of mitral/tufted cells and projection neurons (PNs) respectively, intrinsic local interneurons, as well as centrifugal modulatory neurons. Typical are the numerous glomeruli, spheric-ovoid structures of fine neuropils with condensations of synapses forming a neuronal network; in insects between all four elements. Each glomerulus represents a functional unit receiving information from one set of sensory neurons with the same receptor protein type and sending out the processed information to olfactory areas of higher order (Axel, 1995; Clyne et al., 1999; Vosshall et al., 1999; Buck, 2000; Mombaerts, 2001; Vosshall and Stocker, 2007). In insects, the output neurons are uni- or multiglomerular PNs with axons following one of three major

antennocerebral tracts, the inner (IACT), the middle (MACT) and the outer (OACT) in moths (Homberg et al., 1988; Rø et al., 2007). They project to the calyces of the mushroom bodies, important in learning and memory (Menzel, 2001; Heisenberg, 2003), and to the lateral protocerebrum, a premotoric area. To resolve how biologically relevant odour information is handled by the network, it is essential to determine the relevant input and output of specific glomeruli, which also require identification of the glomeruli across individuals. The atlases of the AL glomeruli of several insect species including heliothine moths have supported the early findings of constant numbers and positions. Thus, they are helpful tools in identifying the glomeruli innervated by physiologically characterised AL neurons.

In herbivorous species of Lepidoptera the AL is organised into two parallel olfactory systems, the macroglomerular complex (MGC) consisting of a few glomerular units dealing with pheromone information in male moths, and the numerous ordinary glomeruli dealing with plant odours in males and females (Anton and Homberg, 1999; Christensen and Hildebrand, 2002; Mustaparta, 2002). Due to available, identified pheromone components as well as the relative simple system, the functional organisation of the MGC is to a large extent resolved in several species, including *H. virescens*, as concerns input and output information (Berg et al., 1998; Vickers et al., 1998; Anton and Hansson, 1999; Galizia et al., 2000; Kanzaki et al., 2003; Vickers and Christensen, 2003). Knowledge about the more complex plant odour system is in general scarce, partly due to unknown relevant plant odorants. However, using chemical analyses linked to electrophysiological recordings from single units, sharply tuned plant odour receptor neurons have been well documented, particularly in *H. virescens* for which numerous primary and secondary plant odorants have been identified (Mustaparta and Stranden, 2005; Røstelien et al., 2005). These results are important in ongoing studies on the processing of plant odour information in the brain of this species. Using intracellular recordings combined with fluorescent staining we are physiologically characterising chemosensory neurons, including PNs, followed by visualisation in confocal laser scanning microscope and three dimensional reconstructions (Rø et al., 2007; Kvello et al., 2009). The neurons are subsequently registered into the SBA for spatially relating the neurons from different preparations in this common frame. In order to identify the PNs it is important to determine the glomeruli they innervate. This may be performed using the separate AL atlas. However, in order to relate the glomeruli giving input to the PNs with their output regions in protocerebrum, integration of the AL glomeruli into the SBA is required.

In this paper we present the *H. virescens* female SBA with a new model of the AL glomeruli integrated into the atlas (SBAGl), i.e. with each of its 66 glomeruli identified with a specific number. The glomeruli in the new atlas are numbered according to the AL atlases of two other heliothine species (Skiri et al., 2005). For identifying female specific glomeruli comparison with the male AL was necessary, which required a new *H. virescens* male AL atlas, included in this paper. As demonstrated by the three registered AL PNs, the SBAGl is a helpful tool for determining the glomeruli innervated as well as the relative position of the axonal projections in the protocerebrum.

MATERIALS AND METHODS

Heliothis virescens (Heliothinae; Lepidoptera; Noctuidae) pupae were imported from a laboratory culture (Syngenta, Basel, Switzerland), separated according to sex and placed in different containers in an incubator (Refritherm 6E, Struers) on a phase-shifted LD photoperiod (14:10 hours) at 22°C. Emerged adults were transferred to new containers and fed *ad libitum* on a 0.15-M sucrose solution. Experiments were performed on 3–5 days old female and male moths.

STAINING OF THE ANTENNAL LOBE AND PROJECTION NEURONS

The moths were mounted in plastic tubes and immobilised with dental wax (Kerr Corporation, Romulus, MI, USA). Cephalic scales and mouthparts were removed before decapitation. Brains were dissected in a saline solution (in mM: 150 NaCl, 3 $CaCl_2$, 3 KCl, 25 $C_{12}H_{22}O_{11}$ and 10 TES buffer, pH 6.9) and fixed in paraformaldehyde (4%) diluted in methanol (50%) over night (4°C). After rinsing in a phosphate buffered saline solution (PBS in mM: 684 NaCl, 13 KCl, 50.7 Na_2HPO_4 and 5 KH_2PO_4, pH 7.2; 10 min), preparations were dehydrated in an increasing ethanol series (50, 70, 90, 96 and 100%, 10 min each) degreased in xylol (5 min), rehydrated in a decreasing ethanol series (100, 96, 90, 70 and 50%, 10 min each) before washed in PBS (10 min) and preincubated in normal goat serum (NGS; Sigma, St. Louis, MO, USA; 10%) in PBS at room temperature (30 min). This was followed by incubation in a monoclonal antibody against the synaptic protein synapsin (SYNORF 1, kindly provided by Prof. E. Buchner, Würzburg, Germany), diluted in PBS (1:10) and NGS (10%) for 48 h (4°C). After rinsing in PBS (5 × 20 min) the preparations were incubated for 24 h (4°C) with a Cy5-conjungated goat anti-mouse secondary antibody (Jackson Immunoresearch; dilution 1:500 in PBS) before rinsing in PBS (5 × 20 min) and dehydrated in increasing ethanol series. Preparations were cleared in methyl salicylate and mounted as whole mounts in double-sided aluminium slides.

For staining of the PNs female moths were restrained and immobilised with wax with the head and antenna protruding. The cuticle between the eyes was removed, exposing the AL and the protocerebrum. Large trachea, intracranial- and antennal muscles were removed to eliminate brain and antennal movements. Neurolemma was perforated with a tungsten hook to facilitate insertion of the microelectrode prior to superfusion with saline solution. Glass microelectrodes were pulled with a Flaming-Brown horizontal puller (P97; Sutter Instruments, Novato, CA, USA), the tips were filled with dye (Micro-Ruby, Invitrogen; 4%) and backfilled with potassium acetate solution (0.2 M). The microelectrodes had a resistance of 150–400 MΩ. Neurons were iontophoretically stained by passing a 1–3 nA depolarising current of 2 Hz with 0.2 s duration. Complete labelling of the neurons required dye injection for 10–15 min. After current injection, the dye was allowed to diffuse over night at 4°C or 3 h at room temperature. The brains were dissected in saline solution, fixed in paraformaldehyde (4%) in PBS and left over night at 4°C. To intensify the staining of the labelled neurons the brains were incubated in Streptavidin-Cy3 (Jackson Immunoresearch, West Grove, PA, USA; diluted 1:200 in PBS) over night at 4°C before rinsed in PBS. Subsequently, the SYNORF1 protocol, as described above, was used on the preparations for background staining.

VISUALISATION OF THE ANTENNAL LOBE GLOMERULI AND THE PROJECTION NEURONS

Stained preparations were visualised with a laser scanning confocal microscope (LSM 510 META Zeiss, Jena, Germany). Stained AL preparations were examined using a Zeiss Plan-Neofluar 40 × 0.75 NA dry lens objective. The fluorescent dye (Cy5) was exited by a 633-nm line of argon laser and scanned with a resolution of 1024 × 1024 pixels in the *xy*-plane and an interslice distance of 2 µm (voxel size of 0.75 µm × 0.75 µm × 2 µm). Intracellular fillings were examined with a Plan-Neofluar 20×/0.5 NA dry lens objective. The intracellular dye was excited by a 543-nm Helium Neon laser and filtered through a bandpass filter BP 565-615 IR. Preparations were scanned with a resolution of 1024 × 1024 pixels in the xy-plane and an interslice distance of 2 µm. The neurons were scanned in several tiles and manually merged in Amira 4.1. To compensate for the refraction indexes of the mountant and that of the dry lens objective, the *z*-axis dimension was multiplied by a factor of 1.6.

RECONSTRUCTION AND IDENTIFICATION OF THE ANTENNAL LOBE GLOMERULI

Grey value image stacks acquired from the confocal microscope were elaborately examined section by section and glomeruli were manually labelled using the segmentation editor in Amira 4.1 (Visage Imaging, Fürth, Germany). In this process any group of voxels belonging to a particular glomerulus was given a unique label resulting in a stack of label images corresponding to the underlying confocal images. The label images were used to create 3D polygonal surface models.

INTEGRATION OF THE ANTENNAL LOBE ATLAS INTO THE STANDARD BRAIN

The digital SBA of *H. virescens* includes the ALs as models solely constituting the glomerular layer labelled as a single material identity (Kvello et al., 2009). Thus, to register the glomeruli of the AL atlas into the SBA, the separately labelled glomeruli had first to be assigned a single material identity corresponding to the AL model of the SBA. The label image stack of the AL glomeruli was then affine- and elastically registered into the corresponding label images of the SBA, i.e. corresponding points in the AL atlas and the AL model of the SBA were transformed into the same coordinates. Subsequently, the glomeruli were relabelled as separate units and given material identity and colour code according to the separate AL atlas.

RECONSTRUCTION AND REGISTRATION OF NEURONS INTO THE NEW STANDARD BRAIN ATLAS WITH GLOMERULI

Gray value image stacks of stained neurons and innervated brain structures acquired from the confocal microscope were examined and reconstructed in the computer software Amira 3.1, as described by Kvello et al. (2009). Brain structures were reconstructed as label images and neurons by using the skeleton tool (Evers et al., 2004; Schmitt et al., 2004). In general, the registration of neurons into the SBA followed the same procedure as described by Brandt et al. (2005). The label images of the innervated brain structures were affine- and elastically registered to the label images of the corresponding structures in the SBA. Then the resulting transformation parameters for the brain structures were applied to the reconstructed neurons. Since the registration of a neuron into any structure of the SBA requires the identification of the corresponding structure in the preparation, the neurons were first registered into the SBA. The SBAGl was then superposed in order to identify the innervated glomeruli. The identification was checked against the confocal images. The innervated glomeruli as well as a few other landmark glomeruli were subsequently reconstructed in the preparation and registered into the corresponding glomeruli of the SBAGl.

RESULTS

ATLAS OF ANTENNAL LOBE GLOMERULI

As expected, the synapsin-specific antibody staining gave a clear labelling of brain structures, particularly the glomeruli of the ALs (**Figure 1**).

In addition the calyces of the mushroom bodies, the optic lobes and the suboesophageal ganglion were clearly stained. Two of the three AL cell body clusters (Berg et al., 2002), the lateral and the medial, were recognised, but were not further described in this study. The results are based on confocal laser images of the glomeruli of four ALs, one right (**Figure 2**), and one left from different females and two left from different males.

Figure 3 shows the 3D reconstructions of each glomerulus in the two female and one male preparations.

The ALs of the two female specimens were compared with the female AL model and the underlying confocal images of two other heliothine moth species, *Helicoverpa armigera* and *Helicoverpa assulta* (Skiri et al., 2005), to identify corresponding glomeruli that were given the same number and colour. The same procedure was carried out for comparing and numbering the male AL glomeruli. Sex specific glomeruli of the female ALs were identified by comparing the glomeruli between the two sexes. Like in the previous studies, the primary landmarks were the antennal nerve entrance, the central large female glomerulus (cLFG), the male specific MGC, the labial pit organ glomerulus (LPOG), the adjacent large glomerulus medially of the LPOG (mLPOG), and the fibre bundles of the lateral and the medial cell clusters, LCCl and MCCl, respectively (**Figure 3**). Surrounding glomeruli of the primary landmarks served as secondary landmarks. This resulted in 4 female specific and 62 ordinary glomeruli in the AL of *H. virescens* females. In males 62 glomeruli corresponded to the ordinary glomeruli in females, whereas 5 glomeruli were male specific, including G63 and the 4 previously described units of the MGC.

FEMALE SPECIFIC GLOMERULI

The four female specific glomeruli of the *H. virescens* ALs, located at the entrance of the antennal nerve, were identified in both preparations. Centrally at the entrance is the large female specific glomerulus (cLFG) (**Figures 2D,E and 3G,H**), previously identified in Berg et al. (2002). Two other female specific glomeruli, F1 and F3, were positioned anterior of cLFG and the fourth, F2, posterior of cLFG. Compared with the other heliothine species (Skiri et al., 2005), cLFG has a similar position and size, whereas the position of F1 and F2 differs among the species. F3 is only present in *H. virescens* and *H. assulta*.

ORDINARY GLOMERULI IN FEMALES

Sixty-six glomeruli were counted in both ALs of the two individuals (**Figure 3**). Among them, 62 glomeruli corresponded to ordinary glomeruli in the AL of *H. virescens* males and of the two other heliothine species, *H. armigera* and *H. assulta*. For instance, easily

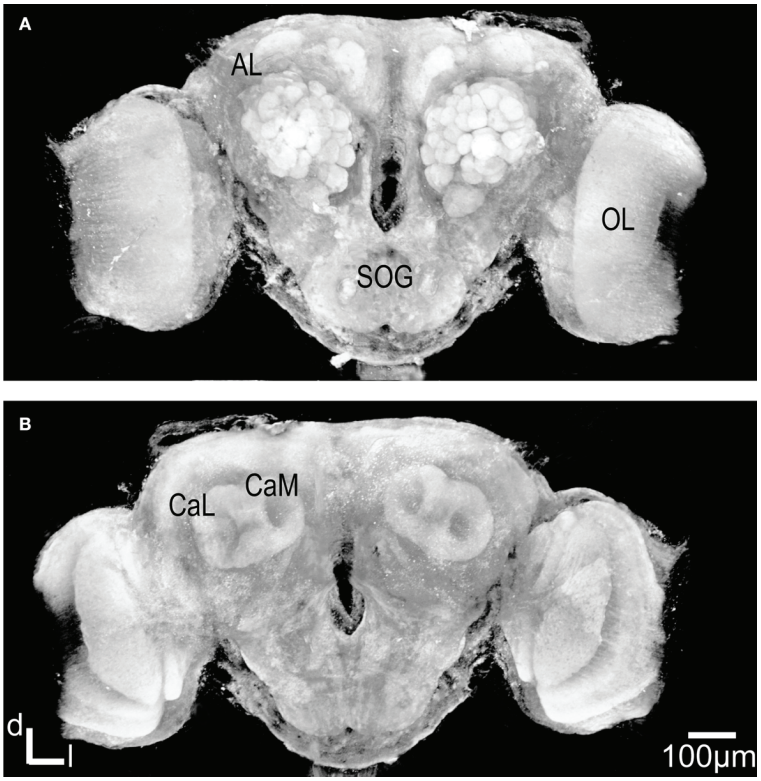

FIGURE 1 | Three dimensional visualisation of the confocal image stack of the *H. virescens* female moth brain. (A) The brain in a frontal view exposing the two antennal lobes (AL) with the numerous glomeruli. **(B)** The brain in posterior view showing the calyces of the mushroom bodies. OL, optic lobes; SOG, suboesophageal ganglion; CaL, lateral calyx; CaM, medial calyx.

recognised in all ALs are the two primary landmarks, the large LPOG and mLPOG, which are given the numbers G38 and G39, respectively, according to Skiri et al. (2005). Posterior of G39 is G53 with five dorso-medially located glomeruli, G58–G62 (**Figures 3J,K**). At the entrance of the antennal nerve, posterior of cLFG, are four recognised glomeruli G51, G52, G56 and G57. Three other glomeruli, G49, G50 and G54, are recognised most dorsal in the AL, and G37, G36 and G35 dorso-medially of the LCCl fibre bundle (**Figures 3G,H**). On the basis of these recognised and identified primary and secondary landmarks, the other 42 glomeruli were identified and given numbers according to the other heliothine atlases (Skiri et al., 2005). This is exemplified in **Figure 3**, showing the clockwise numbering of G1–G23 (**Figures 3A,B**), G24–G34 (**Figures 3D,E**), G35–G48 (**Figures 3G,H**) and G49–G63 (**Figures 3J,K**), appearing in sections from anterior to posterior. In this way, all 62 glomeruli in both *H. virescens* female preparations were found to correspond with the ordinary glomeruli in the atlases of the other heliothine species.

COMPARISON OF NUMBERS AND POSITIONS OF GLOMERULI

Whereas the number of the glomeruli was constant in the ALs of the examined specimens, some variations were found regarding positions and sizes of a few glomeruli. For instance, the position of G1 and G2 is shifted anterior–posterior in the two preparations and the size of G2 and G5 is marked larger in one preparation than in the other (**Figures 3A,B**). Other variations between the two *H. virescens* preparations are the relative positions of G25, G24 and F1 and between G28 and G38. Comparison with the previous *H. virescens* atlas, the differences concern the total number of glomeruli identified as well as the way of numbering the glomeruli. Concerning the female specific glomeruli, only two (cLFG and medially of it the mLFG) were identified by Berg et al. (2002). The eight ordinary glomeruli G11–G13, G25, G34 and G45–G47 in the present atlas were counted as four units in the previous atlas. Oppositely, G62 and G22 in the present atlas seem to be counted as four in the previous atlas. The corresponding numbers of the two atlases are presented in **Table 1**.

MALE SPECIFIC AND ORDINARY GLOMERULI

Like in females, the MGC is located at the entrance of the antennal nerve. As previously described it consists of the cumulus, the dorso-medial and the two ventral glomeruli (**Figures 3C,F**), and differs from the MGC of the two other heliothine species having only three glomeruli (Berg et al., 2002; Skiri et al., 2005). The MGC served as an additional primary landmark in the identification of the ordinary glomeruli. Using the same way of identification as in

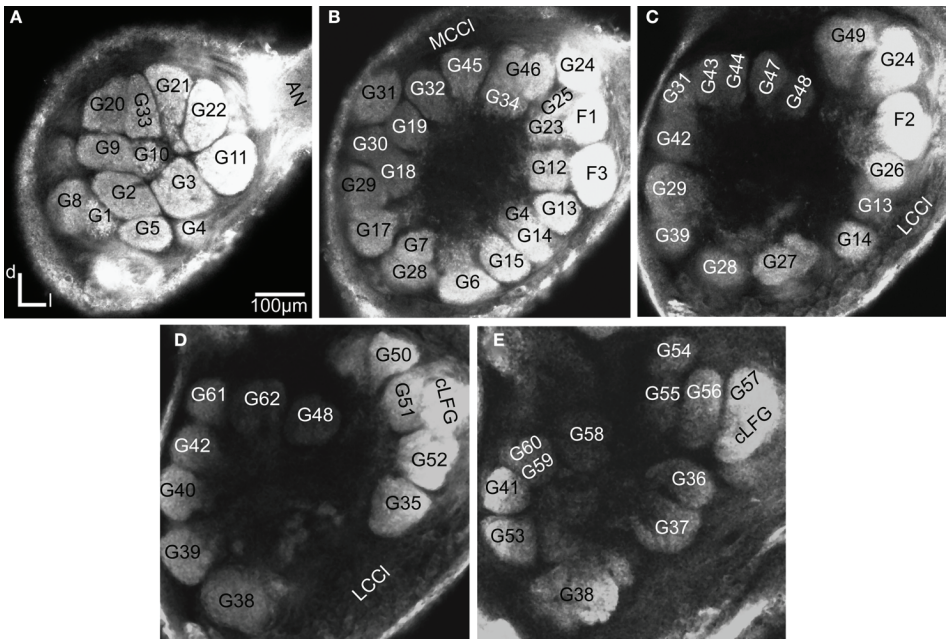

FIGURE 2 | Confocal images at different depths of the right *H. virescens* female antennal lobe, from anterior towards posterior at the following depths: (A) 64 µm, **(B)** 105 µm, **(C)** 144 µm, **(D)** 179 µm, **(E)** 216 µm. Except for G16 all glomeruli are shown. The AL is inverted.

the female AL, 63 ordinary glomeruli were identified in the male AL, of which G1–G62 showed correspondence with the female ordinary glomeruli and G63 being male specific.

INTEGRATION OF THE ANTENNAL LOBE GLOMERULI INTO THE STANDARD BRAIN ATLAS

Registration of the AL glomeruli into the SBA resulted in the new female *H. virescens* SBA with 66 identified glomeruli (SBAGl) (**Figure 4A**).

The two reconstructed female ALs were independently integrated into the SBAGl. After transforming the glomeruli into the SBA, the shape and size of the glomeruli in SBAGl matched the glomerular layer in the SBA. The relative position of the glomeruli was maintained in the transformation process making the glomeruli easily recognisable (**Figures 4B,C**). Thus, they were relabelled and given numbers and colours corresponding to the separate AL atlas. With this new and more detailed anatomical atlas of the *H. virescens* brain, we next wanted to study the specific glomerular innervation of three AL PNs and their projection patterns in the protocerebrum.

INTEGRATION OF ANTENNAL LOBE PROJECTION NEURONS INTO THE SBAGI

The present results include three stained AL PNs registered into the SBAGl (**Figures 5–7**).

These neurons with axons following the IACT are termed PI neurons (Homberg et al., 1988; Rø et al., 2007). The initial registration of each of them into the SBA by transforming the AL as a single material identity revealed the glomerular area of the dendritic innervations in the AL as well as the axonal pathway and branching pattern in the calyces and the lateral protocerebrum. After superposing the glomeruli of the SBAGl, the innervated glomeruli clearly appeared. As exemplified by the neuron shown in **Figures 5A, 6, and 7**, the innervations were identified in three glomeruli, G35, G36 and G37. The dendrite differentially innervated each of the three glomeruli; G37 stronger than G35 and only one branch in G36. The axon following the IACT, passed adjacent and posteriorlaterally to the central body (**Figures 6A,B**). Upon reaching the calyces of the ipsilateral mushroom body, the axon gave off five branches innervating the medial and lateral calyces before turning anteriorlaterally into the lateral protocerebrum, showing a star-like projection pattern. Most branches turned dorsally and only one ventrolaterally into the lateral horn (**Figures 6A–C**), defined as the protrusion from the lateral protocerebrum according to Kvello et al. (2009). The soma was located in the lateral cell cluster close to the innervated glomerulus, G37. A second PN with cell soma in the lateral cluster was registered by the same procedure into the SBAGl (**Figures 5B and 7**). This neuron innervated a single glomerulus identified as G14, located close to its cell body. The axon followed quite closely the axon of the G37 neuron, and also gave off five branches to the calyces before turning anteriorlaterally and extending into the lateral protocerebrum. The same pattern of star-like projections appeared with most branches turning dorsally and one ventrolaterally towards the lateral horn. The third neuron registered into the SBAGl, showed innervation of a single glomerulus identified as G11, located in the anterior part of the AL (**Figures 5C and 7**). The soma was in the anterior

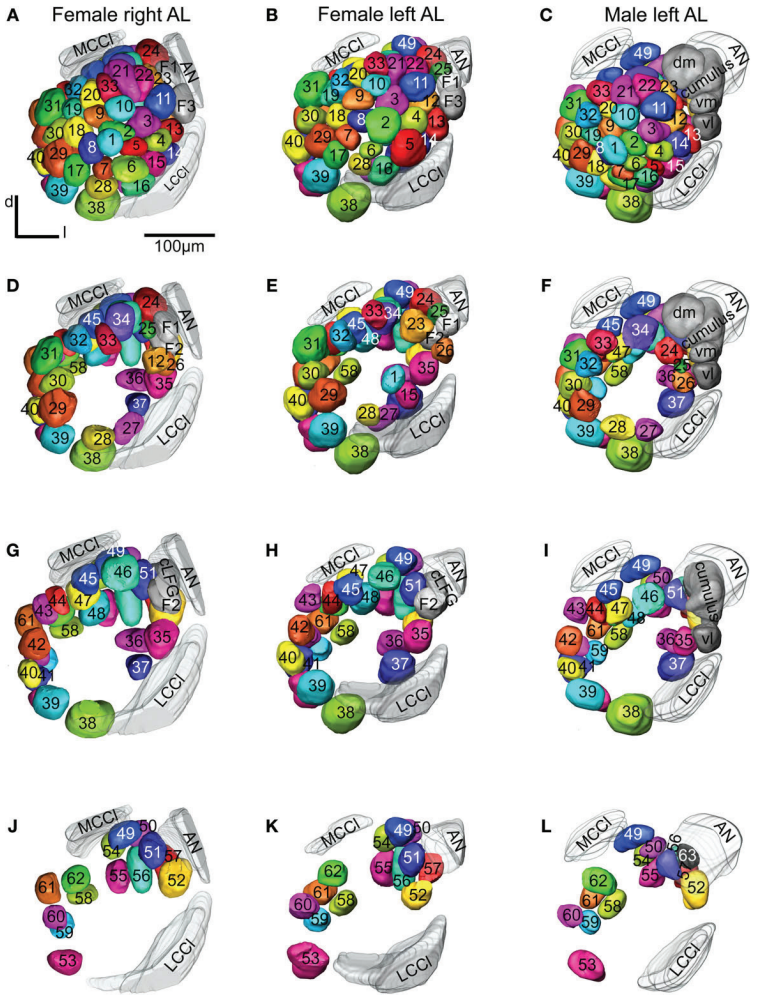

FIGURE 3 | Antennal lobe atlases as 3D reconstructions of two *H. virescens* female (right and left antennal lobe) and one male preparation (left antennal lobe). All glomeruli are reconstructed, identified and given a specific number and colour that corresponded across preparations, including sexes, in accordance with the atlases of two other heliothine species in Skiri et al. (2005). The right and left female and the left male antennal lobes are shown in frontal view at four different sections. **(A–C)** The most anterior part of the three preparations, **(D–L)** the three deeper sections. The right female antennal lobe is inverted for comparison with the left antennal lobe.

cluster, close to the innervated glomerulus. The innervation was extensive throughout the whole glomerulus (**Figure 5C**). The axon followed the IACT sending four branches into the medial and lateral calyces before turning anteriorlaterally towards the lateral protocerebrum, where it projected in the typical star-like pattern with most branches extending dorsally and one ventrolaterally into the lateral horn.

Comparison of the three neurons in the SBAGl shows their relative position from the different glomerular innervation to their projections in the calyces and the lateral protocerebrum (**Figure 7**). The two neurons innervating the more posteriorventrally located G35, G36, G37 and G14, respectively, with soma in the lateral cell cluster have axons running in a ventral pathway into the protocerebrum. The axon of the neuron innervating the dorsoanterior G11 with soma in the anterior cluster runs more dorsally in the AL and protocerebrum before joining the other axons in the IACT anteriorly and close to the central body. The axonal projections of the three neurons in the calyces intermingle, whereas in the lateral protocerebrum the axonal projections appears organised in a dorsoventral axis with partly overlap. The projections of the G14 neuron are dorsally to those of the G11 neurons, which are again dorsally to those of the G37 neuron.

Table 1 | Glomeruli of *H. virescens* antennal lobe atlases with corresponding numbers in the new and the previous atlas.

New atlas F and M	Previous atlas		New atlas F and M	Previous atlas	
	F	M		F	M
G1	G1	G8	G36	G45	G57
G2	G7	G3	G37	G37	G41
G3	G57	G6	G38	G19	G39
G4	G8	G2	G39	G21	G35
G5	G2	G7	G40	G22	G42
G6	G6	G17	G41	G43	G48
G7	G3	G23	G42	G42	G47
G8	G4	G1	G43	G24	G38
G9	G5	G12	G44	G23	G40
		G18	G45	G33[1]	G33
G10	G11	G5	G46	G32[1]	G24[1]
G11	G58[1]	G4	G47	G33[1]	G45
G12	G36[1]	G22	G48	G26	G53
G13	G36[1]	G25	G49	G54	G54[1]
G14	G30	G10	G50	G39	G55
G15	G18	G19	G51	G41	[3]
G16	G9	G21[1]	G52	G38	G58
G17	G20	G16			G59
G18	G12	G15	G53	G44	G36
G19	G27	G26			G49
G20	G15	G27	G54	G53	G54[1]
G21	G17	G13	G55	G52	[3]
G22	G32[2]	G9	G56	G51	G56
	G60	G62	G57	G40	G60
G23	G59	G11			G61
G24	mLFG	[3]	G58	G48	[3]
G25	G58[1]	G14	G59	G50	G51
G26	G35	G43	G60	G49	G46
G27	G28	G32	G61	G47	G50
		G21[2]	G62	G55	G52
G28	G10	G31		G56	
G29	G14	G28	G63		Cumulus[2]
		G34	Cumulus		Cumulus[1]
G30	G13	G30	dm		dm
G31	G25	G29	vm		vm
G32	G29	G37[1]	cLFG	cLFG	
G33	G16	G20	F1	G31	
		G37[2]	F2	G34	
G34	G32[1]	G24[1]	F3	[3]	
G35	G46	G44			

F, female; M, male.
[1]Two glomeruli counted as one.
[2]Includes a part of adjacent glomerulus.
[3]Glomeruli not found.

DISCUSSION

ANTENNAL LOBE GLOMERULI INTEGRATED INTO THE STANDARD BRAIN ATLAS

How glomerular activity in the primary olfactory centres represents odour information and how this topographic organisation is further reflected in higher olfactory areas, are central questions in studies on the functional organisation of vertebrate as well as insect olfactory systems. A major challenge is to map in higher olfactory brain neuropils the target areas of the primary olfactory centre's output neurons, according to the glomerular input; in *Drosophila* made possible by the use of molecular labelling of PNs (Wong et al., 2002; Tanaka et al., 2004; Jefferis et al., 2007). In the honeybee and the moth *H. virescens*, whole brain standard atlases have been demonstrated as helpful tools in determining the projections in the calyces and the lateral protocerebrum of AL PNs (Brandt et al., 2005; Kvello et al., 2009). Particularly in the lateral protocerebrum with no visible substructures, integrated PNs from different preparations give important information about their relative positions. However, because of the low resolution confocal scans used for creating the whole brain atlases, separate atlases with higher resolution are better suited for determining the PNs input and output regions, respectively. By integration of the AL glomeruli into the *H. virescens* SBA as shown in the present study, the PN input and output regions were standardised in this common framework, SBAGl. This integration process was facilitated by the fact that the AL of this atlas included the glomerular layer only, excluding tracts and cell clusters; different from the four other atlases. Therefore, the AL atlas glomeruli could be directly registered into the SBA, after being assigned a single material identity. Since the relative position of the glomeruli was maintained in the transformation process, all 66 glomeruli could easily be recognised, relabelled and numbered according to the AL atlas (**Figure 4**). The anatomically more detailed SBAGl provides a stronger basis for studying the specific innervations in the AL as well as the connections to higher brain areas, like the calyces and the lateral protocerebrum.

ANTENNAL LOBE PROJECTION NEURONS INTEGRATED INTO THE SBAGI

In principle, the integration of reconstructed AL neurons into the SBAGl is a two-step process as described for the neurons presented in **Figures 5–7**. The first step constitutes a registration into the SBA which guides the localisation of the dendritic innervation to a particular area of the AL. Then, superposing the SBAGl reveals the innervated glomeruli. This procedure used for the well stained preparations in the present study allowed verification of the glomerular innervation in confocal images. This means that the procedure can be used even for preparations where glomeruli may not be well distinguished, as long as the glomerular borderline is clearly detectable. The well stained preparations in the present study made reconstruction of the innervated and landmark glomeruli possible. The registration of these glomeruli into the SBAGl resulted in a precise position of the dendritic innervation within the glomeruli. Thus, the SBAGl is an extended and more elaborate tool that together with the confocal images expands the possibility for making accurate judgments of dendritic arborisation and identification of the innervated glomeruli.

In addition to the high resolution model of the AL facilitating the identification of glomerular innervation, the SBAGl also provides the frame for visualising the relative position of whole neurons in the brain. As shown in **Figures 6 and 7**, the details on the neuronal pathways are for instance visualised by the different axonal trajectories in the AL before joining in the IACT. The uniglomerular innervation and extensive branching throughout the glomerulus as

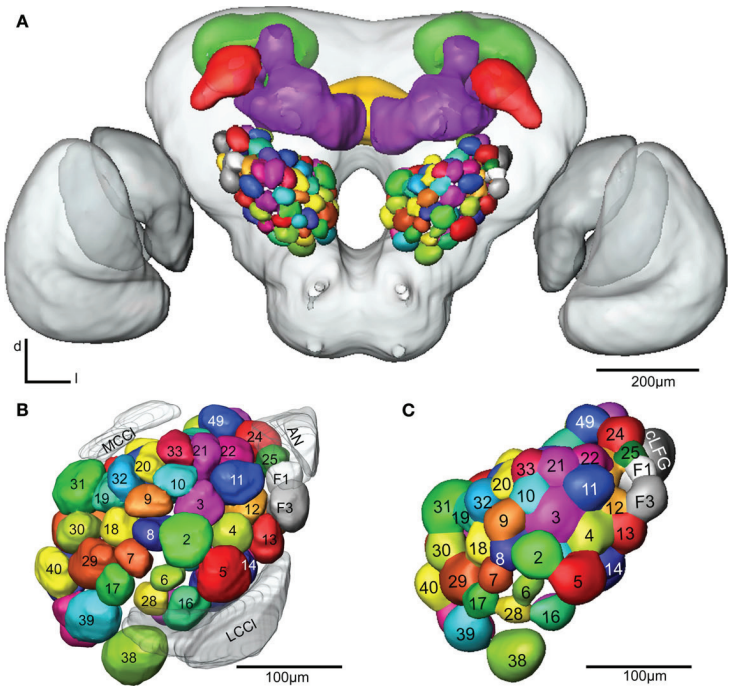

FIGURE 4 | (A) The female H. virescens standard brain atlas with the glomeruli of one left and one right antennal lobe integrated. **(B,C)** The left female antennal lobe atlas with numbered glomeruli and cell clusters, showing the glomerular layer before **(B)** and after **(C)** registration into the standard brain atlas.

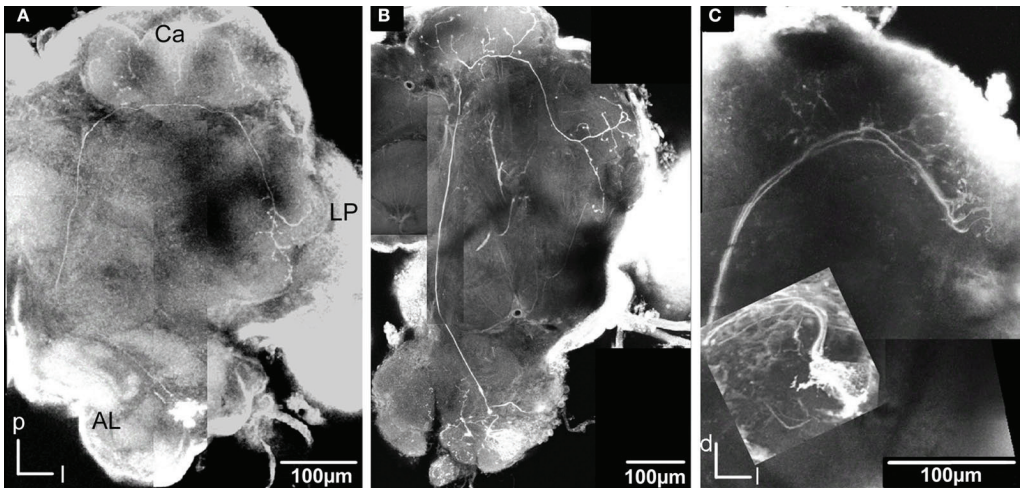

FIGURE 5 | Stacks of confocal images of three preparations each with one stained projection neuron having axon in the inner antennocerebral tract. **(A)** Dorsal view: This neuron innervated three glomeruli (G35, G36 and G37) and projected in the calyces with five branches (three visible) before turning anterior-laterally and projecting in lateral protocerebrum. **(B)** Dorsal view: This neuron innervated G14 and projected in calyces with five branches before turning anterior-laterally into the lateral protocerebrum. The starlike projection with dorsal branches as well as a single ventral branch into the lateral horn is visible. **(C)** Frontal view: This neuron (co stained with a second neuron, from Kvello et al., 2009) innervated G11. The projection in the calyces and the lateral protocerebrum is shown.

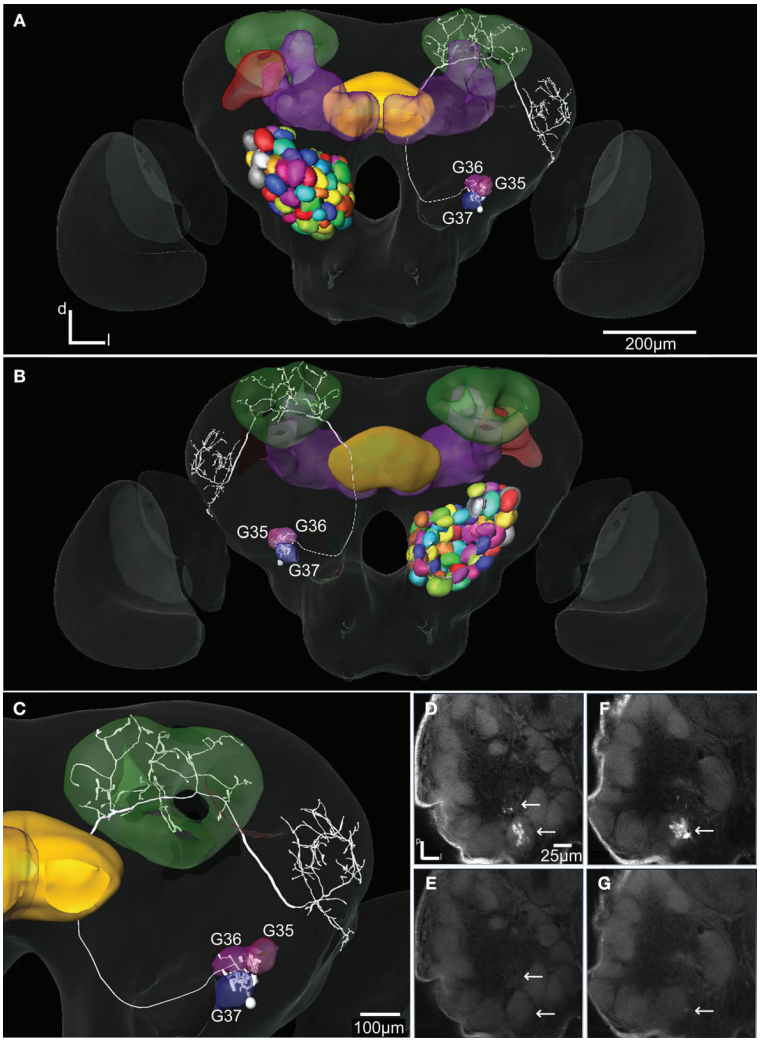

FIGURE 6 | The *H. virescens* standard brain atlas with one integrated antennal lobe projection neuron (the same as in Figure 5A). (A) Frontal view. **(B)** Posterior view. **(C)** Magnified frontal view showing the innervated glomeruli and projection pattern in the medial and lateral calyces and in the lateral protocerebrum. **(D–G)** Confocal images showing the triple glomerular innervation in two different sections scanned with two channels. **(D)** Micro-ruby staining showing the innervation of glomeruli G37 and G36. **(E)** Synapsin staining visualising the glomeruli of the same section. **(F)** Micro-ruby staining showing the innervation of glomerulus G35. **(G)** Synapsin staining visualising the glomeruli of the same section. Arrows indicate innervated glomeruli.

shown for the G11 and G14 neurons are typical features for IACT PNs (category PIa in Homberg et al., 1988; Rø et al., 2007). These neurons found in most insect species belong to a conserved group of PNs (Schachtner et al., 2005). IACT neurons innervating a few adjacent glomeruli have also been identified in *H. virescens* (category PIc in Rø et al., 2007), similar to the G37 neuron with dendritic arborisations in the two adjacent glomeruli, G35 and G36. The innervation pattern in protocerebrum, shown for the three neurons in **Figure 7**, is typical for IACT neurons. As previously described, they send three to five branches into the calyces and extend the axon into the lateral protocerebrum ending in a star-like projection, where most branches project dorsally and one branch ventrolaterally towards or into the lateral horn, like the IACT neurons in the present study. By using the SBAGl combined with registration algorithms for integrating the neurons we have here found that the three IACT neurons innervate distinct but overlapping areas

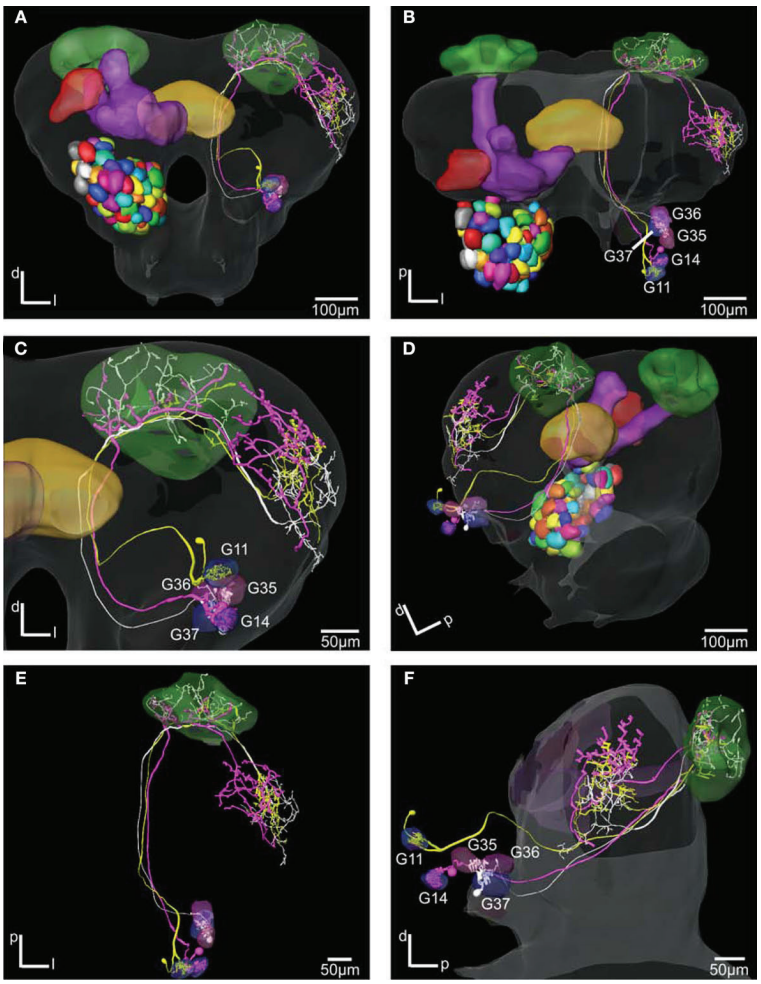

FIGURE 7 | The *H. virescens* standard brain atlas with three antennal lobe projection neurons integrated. (A,C) Frontal view. **(B,E)** Dorsal view. **(D)** Posterior lateral view. **(F)** Lateral view. The relative positions of the innervated glomeruli and projections as well as the axonal pathways are shown in the different views. The projections pattern in the lateral protocerebrum in different but overlapping areas along a dorsoventral axis appears particularly in **(C)** and **(F)**. The dorsal axonal pathway in the antennal lobe of the G11 neuron before joining the other axons in the inner antennocerebral tract is clearly seen in **(A)** and **(B)**.

along a dorsoventral axis in the lateral protocerebrum (**Figure 7**). Whether this organisation is consistent with the actual organisation or due to methodological limitations remains to be verified. In contrast, the two PNs innervating the same glomerulus showed intermingled projections in the same area (Kvello et al., 2009). A similar principle for the organisation of PN projections is found in the lateral horn of *Drosophila*, where molecularly labelled neurons innervating the same glomerulus exhibited similar axonal topography, whereas neurons from different glomeruli displayed different projection patterns (Wong et al., 2002). A further division of the lateral horn in *Drosophila* into sub-regions according to different PN projection clusters is described by Jefferis et al. (2007). How the projection pattern of PN populations in *H. virescens* are organised in the lateral protocerebrum according to the innervated glomeruli as well to the different tracts, are interesting questions to be resolved when more PNs have been integrated into the SBAGl.

COMPARISON OF ANTENNAL LOBE ATLASES BETWEEN SEXES AND SPECIES

In the present study we provided a new atlas of the AL of *H. virescens* females, based on the numbering system of two other heliothine moth species (Skiri et al., 2005). In general, the challenge in this kind of work is to detect the borders between the glomeruli. The difference from the previous *H. virescens* atlas in

respect to the number of glomeruli included seems to be due to the lack of detectable borderlines between pairs of glomeruli in the lower resolution confocal images of the previous atlas (Berg et al., 2002). The glomeruli in the present *H. virescens* atlas showed a striking correspondence with the glomeruli of the atlases of the two other heliothine species (Skiri et al., 2005), which is the basis for the identification of the glomeruli with corresponding numbers. Thus, the new *H. virescens* atlas is more reliable for identifying the glomeruli innervated by a neuron, as well as suited for comparing the results between heliothine species. For instance, a challenging question is whether corresponding glomeruli in the three species also receive and process information about the same odorants or the odorant specificity has changed through evolution. An interesting example on possibly conserved specificity is for the large LPOG or G38, present in the typical position in the AL of lepidopteran species, and in *Manduca sexta* shown to be involved in mediating information about CO_2 (Gurenstein et al., 2004). The male AL atlas included in this study provides a basis for detecting similarities and differences with the female olfactory system both concerning morphology and physiology. Interestingly, except for one additional glomerulus, G63, in the male AL, the numerous ordinary glomeruli corresponded well between the two sexes as well as between the species. Because of this correspondence within and between sexes and species (all together 12 individual ALs), we find that the present results are reliable as concerns numbers and relative positions of the glomeruli. In the present study we have integrated the AL glomeruli into the SBA of *H. virescens* and shown its suitability for integrating and visualising AL neurons. So far, we have only registered PNs of the IACT, showing their relative positions. The intention is to integrate physiologically characterised PNs of all tracts for relating glomerular innervation in the AL to axonal projections in the protocerebrum. Functional similarities and differences among the PNs may in this way be related to specific input, output or ACTs, the latter associated with functionally different PNs in the honeybee (Müller et al., 2002). In a previous study, we have compared the spatial relationship between a few olfactory and gustatory neurons showing adjacent projection areas in the lateral protocerebrum (Kvello et al., 2009). Thus, integration of more physiologically characterised chemosensory neurons may visualise the neuronal network underlying chemosensory coding in this moth species.

ACKNOWLEDGMENTS

The project was financed by the Royal Norwegian Society of Sciences and Letters. We also acknowledge Dr. Hanne Skiri for help with making the AL atlas, Prof. Erich Buchner (Universität Würzburg, Germany) for providing antibodies, and the Insect Rearing Team of Syngenta (Basel, Switzerland) for providing insect materials.

REFERENCES

Anton, S., and Hansson, B. S. (1999). Physiological mismatching between neurons innervating olfactory glomeruli in a moth. *Proc. R. Soc. Lond., B, Biol. Sci.* 266, 1813–1820.

Anton, S., and Homberg, U. (1999). Antennal lobe structure. In Insect Olfaction, B. S. Hansson, ed. (Berlin, Springer), pp. 97–124.

Axel, R. (1995). The molecular logic of smell. *Sci. Am.* 273, 154–159.

Berg, B. G., Almaas, T. J., Bjaalie, J. G., and Mustaparta, H. (1998). The macroglomerular complex of the antennal lobe in the tobacco budworm moth *Heliothis virescens*: specified subdivision in four compartments according to information about biologically significant compounds. *J. Comp. Physiol. A* 183, 669–682.

Berg, B. G., Galizia, C. G., Brandt, R., and Mustaparta, H. (2002). Digital atlases of the antennal lobe in two species of tobacco budworm moths, the oriental *Helicoverpa assulta* (male) and the American *Heliothis virescens* (male and female). *J. Comp. Neurol.* 446, 123–134.

Brandt, R., Rohlfing, T., Rybak, J., Krofczik, S., Maye, A., Westerhoff, M., Hege, H. C., and Menzel, R. (2005). Three-dimensional average-shape atlas of the honeybee brain and its applications. *J. Comp. Neurol.* 492, 1–19.

Buck, L. B. (2000). The molecular architecture of odor and pheromone sensing in mammals. *Cell* 100, 611–618.

Chiang, A.-S., Liu, Y.-C., Chiu, S.-L., Hu, S. H., Huang, C.-Y., and Hsieh, C.-H. (2001). Three-dimensional mapping of brain neuropils in the cockroach, *Diploptera punctata*. *J. Comp. Neurol.* 440, 1–11.

Christensen, T. A., and Hildebrand, J. G. (2002). Pheromonal and host-odor processing in the insect antennal lobe: how different? *Curr. Opin. Neurobiol.* 12, 393–399.

Clyne, P. J., Warr, C. G., Freeman, M. R., Lessing, D., Kim, J., and Carlson, J. R. (1999). A novel family of divergent seven-transmembrane proteins: candidate odorant receptors in *Drosophila*. *Neuron* 22, 327–338.

el Jundi, B., Heinze, S., Lenschow, C., Kurylas, A., Rohlfing, T., and Homberg, U. (2010). The locust standard brain: a 3D standard of the central complex as a platform for neural network analysis. *Front. Syst. Neurosci.* 3:21. doi: 10.3389/neuro.06.021.2009.

el Jundi, B., Huetteroth, W., Kurylas, A. E., and Schachtner, J. (2009). Anisometric brain dimorphism revisited: implementation of a volumetric 3D standard brain in *Manduca sexta*. *J. Comp. Neurol.* 517, 210–225.

Evers, J. F., Schmitt, S., Sibila, M., and Duch, C. (2004). Progress in functional neuroanatomy: precise automatic geometric reconstruction of neuronal morphology from confocal image stacks. *J. Neurophysiol.* 93, 2331–2342.

Flanagan, D., and Mercer, A. R. (1989). An atlas and 3-D reconstruction of the antennal lobes in the worker honey bee, *Apis mellifera* L. (*Hymenoptera*: Apidae). *Int. J. Insect. Morphol. Embryol.* 18, 145–159.

Galizia, C. G., McIlwrath, S. L., and Menzel, R. (1999). A digital three-dimensional atlas of the honeybee antennal lobe based on optical sections acquired by confocal microscopy. *Cell Tissue Res.* 295, 383–394.

Galizia, C. G., and Menzel, R. (2000). Probing the olfactory code. *Nat. Neurosci.* 3, 853–854.

Galizia, C. G., Sachse, S., and Mustaparta, H. (2000). Calcium responses to pheromones and plant odours in the antennal lobe of the male and female moth *Heliothis virescens*. *J. Comp. Physiol. A* 186, 1049–1063.

Greiner, B., Gadenne, C., and Anton, S. (2004). Three-dimensional antennal lobe atlas of the male moth, *Agrotis ipsilon*: a tool to study structure–function correlation. *J. Comp. Neurol.* 475, 202–210.

Gurenstein. P. G., Christensen. T. A., and Hildebrand. J. G. (2004). Sensory processing of ambient CO_2 information in the brain of the moth *Manduca sexta*. *J. Comp. Physiol.* A. 190, 707–725.

Heisenberg, M. (2003). Mushroom body memoir: from maps to models. *Nat. Rev. Neurosci.* 4, 266–275.

Hildebrand, J. G., and Shepherd, G. M. (1997). Mechanisms of olfactory discrimination: converging evidence for common principles across phyla. *Annu. Rev. Neurosci.* 20, 595–631.

Homberg, U., Montague, R. A., and Hildebrand, J. G. (1988). Anatomy of antenno-cerebral pathways in the brain of the sphinx moth *Manduca sexta*. *Cell Tissue Res.* 254, 255–281.

Huetteroth, W., and Schachtner, J. (2005). Standard three-dimensional glomeruli of the *Manduca sexta* antennal lobe: a tool to study both developmental and adult neuronal plasticity. *Cell Tissue Res.* 319, 513–524.

Iyengar, B. G., Chou, C. J., Sharma, A., and Atwood, H. L. (2006). Modular neuropile organization in the *Drosophila* larval brain facilitates identification and mapping of central neurons. *J. Comp. Neurol.* 499, 583–602.

Jefferis, G. S. X. E., Potter, C. J., Chan. A. I., Marin, E. C., Rohlfing, T., Maurer, C. R., and Luo, L. Q. (2007). Comprehensive maps of *Drosophila* higher olfactory centers: spatially segregated fruit and pheromone representation. *Cell* 128, 1187–1203.

Kanzaki, R., Soo, S., Seki, Y., and Wada, S. (2003). Projections to higher olfactory centers from subdivisions of the antennal lobe macroglomerular complex of the male silkmoth. *Chem. Senses* 28, 113–130.

Kazawa, T., Namiki, S., Fukushima, R., Terada, M., Soo, K., and Kanzaki, R. (2009). Constancy and variability of glomerular organization in the antennal lobe of the silkmoth. *Cell Tissue Res.* 336, 119–136.

Kloppenburg, P., and Mercer, A. R. (2008). Serotonin modulation of moth central olfactory neurons. *Annu. Rev. Entomol.* 53, 179–190.

Kurylas, A. E., Rohlfing, T., Krofczik, S., Jenett, A., and Homberg, U. (2008). Standardized atlas of the brain of the desert locust, *Schistocerca gregaria*. *Cell Tissue Res.* 33, 125–145.

Kvello, P., Løfaldli, B. B., Rybak, J., Menzel, R., and Mustaparta, H. (2009). Digital, three-dimensional average shaped atlas of the *Heliothis virescens* brain with integrated gustatory and olfactory neurons. *Front. Syst. Neurosci.* 3:14. doi: 10.3389/neuro.06.014.2009.

Laissue, P. P., Reiter, C., Hiesinger, P. R., Halter, S., Fischbach, K. F., and Stocker, R. F. (1999). Three-dimensional reconstruction of the antennal lobe in *Drosophila melanogaster*. *J. Comp. Neurol.* 405, 543–552.

Laurent, G., Wehr, M., and Davidowitz, H. (1996). Temporal representations of odors in an olfactory network. *J. Neurosci.* 16, 3837–3847.

Lledo, P.-M., Gheusi, G., and Vincent, J.-D. (2005). Information processing in the mammalian olfactory system. *Physiol. Rev.* 85, 281–317.

Masante-Roca, I., Gadenne, C., and Anton, S. (2005). Three-dimensional antennal lobe atlas of male and female moths, *Lobesia botrana* (Lepidoptera: Tortricidae) and glomerular representation of plant volatiles in females. *J. Exp. Biol.* 208, 1147–1159.

Menzel, R. (2001). Searching for the memory trace in a mini-brain, the honeybee. *Learn. Mem.* 8, 53–62.

Mombaerts, P. (2001). How smell develops. *Nat. Neurosci.* 4, 1192–1198.

Müller, D., Abel, R., Brandt, R., Zöckler, M., and Menzel, R. (2002). Differential parallel processing of olfactory information in the honeybee, *Apis mellifera* L. *J. Comp. Physiol.* A. 188, 359–370.

Mustaparta, H. (2002). Encoding of plant odour information in insects: peripheral and central mechanisms. *Entomol. Exp. Appl.* 104, 1–13.

Mustaparta, H., and Stranden, M. (2005). Olfaction and learning in moths and weevils living on angiosperm and gymnosperm hosts. *Recent Adv. Phytochem.* 39, 269–292.

Rein, K., Zöckler, M., Mader, M. T., Grübel, C., and Heisenberg, M. (2002). The *Drosophila* standard brain. *Curr. Biol.* 12, 227–231.

Reischig, T., and Stengl, M. (2002). Optic lobe commissures in a three-dimensional brain model of the cockroach *Leucophaea maderae*: a search for the circadian coupling pathways. *J. Comp. Neurol.* 443, 388–400.

Rø, H., Müller, D., and Mustaparta, H. (2007). Anatomical organization of antennal lobe projection neurons in the moth *Heliothis virescens*. *J. Comp. Neurol.* 500, 658–675.

Rospars, J. P., and Chambille, I. (1981). Deutocerebrum of the cockroach *Blaberus craniifer* burm. Quantitative study and automated identification of the glomeruli. *J. Neurobiol.* 12, 221–247.

Rospars, J. P., and Hildebrand, J. G. (2000). Sexually dimorphic and isomorphic glomeruli in the antennal lobes of the sphinx moth *Manduca sexta*. *Chem. Senses* 25, 119–129.

Røstelien, T., Stranden, M., Borg-Karlson, A.-K., and Mustaparta, H. (2005). Olfactory receptor neurones in two heliothine moth species responding selectively to aliphatic green leaf volatiles, aromatics, monoterpenes and sesquiterpenes of plant origin. *Chem. Senses* 30, 443–461.

Sadek, M. M., Hansson, B. S., Rospars, J. P., and Anton, S. (2002). Glomerular representation of plant volatiles and sex pheromone components in the antennal lobe of the female *Spodoptera littoralis*. *J. Exp. Biology*. 205, 1363–1376.

Schachtner, J., Schmidt, M., and Homberg, U. (2005). Organization and evolutionary trends of primary olfactory brain centers in Tetraconata (Crustacea + Hexapoda). *Arthropod Struct. Dev.* 34, 257–299.

Schmitt, S., Evers, J. F., Duch, C., Scholz, M., and Obermayer, K. (2004). New methods for the computer-assisted 3-D reconstruction of neurons from confocal image stacks. *Neuroimage* 23, 1283–1298.

Skiri, H. T., Rø, H., Berg, B. G., and Mustaparta, H. (2005). Consistent organization of glomeruli in the antennal lobes of related species of heliothine moths. *J. Comp. Neurol.* 491, 367–380.

Smid, H. M., Bleeker, M. A., Van Loon, J. J. A., and Vet, L. E. (2003). Three-dimensional organization of the glomeruli in the antennal lobe of the parasitoid wasps *Cotesia glomerata* and *C. rubecula*. *Cell Tissue Res.* 312, 237–248.

Stocker, R. F, Lienhard, M. C., Borst, A., and Fischbach, K. F. (1990). Neuronal architecture of the antennal lobe in *Drosophila melanogaster*. *Cell Tissue Res.* 262, 9–34.

Stopfer, M. (2007). Olfactory processing: massive convergence onto sparse codes. *Curr. Biol.* 17, 363–364.

Tanaka, N. K., Awasaki, T., Shimada, T., and Ito, K. (2004). Integration of chemosensory pathways in the *Drosophila* second-order olfactory centers. *Curr. Biol.* 14, 449–457.

Toga, A. W. (2002). Neuroimage databases: the good, the bad and the ugly. *Nat. Rev. Neurosci.* 3, 302–309.

Toga, A. W., and Thompson, P. M. (2001). Maps of the brain. *Anat. Rec.* 265, 37–53.

Van Essen, D. C. (2002). Windows on the brain: the emerging role of atlases and databases in neuroscience. *Curr. Opin. Neurobiol.* 12, 574–579.

Varela, N., Couton, L., Gemeno, C., Avilla, J., Rospars, J. P., and Anton, S. (2009). Three-dimensional antennal lobe atlas of the oriental fruit moth, *Cydia molesta* (Busck) (Lepidoptera: Tortricidae): comparison of male and female glomerular organization. *Cell Tissue Res.* 337, 513–526.

Vickers, N. J., and Christensen, T. A. (2003). Functional divergence of spatially conserved olfactory glomeruli in two related moth species. *Chem. Senses* 28, 325–338.

Vickers, N. J., Christensen, T. A., and Hildebrand, J. G. (1998). Combinatorial odor discrimination in the brain: Attractive and antagonist odor blends are represented in distinct combinations of uniquely identifiable glomeruli. *J. Comp. Neurol.* 400, 35–56.

Vosshall, L. B., Amrein, H., Morozov, P. S., Rzhetsky, A., and Axel, R. (1999). A spatial map of olfactory receptor expression in the *Drosophila* antenna. *Cell* 96, 725–736.

Vosshall, L. B., and Stocker, R. F. (2007). Molecular architecture of smell and taste in *Drosophila*. *Annu. Rev. Neurosci.* 30, 505–533.

Wilson, R. I., and Mainen, Z. F. (2006). Early events in olfactory processing. *Annu. Rev. Neurosci.* 29, 163–201.

Wong, A. M., Wang, J. W., and Axel, R. (2002). Spatial representation of the glomerular map in the *Drosophila* protocerebrum. *Cell* 109, 229–241.

Conflict of Interest Statement: The authors declare that the research was conducted in the absence of any commercial or financial relationships that could be construed as a potential conflict of interest.

Received: 05 December 2009; paper pending published: 18 January 2010; accepted: 26 January 2010; published online: 12 Febuary 2010.

*Citation: Løfaldli BB, Kvello P and Mustaparta H (2010) Integration of the antennal lobe glomeruli and three projection neurons in the standard brain atlas of the moth Heliothis virescens. Front. Syst. Neurosci. **4**:5. doi: 10.3389/neuro.06.005.2010*

Paper III

frontiers IN SYSTEMS NEUROSCIENCE

A putative neuronal circuit handling information about a ten component plant odor blend in the brain of H. virescens

Bjarte Bye Løfaldli, Pål Kvello, Nicholas Kirkerud and Hanna Mustaparta

Standard Text:	This Provisional PDF corresponds to the article as it appeared upon acceptance, after rigorous peer-review. Fully formatted PDF and full text (HTML) versions will be made available soon.
Journal Name:	Frontiers in Systems Neuroscience
ISSN:	1662-5137
Article type:	Original Research Article
Received on:	03 Apr 2012
Frontiers website link:	www.frontiersin.org

A putative neuronal circuit handling information about a ten component plant odor blend in the brain of *H. virescens*

Authors
Bjarte Bye Løfaldli[1,2,3], Pål Kvello, Nicholas Kirkerud and Hanna Mustaparta[1]*

Institutional affiliation

[1]Neuroscience Unit, Department of Biology, Norwegian University of Science and Technology, Trondheim, Norway

Abbreviated title
A putative circuit in *H. virescens*

Key words
Insect olfaction, protocerebral neurons, antenno-protocerebral tracts, lateral protocerebrum, superior protocerebrum, descending neuron and odor mixture.

Figures/tables: 11/2
Words in manuscript/characters in abstract: 9375/1121

[2]Bjarte Bye Løfaldli
Norwegian University of Science and Technology
The Faculty of Medicine,
Kavli Institute for Systems Neuroscience/
Centre for Biology of Memory, MTFS
Olav Kyrres gt. 9,
NO-7030 Trondheim, Norway
Bjarte.lofaldli@ntnu.no

[3]High resolution figures, reconstructions and files from the standard brain project are available by contact at the following blog address: http://olfactoryblog.wordpress.com/ or by email: olfactoryblog@gmail.com.

*** Correspondence:**
Prof. Hanna Mustaparta
Norwegian University of Science and Technology
Department of Biology
Neuroscience Unit, MTFS
Olav Kyrres gt. 9,
No-7030 Trondheim, Norway
hanna.mustaparta@bio.ntnu.no

Abstract
The olfactory pathway in the insect brain is anatomically well described from the antennal lobe to the mushroom bodies and the lateral protocerebrum in several species. Less is known about the further connections of the olfactory network in protocerebrum and how information about relevant plant odorants and mixtures are represented in this network, resulting in output information mediated by descending neurons. In the present study we have recorded intracellularly followed by dye injections from neurons in the lateral- and superior protocerebrum of the moth, *Heliothis virescens*. As relevant stimuli, we have used selected primary plant odorants and mixtures of them. The results provide the morphology and physiological responses of neurons involved in a putative circuit connecting the mushroom body lobes, the superior and the lateral protocerebrum, as well as input to superior and lateral protocerebrum by one multiglomerular antennal lobe neuron and output from the lateral protocerebrum by one descending neuron. All neurons responded to one particular mixture of ten primary plant odorants, some neurons also to single odorants of the mixture. Altogether, the physiological data suggest a combinatorial coding mechanism involved in handling information about this mixture of primary plant odorants.

Introduction
The intimate relationship between insects and plants relies to a large extent on plant produced chemical cues and sophisticated olfactory and gustatory systems evolved in insects. The importance of these senses is reflected in the numerous sensory organs, sensilla, on the various appendages and the large areas of the brain devoted to chemosensory coding and learning. Important questions in studying olfactory and gustatory mechanisms concerns stimulation with relevant odorants and tastants involved in attraction and selection of host plants, how receptor neurons detect the large diversity of odour and taste molecules, and how innate and learned odour and taste information is handled in the brain, resulting in particular motor output and behaviour.

The olfactory system of many insect species is anatomically and partly functionally described with common structures and organisation, from receptor neurons projecting in the primary olfactory centre, the antennal lobe (AL), to the second order olfactory areas in protocerebrum, like the mushroom bodies (MB), the lateral- and the superior protocerebrum (LP and SP) (Galizia and Rössler, 2010). As shown in the fruit fly (*Drosophila melanogaster*) and other species, the olfactory receptor neurons (ORNs); consists of subtypes, each subtype expressing one and the same type of receptor proteins and sending their primary axons to one specific glomerulus, exceptionally two, in the AL (Vosshall et al., 1999; Vosshall and Stocker, 2007). Thus, each glomerulus is considered to receive odour information from one type of ORNs. The number of glomeruli is species specific, like 43 in the fruit fly, 60-67 in moth species, including *H. virescens* (66 in females), and 160 in the honeybee (*Apis melifera*) (Flanagan and Mercer, 1989; Stocker et al., 1990; Berg et al., 2002; Løfaldli et al., 2010). The information is processed in the neuronal network formed by the synapses between the ORNs and the local and projection neurons (LNs and PNs) in the AL, and modulated by centrifugal neurons also innervating the glomeruli. Like in most insect species studied, the majority of PNs in moths are uniglomerular, innervating single glomeruli, in contrast to the multiglomular PNs present

in a smaller number (Homberg et al., 1988; Stocker et al., 1990; Jefferis et al., 2007; Rø et al., 2007). The processed information is then mediated to the protocerebral areas, mainly via three parallel antenno-protocerebral tracts (APTs), the medial (also called the inner antenno-cerebral tract ACT), the lateral (also called the outer ACT) and the medio-lateral APT. Whereas the medial and the lateral APT both project in the calyces of the MB and in the LP lobe, but in opposite order, the mediolateral APT projects in the LP and the SP, avoiding the calyces of the MB (Homberg et al., 1988; Kirschner et al., 2006; Rø et al., 2007; Galizia and Rössler, 2010).

The MB has been studied particularly in social insects, like honeybees and ants, because of its importance in learning and memory (Heisenberg et al., 1985; Menzel, 2001; Heisenberg, 2003; Gerber et al., 2004). The dendrites of the numerous kenyon cells, receiving information from the PNs of the AL, form the calyces, and the axons the peduncle and the lobe system that is divided into several subsystem of the medial and vertical lobes (Ito et al., 1998; Strausfeld, 2002; Fukushima and Kanzaki, 2009). Several types of extrinsic MB neurons have been morphologically described with dendritic innervations along the pedunculus and the lobes and axon projecting in other protocerebral areas, like the LP (Homberg, 1984; Ito et al., 1998; Li and Strausfeld, 1999; Tanaka et al., 2008). One physiologically characterised MB extrinsic neuron, the PE1 of the honeybee projecting in LP as well as other areas, is particularly interesting by showing changed responses after odour conditioning (Mauelshagen, 1993; Rybak and Menzel, 1998; Okada et al., 2007). The LP, receiving direct information from the AL as well as via the MB, is considered as a premotoric area, from where descending neurons mediate the information out of the brain. Whereas descending neurons responding to pheromones have been described in the lateral accessory lobes (Kanzaki et al., 1991; Kanzaki et al., 1994), the knowledge is scarce about descending LP neurons responding to plant odours. In flies a ventral area of the LP is shown to house descending neurons and to receive information of different modalities, including olfactory information from the lateral horn (LH) (Strausfeld, 1976; Tanaka et al., 2004).

In general, little knowledge exits on the anatomical and functional organisation of the LP/LH. Studies both in the fruit fly and in the *H. virescens* have indicated a stratified projection pattern among m-APT PNs in the LH (fruit fly) and the LP (*H. virescens*); similar and close projections of neurons innervating the same glomerulus and partly overlapping projections of neurons innervating different glomeruli (Marin et al., 2002; Wong et al., 2002; Jefferis et al., 2007; Løfaldli et al., 2010). In *H. virescens* the olfactory projection area in the LP is termed olfactory axis (OA). Regarding the functionality of the LP/LH it has been proposed that the AL-LH pathway represents a naïve or inexperience odour processing route from the AL to motor control, compared to the associative and experience dependent MB pathway (Heimbeck et al., 2001; Keene and Waddell, 2007). In a recent study of the fruit fly, Ruta et al., (2010) mapped the information pathway of a pheromone from the responding PNs in the AL to descending neurons in the LP. They showed that information about the pheromone was transferred to third order LP neurons having dendritic overlap with the PN projections and axonal overlap with the dendrites of descending neurons that responded to stimulation with the pheromone, thus showing a functional pathway from the input to the output of the brain.

142 Coding mechanisms have particularly been studied in the AL of many insect species,
143 reporting both spatial and temporal principles for odour quality coding (Laurent et al.,
144 1996; Joerges et al., 1997; Galizia and Menzel, 2000; Stopfer et al., 2003; Wang et al.,
145 2003a; Lei et al., 2004; Riffell et al., 2009b). In moths, spatial coding principles are
146 demonstrated by the functional organisation of the well defined macroglomerular
147 complex innervated by PNs, of which some show specific responses to single compounds
148 and others integration of the pheromone information (Anton and Hansson, 1994; Berg et
149 al., 1998; Vickers et al., 1998; Christensen and Hildebrand, 2002). Likewise, in the more
150 complex plant odour system of moths, PNs responding specifically to single odorants and
151 others to several odorants have been shown by electrophysiological recordings as well as
152 calcium imaging studies (Müller et al., 2002; Sadek et al., 2002; Skiri et al., 2004;
153 Reisenman et al., 2005; Krofczik et al., 2009; Yamagata et al., 2009; Deisig et al., 2010;
154 Kuebler et al., 2011). Using calcium imaging, similar results have been obtained in the
155 honeybee, proposing a combinatorial coding mechanism where single odorants and
156 blends elicit specific activity patterns among some glomeruli and neurons in the AL
157 network (Galizia and Menzel, 2000; Galizia and Szyszka, 2008). In contrast, in the locust
158 AL, exclusively containing multiglomerular PNs, odour coding is shown to relay more on
159 the temporal synchronous activities than the spatial activity (Laurent et al., 1996; Perez
160 Orive et al., 2002). In a recent multiunit recording study in the hawk moth (*Manduca*
161 *sexta*) stimulation with complex mixtures containing particular odorants derived from
162 host plants elicited synchronous intensity invariant firing patterns among the recorded
163 neuronal units (Riffell et al., 2009a; Riffell et al., 2009b). It was found that the mixture
164 was differently represented from the single constituents in a spatio-temporal activity
165 pattern, similar to findings in the honeybee by imaging and electrophysiological
166 recordings from PNs (Deisig et al., 2006; Yamagata et al., 2009). Furthermore,
167 differentiation between information mediated by single odorants and blends have been
168 proposed for the m- and the l-APT, the PNs of the l-APT processing synthetically and the
169 m-APT PNs elementally information about mixtures (Krofczik et al., 2009). In spite of
170 results provided by numerous studies in insects, we need more specific knowledge about
171 the processing of relevant odour information both in the AL and in the protocerebral
172 networks.
173
174 The present study focuses on how information about relevant plant odours is handled by
175 neurons projecting in two APT target areas in the protocerebrum of *H. virescens*. It is
176 based on knowledge about primary plant odorants, previously identified by the use of gas
177 chromatography linked to electrophysiological recordings from single receptor neurons
178 (Røstelien et al., 2005). From these long-lasting recordings of testing large numbers of
179 naturally produced plant volatile mixtures (“head-space”), we know that ORNs
180 responding to plant odorants in this species belong to functional subtypes, each subtype
181 responding best to one primary odorant and weakly to a few others of molecular
182 similarity. Furthermore, with one exception, the molecular receptive ranges of the
183 functionally described ORN types do not overlap. This indicates that responses of a
184 central neuron to a primary odorant originate from one particular ORN type. In the
185 present study we have stimulated with selected primary odorants and defined mixtures of
186 them during intracellular recordings from protocerebral neurons, followed by dye
187 injection for morphological characterisation. We have asked how information about

relevant plant odorants and mixtures are represented among neurons in higher order protocerebral areas. The results revealed neurons that are part of a putative circuit handling information about a defined ten component plant odour blend.

Materials and Methods

Insects, stimulation protocol, recordings and staining

H. virescens (Heliothinae; Lepidoptera; Noctuidae) pupae were imported from a laboratory culture (Syngenta, Basel, Switzerland), separated according to sex, enclosed and kept with access to 0.1M sucrose solution in an incubator (Refritherm 6E, Struers) on a phase-shifted LD photoperiod (14:10 hours) at 25^{o}C. Experiments were performed on three to six days old female moths.

Moths were mounted in plastic tubes and immobilized with dental wax (Kerr Corporation, Romulus, MI). Part of head cuticle was removed to expose the superior and lateral parts of the protocerebrum. Large trachea, intracranial- and antennal muscles were removed to eliminate movements. Glass microelectrodes were pulled with a Flaming-Brown horizontal puller (P97; Sutter Instruments, Novarto, Ca, USA), the tips were filled with dye (Micro-Ruby, Invitrogen; 4%) and backfilled with potassium acetate solution (0.2 M). The microelectrodes had a resistance of 150–400 MΩ. Neurolemma was perforated with a tungsten hook to facilitate insertion of the microelectrode prior to super fusion with saline solution.

Neuronal activity was recorded with an axoprobe amplifier (Molecular devices) and a CED data acquisition unit (Cambridge electronic design) during stimuli protocol application. Olfactory stimuli were applied as air puffs (0,8 ml/300 ms) into a continuous air stream through glass cartridges. Each cartridge containing one of the following primary odorants: Hexanol, (3Z)-Hexen-1-ol, (3Z)-Hexenyl acetate, Ocimene, racemic-Linalool, Geraniol, (+)-3-Carene, trans-Verbenol, Methyl benzoate, 2-Phenylethanol, (-)-Germacrene D, Farnesene, (odorants described in Røstelien et al., (2005), defined blends with equally amount of each odorant (from a binary to a twelve component mixture), and other blends (Ylang oil and magnet), applied (10µg) to a filter paper (1,5 cm). All neurons were tested with purified air as control. Tactile and taste stimulation (sucrose, quinine hydrochloride, salt and distilled water) as described in Kvello et al., (2010), as well as sound and light stimulation were applied to some neurons.

Neurons were iontophoretically stained by passing a 1-3 nA depolarizing current of 2 Hz with 0.2 seconds duration. Complete labelling of the neurons required dye (4% micro ruby, Invitrogen) injection for 10 to 15 minutes. After current injection, the dye was allowed to diffuse over night at 4^{o}C. The brains were dissected in saline solution, fixed in paraformaldehyde (4%) in PBS and left over night (4^{o}C). Stained neurons was intensified by Streptavidin-Cy3 (Jackson immunoresearch, West Grove, PA; diluted 1:200 in PBS) over night (4^{o}C) before PBS rinsing, dehydration (ethanol series: 50, 70, 90, 96 and 100 % 10 min each) and mounting in methyl salicylate. Most preparations with successful neuronal staining underwent a subsequent background staining with a SYNORF1 protocol; rehydration in ethanol (100%, 96%, 90%, 70%, 50%, 10 minutes each), washing (PBS, 10 minutes) and preincubation in normal goat serum (NGS; Sigma, St.

Louis, MO; 10%) in PBS at room temperature (30 minutes). Subsequently, the preparations were incubated in a monoclonal antibody against the synaptic protein synapsin (SYNORF 1, Prof. E. Buchner, Würzburg, Germany), diluted in PBS (1:10) and NGS (10%) for 48 hours (4°C). Rinsed in PBS (5x20 minutes) before incubated for 24 hours (4°C) with a Cy5-conjungated goat anti-mouse secondary antibody (Jackson Immunoresearch; dilution 1:500 in PBS), rinsed again (PBS, 5x20 minutes), and dehydrated before mounted in methyl salicylate on double-sided aluminium slides.

Visualization, reconstruction and registration of neurons into the standard brain atlas (SBA).

Stained preparations were visualized in a laser scanning confocal microscope (LSM 510 META Zeiss, Jena, Germany and a Leica TCS SP5, Leica microsystems). Intracellular fillings were examined with a Plan-Neofluar 20x/0.5 NA dry lens objective and a C-Achroplan 40x/0.8 NA water objective in the Zeiss microscope and a 10x/0,4 NA dry lens objective in the Leica microscope. The intracellular dye was excited by a 543 nm Helium Neon laser and filtered through a bandpass filter BP 565-615 IR (561 HeNe laser in Leica), and the fluorescent dye Cy5 was exited by a 633 nm line of argon laser. Preparations were scanned with a resolution of 1024 x 1024 pixels in the xy-plane and an interslice distance of 2µm. Neurons was scanned in several tiles and manually merged in Amira (Visage Imaging). To compensate for the refraction indexes the z-axis dimension was multiplied by a factor of 1.6. Gray value image stacks of stained neurons and innervated brain structures acquired from the confocal microscope were examined and semi-automatically reconstructed (Evers et al., 2005; Schmitt et al., 2004 and Kvello et al., 2009). The registration of reconstructed neurons into the standard brain atlas (SBA) followed the same procedure as described by Brandt et al., (2005), Kvello et al., (2009) and Løfaldli et al., (2010). Selected brain structures in the preparations with stained neurons were reconstructed as label images and affine and elastically registered to the corresponding label imaged in the SBA. The transformation parameters were then applied to the corresponding reconstructed neuron. The results were then carefully evaluated by comparing the grey value images with the obtained model. The SBA contains only label images of neuropile areas and not cell clusters.

Physiological analysis.

All obtained intracellular voltage traces were processed with a wave form analysis mode in the computer program Spike 2 (Cambridge electronic design). The recordings were reviewed for odour evoked responses and sorted in a response table. Recordings that qualified for further response analyses had to fulfil the following criteria: In addition to control and B10, the neurons had to be tested for one or more of the four most frequently tested primary odorants, the responses had to be repeated and the recording had to be stable and reliable with low levels of noise. The responses were quantified in bins of 50ms across all stimuli for all neurons except those with exceptionally wide response windows. The response window was defined as the period between stimulus onset and the first bin where the consecutive 400ms did not deviate significantly from spontaneous activity. The response window width (number of bins) of a neuron was kept constant across all stimuli, the duration of the longest response determining the width of the response window. Mean frequency and variance of the spontaneous activity were

estimated for each neuron. The estimation was based on the weighted average of spike rates from two periods: 200ms prior to stimuli onset and 1500ms recorded 400ms after the end of the defined response windows. The interval of 400ms after the response window was excluded from the estimation. This in order to ensure that neurons had returned to spontaneous activity. Any considerable change in spontaneous activity during the continuous recording was taken into account.

Temporal response strength was quantified for each response window following an odor stimulus by calculating the mean deviation (in frequency) from estimated spontaneous activity (MDS):

$$MDS = \frac{1}{n}\sum_{i=1}^{n} r_i - r_{sp} \qquad [1]$$

n is the number of bins, r_i is the firing rate of bin *i* and r_{sp} is the estimated spontaneous activity. By taking the absolute value of the deviation, both positive and negative deviations contribute similarly to the MDS. This method enables quantification of complex responses consisting of both inhibitory and excitatory elements without neutralizing each other.

To ascertain the excitatory and inhibitory parts of the responses, the contribution of positive deviation (eMDS) and negative deviation (iMDS) was also calculated. Mean response frequency (MRF) across bins of the response window and maximum frequency (maximum observed frequency in the response) was calculated as well. Odor responses were considered significant if either the excitatory or the inhibitory average MDS of two stimulations with the same odor exceeded the neuron's standard deviation (SD) of spontaneous activity by a factor of 2. Absolute MDS had to exceed the SD in spontaneous activity by four times. Neurons were grouped according to their MDS response profiles for different odorants. To visualize the neurons response profile curves the significant responses were plotted over response window time. Responses to single odorants and mixtures in a neuron were determined as different if their average MDS differed more than the pooled SD for all repetitions of the significant responses in that particular neuron. If the average MDS between the mixture response and the single odorant response differed less than the pooled SD, the term hypoadditivity is used. If the single odorants MDS was stronger than the blend MDS, the term suppression is used. Hypoadditivity was only used to describe differences between responses to a blend and a particular single odorant, and not as a general mixture effect, because all constituents of the complex mixture were not tested. To compared the MDS response strength to control and selected single odorants and blends in the population of selected neurons, two-tailed Wilcoxon rank-sum tests were carried out on all significant responses. The stimuli were grouped as control, single odorants and blends and tests were carried out between these groups on the excitatory, the inhibitory and the absolute MDS in neurons grouped as excitatory, inhibitory or complex responding, respectively.

Terminology

In naming the antenna-cerebral tracts (ACT's) we followed the nomenclature proposed by Galizia and Rössler (2010) using terms according to the position in the brain. Thus, the inner, the medial and the outer ACTs were in this study termed the medial (m), the medio-lateral (ml) and the lateral (l) antenno-protocerebral tract (APT), respectively. The term superior protocerebrum is according to Rø et al., (2007) the area proximately to and dorsally of the MB lobes, extending from the anterior to the posterior part. Concerning the anatomy of the mushroom body (MB) lobes, we employ the system described in Rø et al., (2007) in *H. virescens*. Here the α and α' together with one arm of the γ lobe makes up the vertical lobes and the second arm of the γ lobe and the β and β' constitutes the horizontal lobes. The heel (H) lays on the horizontal part anterior to the pedunculus. Lateral protocerebrum (LP) and lateral horn (LH) denotes to the areas defined in Kvello et al., (2009) and Løfaldli et al., (2010), i.e. LH is the small protrusion from the LP.

Results

Output areas of the antenno-protocerebral tracts

Injection of dye in the antennal lobe of *H. virescens* revealed staining of the three major antenno-protocerebral tracts, the medial, the medio-lateral and the lateral (m-APT, ml-APT and l-APT) and their target areas in protocerebrum (**Figure 1A**).

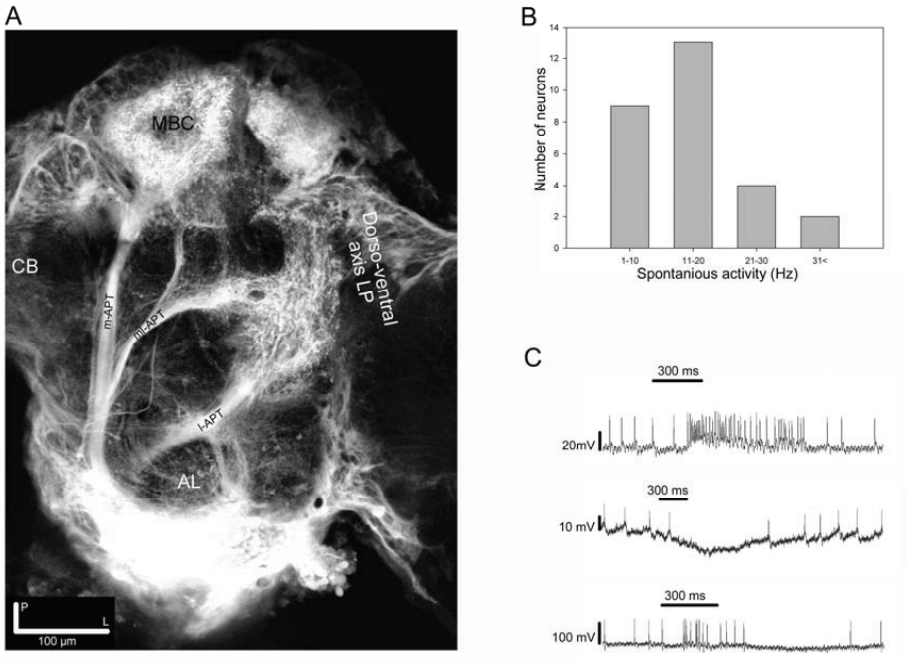

The calyces of the mushroom bodies (MB calyx) clearly appeared with projections from the medial and the lateral tract. In the lateral protocerebrum (LP) the dorso-ventral area of the olfactory axis (OA) received projections from all tracts. The third important olfactory area, the superior protocerebrum (SP) located dorsally of the posterior parts of the MB lobes, appeared with projections exclusively from the medio-lateral tract.

Electrophysiological recordings from protocerebral neurons

The presented results are based on recordings from 87 neurons obtained in the LP and in the SP. These neurons responded to stimulation with single odorants and blends of the selected primary plant odorants (**Table 1**).

Table 1: Overview of the most tested single primary odorants and blends in all of the 87 recorded odor responding neurons. The four single odorants and the two blends selected for further analysis as well as control are shaded. The weighted probability (P) to elicit responses is indicated for control, the four single odorants and the two blends (B10 and B12).

Odorants	Neurons tested (n)	Responses (%)	Blends	Neurons tested (n)	Responses (%)
Air (control)	87	32	Plant blend 2	23	87
3Z-Hexenyl acetate	43	61	Plant blend 3	12	66
Linalool	27	82	Plant blend 9	31	81
Ocimene	11	64	Plant blend 10	83	92
Geraniol	11	46	Plant blend 11	28	64
Germacrene D	38	82	Plant blend 12	50	96
Farnesene	11	46	Air P(r): 0,32 Singles P(r): 0,76 Blends P(r): 0,93		
2-Phenylethanol	40	85			

A puff of purified air (control) resulted in a weak response in about 32 percent of the neurons. The response probability varied between the primary plant odorants and the plant odor blends. The summated response probability (P) was higher for the two most effective blends (P 0,93, B10 and B12) than for the four most effective single odorants (0,76, 3Z- hexenyl acetate, linalool, 2-phenyl ethanol and germacrene D. **Table 1**). The odorants constituting the six most tested plant odor blends are listed in table 2.

The limited duration of the intracellular recordings, in emphasizing repetition as well as randomization of the stimuli, did not allow every neuron to be tested for all stimuli. We selected twenty-eight of the 87 neurons for further response analysis, based on the required recording quality and the applied stimuli, as given in the method. Spontaneous activity in these neurons ranged from 1 - 42Hz (**Figure 1B**). The identified response types to olfactory stimulation were excitation, inhibition and complex responses consisting of inhibitory and excitatory phases (**Figure 1C**). Most responses outlasted the applied stimulus period. In the subsequent analyses of the 28 neurons, the focus was on the responses to the following stimuli; control, the four primary odorants, 3Z- hexenyl acetate, linalool, 2-phenyl ethanol and germacrene D, and the two most complex plant odor blends, the ten component B10 and the twelve component B12 (**Table 1**, shaded).

B12 contained all of the four mentioned odorants and B10 all, but germacrene D (**Table 2**).

Table 2: Single odorants (shaded) constituting the six most tested blends, from the binary, B2, to the most complex, B12.

Single odorants	Plant blends					
	PB2	PB3	PB9	PB10	PB11	PB12
3Z-hexanol						
3Z-hexen-1-ol						
3Z-hexenyl acetate						
Ocimene						
Linalool						
Geraniol						
(+)3-carene						
E-verbenol						
Methyl benzoate						
2-phenylethanol						
Farnesene						
(-)-germacrene D						

The two blends and the four odorants showed highest response probability and was the most tested stimuli in all of the 87 recorded neurons. Twelve of the 28 neurons were tested for responses to stimulation with tastants. Three of them responded, one excitatory to sucrose and quinine applied to the left antenna (also excitatory responses to odors) and the two other to sucrose applied to the proboscis (one with excitatory and one with complex responses to odor stimuli). Occasional light and sound stimulation did not elicit responses in the 28 neurons.

MDS and MRF

The average responses of the 28 neurons to odor stimuli was calculated as mean deviation from spontaneous activity (MDS) indicating response strengths (both excitatory and inhibitory), mean response frequency (MRF) and maximum frequency (**Figures 2A-I**).

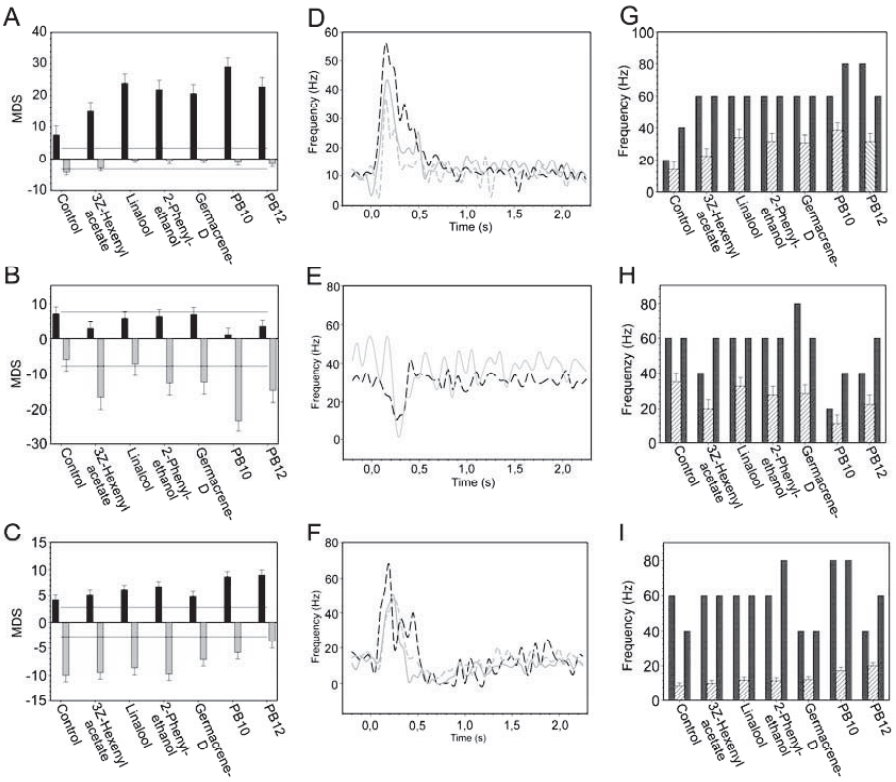

The response chart in **Figure 3A-G** gives an overview of the significant responses of the 28 neurons to stimulation with control, the four single odorants and the blends.

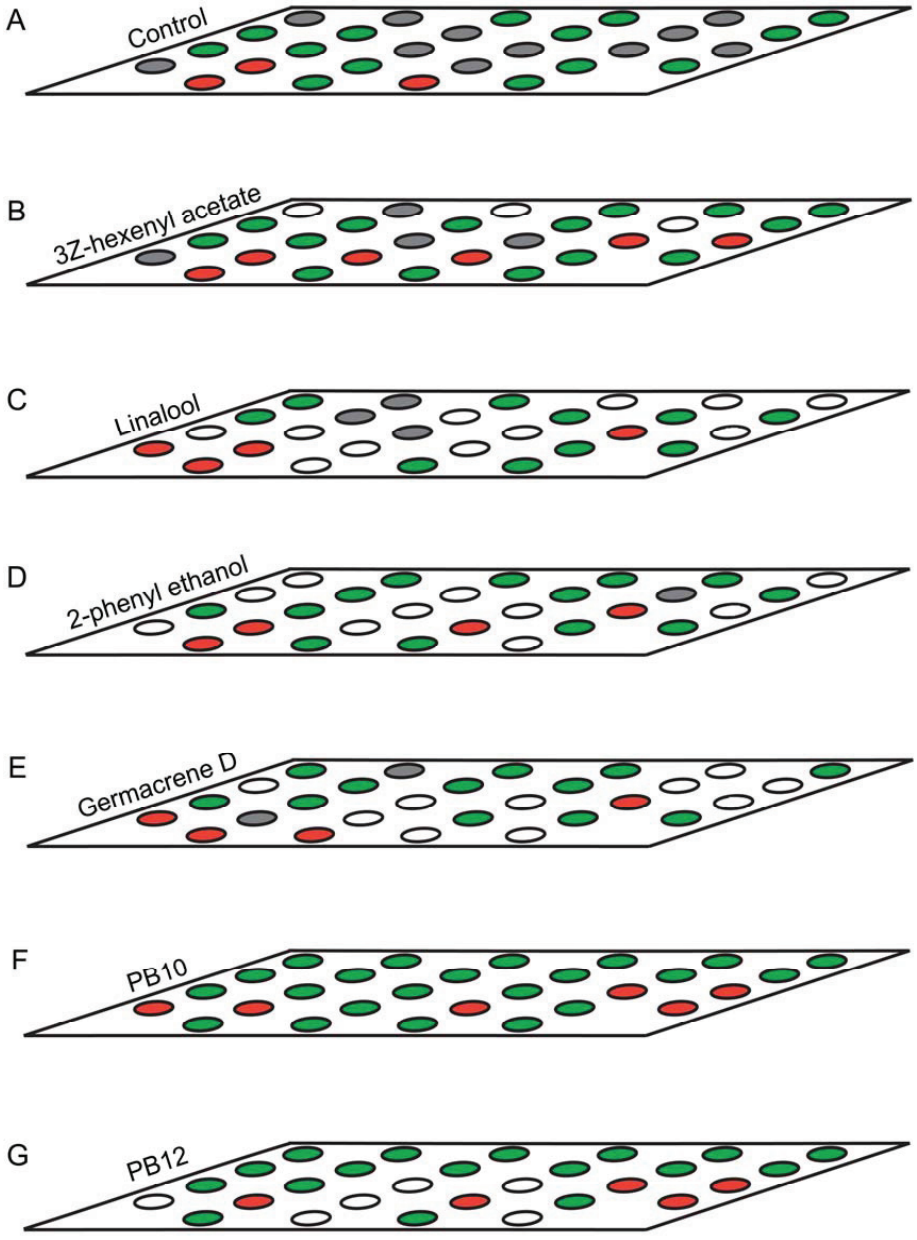
A
Control
B
3Z-hexenyl acetate
C
Linalool
D
2-phenyl ethanol
E
Germacrene D
F
PB10
G
PB12

408
409

Responses are marked as excitatory or inhibitory modes, according to which of the two phases were strongest. Thus, the chart does not give the response strength. Neurons were further grouped according to their MDS response pattern as exemplified in **Figure 2A-C**. Sixteen neurons (1–16) appeared with clear excitatory response profiles to odor stimuli, four neurons (17-20) mainly with inhibitory responses and seven neurons (21-27) with a complex response pattern of both excitatory and inhibitory phases. One neuron was unassigned because of a particular response pattern of two excitatory phases separated by a long inter-response interval (several seconds). The MDS response pattern of the individual neurons (**Figure 2B, E** and **H**) is also reflected in the response profile curve of the neurons in **Figure 2A**, **D** and **E**. All neurons assigned to the group of excitatory and inhibitory responses, showed positive or negative MDS, respectively, in the main part of the response window (**Figures 2A-B** and **D-E**). In a few cases a transient change of the response appeared as exemplified by the MDS (**Figure 2B**) and the dotted curve (**Figure 2E**) showing a small excitation following the inhibitory responses. This kind of changes was rarely significant. In the complex responding neurons exemplified in **Figure 2F**, a strong inhibitory response phase followed a stronger excitatory phase, also reflected by the single responses in **Figure 2C**. These transient changes of response phases are obviously not reflected in the MRF (**Figure 2I**). The response duration of the excitatory responding neurons varied, 14 showing short responses (150 – 600ms) and two longer responses (1000-3000ms). The latency also differed, being 100-200ms in the former and 250-350ms in the latter group. Among the four inhibitory responding neurons, two showed short lasting (400-600ms) and two longer lasting (1500-1800ms) responses. Neurons placed in the complex responding group showed latency between 150-300ms and response duration between 400 and 1100ms.

The response modes of all 28 neurons given in the chart of **Figure 3A-G** showed more frequently excitatory than inhibitory responses for all stimuli, also applying to the control (excitation in 14, no response in 11 and inhibition in 3). The control stimulus elicited responses in 60 % of the 28 neurons, somewhat more frequently than among all 87 neurons (**Table 1**). The two mixtures B10 and B12 was the most potent stimuli, B10 elicited responses in all 28 neurons and in 92 percent of totally 83 tested neurons and B12 in all 22 tested among the 28 neurons and in 96 percent of 50 tested neurons (**Table 1**). A few neurons showed specific responses to a single odorant and the blends (**Figure 3A-G**), in contrast to most neurons which responded to many single odorants and the blends. Two particular neurons (15 and 16 in **Figure 3A-G**, only one single odorant tested in the latter) responded to the blend B10, but not to the single odorants tested.

Odor discrimination expressed by response strength

A comparison of the odor responses revealed different MDS and MRF in most of the 28 neurons to the control, the single odorants and the mixtures, as exemplified in **Figure 2A-C and G-I**. In the 16 neurons with excitatory responses, stimulation with the blends yielded the strongest responses, largest MDS and highest MRF in eleven of them (B10 strongest in four and B12 in five neurons, the two neurons with long lasting excitation were only tested with B10, **Figure 3A-G** neuron 15 and 16). Suppression was observed in two neurons for which a single odorant (linalool and 2-Phenyl ethanol, respectively) yielded stronger MDS than the blends, B10 and B12. Hypoadditivity was seen in three neurons for which the strongest single odorant and the strongest blend yielded equal

responses among the tested odorants. A more intricate relation was often found when comparing the responses to single odorants and the blends (**Figure 2A-C** and **Figure 4**).

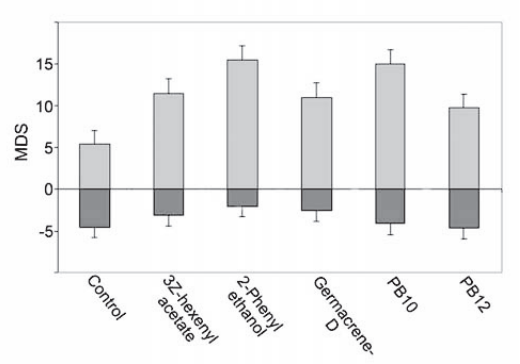

In the neuron in **Figure 4** the response to the strongest blend (B10) and the strongest single odorant (2-phenyl ethanol) was about equal, implying hypoadditivity. However, in spite of the two added odorants, germacrene D and farnesenes, B12 showed suppression in relation to 2-phenyl ethanol, but hypoadditivity in relation to germacrene D and 3Z-hexenyl acetate. All responses were clearly stronger than to the control. Different response strength to the single odorants was found in most neurons between the strongest and the weakest odorants and only in four neurons between the two strongest single odorants. The statistical analysis of the grouped MDS strength in the excitatory responding neurons (**Figure 5A**) showed significant stronger responses to the odorants than to control (air vs. singles p = 1,14E-06 and air vs. blends p = 4,52E-11) and significant stronger responses to blends than to single odorants (p = 3,11E-03).

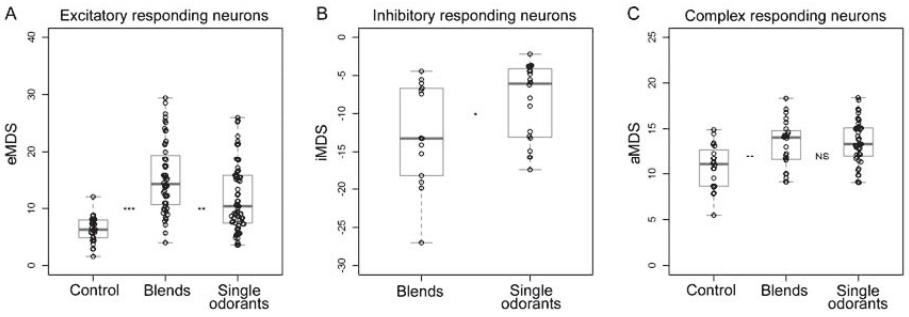

Among all sixteen excitatory neurons the highest observed MDS value (29Hz) and MRF (39Hz) was obtained for B10. The highest observed maximum response frequency (140 Hz) was elicited by stimulation with 3Z-hexenyl acetate, 2-phenyl ethanol and B12 in one neuron. The inhibitory responding neurons also displayed different MDS strength in their responses to stimulation with the single odorants and mixtures. Two neurons responded stronger to B10 than to any of the other odorants (only one of them tested with B12). The other two inhibitory responding neurons showed hypoadditivity and did not differ in

response strength to the strongest single odorant and the strongest mixture. The control elicited response in one neuron, which was clearly weaker than the responses to the odors. The statistical tests of grouped MDS strength showed stronger responses to the blends than to the single odorants in the neurons responding by inhibition ($p = 0{,}02997$. **Figure 5B**).

In the complex responding neurons the effect of the single odorants and mixtures varied more than in the two previously described groups. All neurons showed either suppression (four neurons; one in both phases, two in the inhibitory and one in the excitatory phase) or hypoadditivity (three neurons; two in both phases and one in the excitatory phase) in one or both of the response phases. Discrimination between the two complex mixtures and between the two strongest single odorants also varied across neurons as well as within a neuron. Four neurons had stronger MDS to one of the two mixtures (two to B10 in the excitatory phase and two to B12 in the inhibitory phase) and two neurons showed different MDS to the two strongest single odorants (one neuron in the inhibitory phase and the other in the excitatory phase). Statistical analysis on the absolute MDS values in complex responding neurons revealed that single odorants ($p = 0{,}000189$) and blends ($p = 0{,}004335$) elicited significantly stronger responses than the control (**Figure 5C**). Although the difference in MDS strength between single odorants and blends was not significant, the data pointed towards a stronger absolute MDS for the single odorants than for the blends. In the unassigned neuron MDS analysis on the first response phase revealed strongest excitatory response to 3Z-hexenyl acetate, whereas B10 and linalool elicited similar responses as control. As shown by the staining this neuron was bi-lateral having dendritic arborisations in the right LP and axonal projections in the OA of the left LP.

Neurons innervating olfactory areas in protocerebrum.

Nine of the 28 neurons were fully stained, showing innervation in the three main olfactory protocerebral areas, the SP, the LP and the MB. The focus here is on five neurons, all responding to the blend B10 (**Figure 6A-E**).

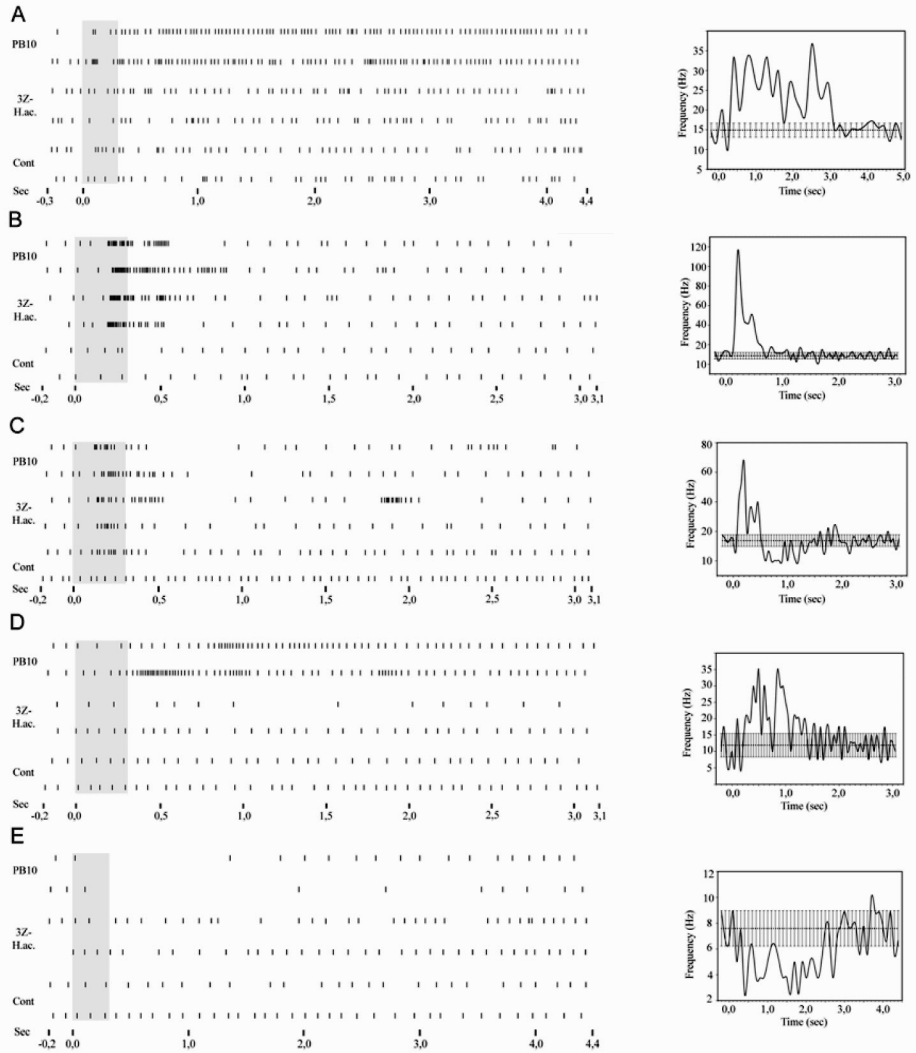

One neuron was a medial antenno-protocerebral tract projection neuron (ml-APT PN) showing similar morphology as another neuron stained by electroporation, but not physiologically studied. The other four neurons inspected in confocal images and 3D-reconstructed were protocerebral neurons with projections in partly overlapping areas in the SP and the OA of LP (**Figures 7- 11**). All neurons were transformed into the standard brain atlas.

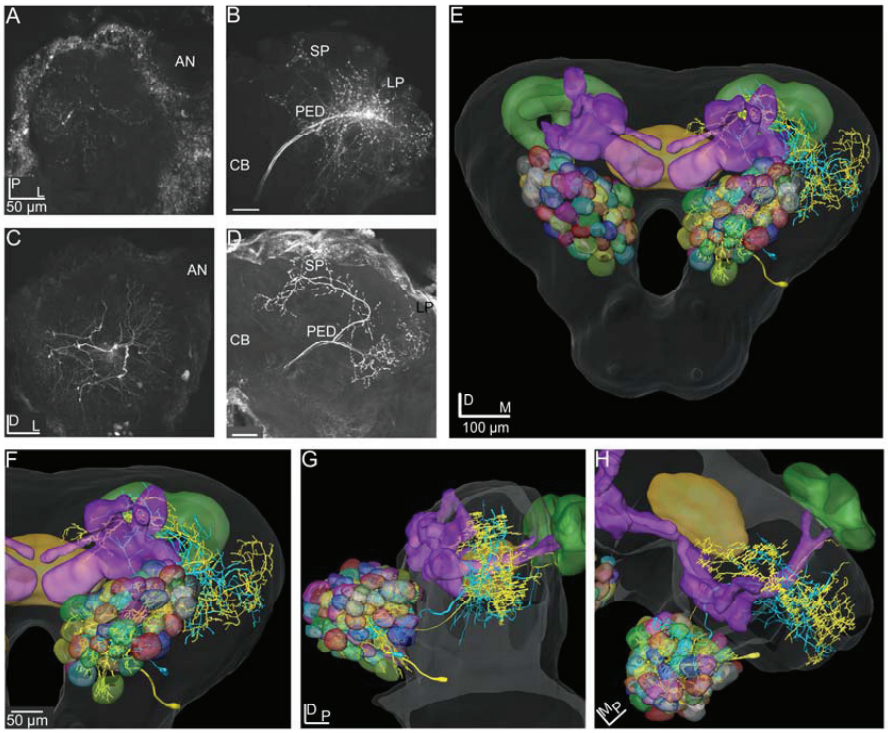
A
AN
P
L
50 µm
B
SP
LP
PED
CB
C
AN
D
L
D
SP
LP
CB
PED
E
D
M
100 µm
F
50 µm
G
D
P
H
M
P

522
523
524

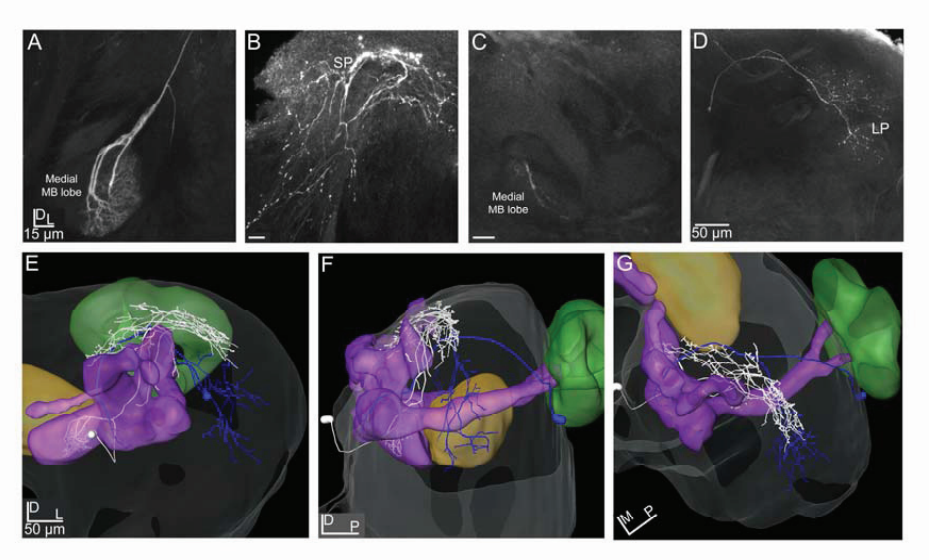

525
526
527

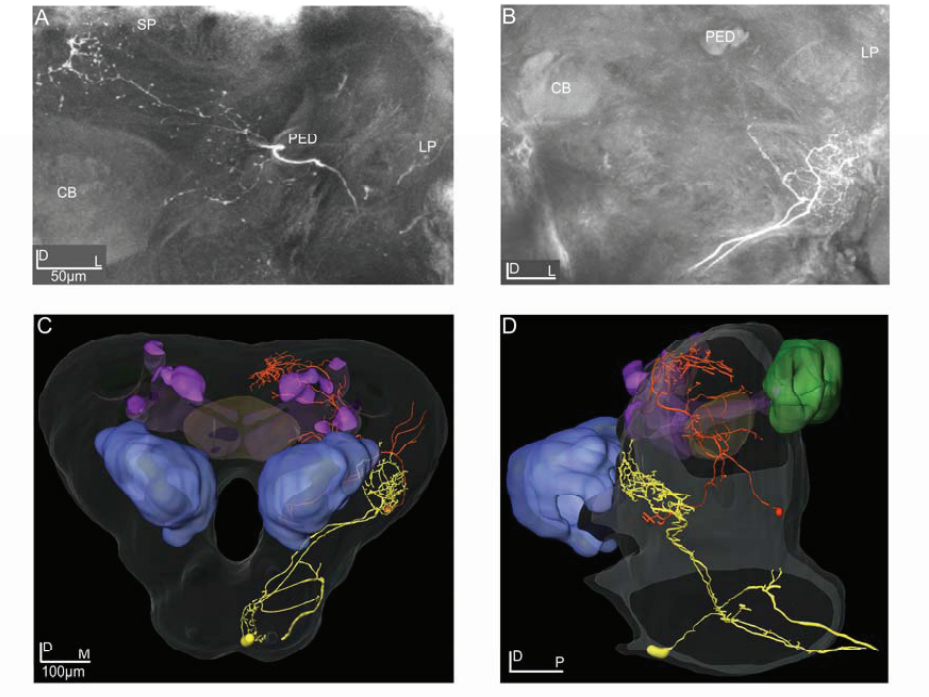

528
529

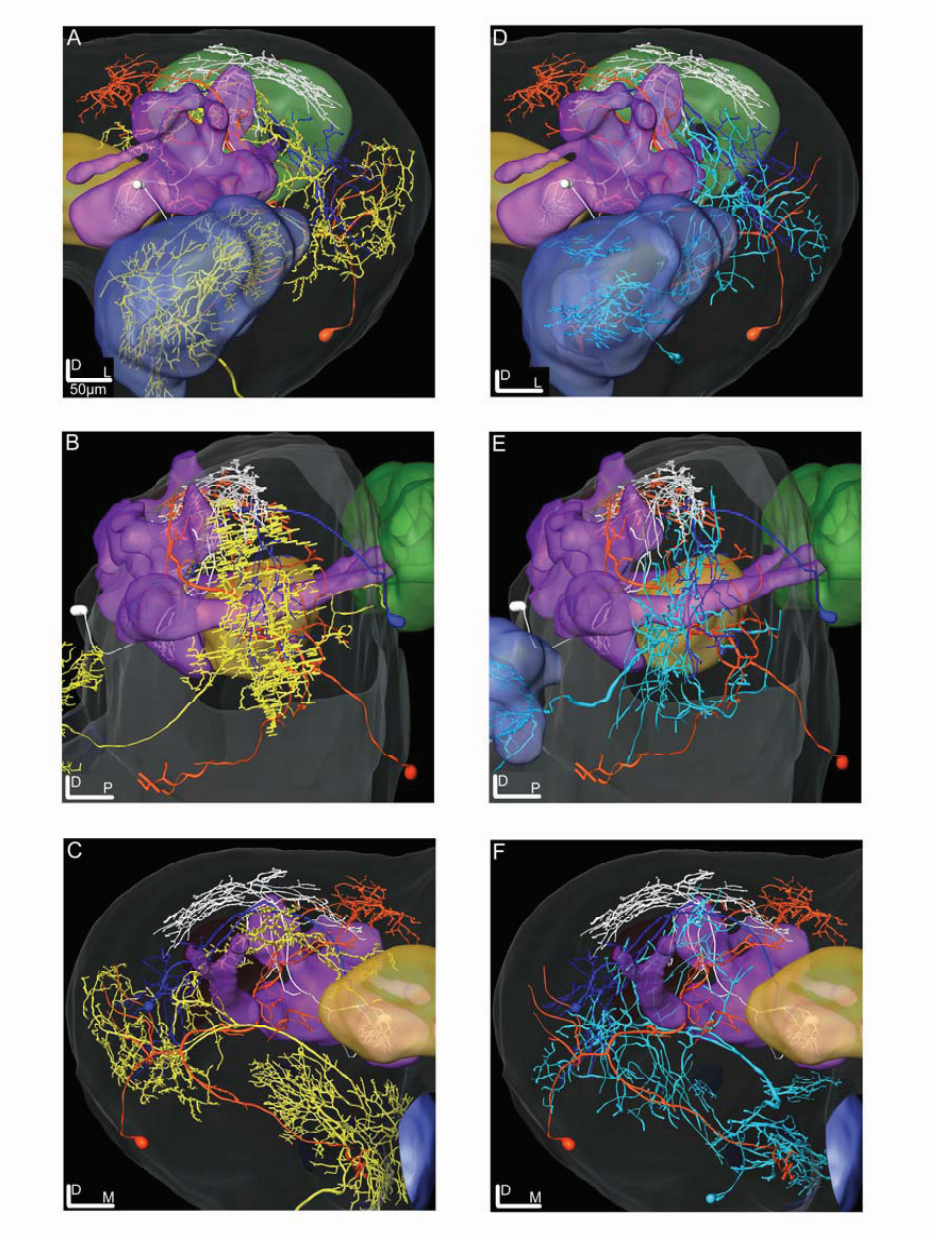

530
531

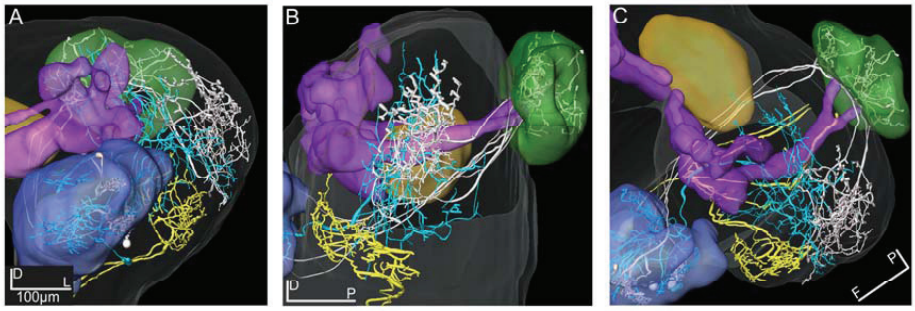

Mediolateral APT projection neurons

The two stained ml-APT PNs revealed different but partly overlapping axonal projections as well as different glomerular innervation patterns in the antennal lobe (**Figure 7A-H**). Both were multiglomerular, the Type 1 having a sparsely dendritic arborisation in each of the innervated glomeruli, most of them located laterally and medially in the AL (Figure 5A,B,E-H, two Type 1 neurons stained during the same recording, blue color). The Type 2 neurons (n=2, only one shown. **Figure 7C,D,E-H**, yellow colored reconstruction) innervated densely almost all glomeruli of the AL. All four PNs had soma in the ventral part of the lateral cell cluster. The axons of the Type 1 ml-APT PNs projected in the medial part of the dorso-ventral olfactory axis in the LP, with some overlap with the more dorsal projections of m-APT PNs (**Figure 11A-C**, m-APT PNs from Løfaldli et al., (2010), termed IACT PNs). A few branches of the ml-APT PNs extended into LH and two others posteriorly towards the ipsilateral calyces. Some side branches turning more dorso-medially from the LP into to the SP. Here they branched off close to the MB lobes and the pedunculus, dorsally and posterior to the α, α` (vertical lobes) and the γ lobe, the heel and pedunculus.

The axons of Type 2 ml-APT PNs divided after passing ventro-laterally to the pedunculus (**Figure 7D and E-H**, only one included). One branch turned dorso-medially into SP where it showed extensive arborisations proximately to the MB lobes, partly overlapping with the Type 1 ml-APT PNs. A few smaller branches extended more dorso-medially and posterior to the medial part of β`, β (medial lobes) and γ lobes (**Figure 7E-H**, only one showed). The second major branch ran laterally into the dorso-ventral axis of LP overlapping with the projections of Type 1 ml-APT PNs (**Figure 7E-H**, only one showed). One single projection ran along and within the outer part of the pedunculus in posterior direction toward the ipsilateral calyces where it branched off in a confined area external to the calyces.

Raster plot and the response curve from the recording of one Type 1 ml-APT PN is shown in **Figure 6A**. The responses appeared as a long lasting excitation to stimulation with B10 with latency around 300ms. No response was recorded to stimulation with control, other mixtures (B5 and ylang oil) or single odorants (3Z hexenyl acetate, linalool, geraniol) (neuron number 15 in **Figure 3A-G**). In the recording of the Type 2 ml-APT PN no response was obtained to stimulation with control, single odorants or blends (not included among the 28 physiologically described neurons in this study).

Mushroom body extrinsic neurons

Two MB extrinsic neurons have been reconstructed and transformed into the standard brain atlas (**Figure 8A-G**). Both neurons have their dendritic arborisations within the medial lobe of the MB. One, named MB-SP extrinsic neuron (**Figure 8A, B and E-G**, white color), has dense arborisations in a confined area of the swelling part of the lobe, whereas the other extrinsic neuron (MB-LP) shows a sparse pattern with only one dendritic branch within the lobe (**Figure 8C, D and E-G**, blue color). The soma of the MB-SP extrinsic neuron was located frontally of the MB lobes and of the MB-LP extrinsic neuron posteriorly and closely to the MB calyces. As indicated by the name, the MB-SP extrinsic neuron had its axonal projections located in the SP with branches posteriorly and dorsally to the α, α· (vertical) and the γ lobe. Some branches extended more laterally terminating in a dense projecting pattern (**Figure 8E-G**). The axonal projections of this extrinsic MB neuron partly overlapped with the axons of both types of ml-APT PNs in the SP (**Figure 10A-F**). This implies that SP in *H. virescens* receives input from both types of neurons in the same or partly overlapping areas. The stained MB-LP extrinsic neuron projected in the OA of LP, with relatively sparse branches extending from dorso-medial to more ventro-lateral areas (**Figure 8E-G**). The projections partly overlapped in the LP with the axonal projections of both types of ml-APT PNs (**Figure 10A-F**). This implies that LP like the SP in *H. virescens* receives information from the MB lobes as well as from the AL.

Raster plots for the MB-SP extrinsic neuron (**Figure 6B**) and for the MB-LP extrinsic neuron (**Figure 6C**) show a strong response of both neurons to stimulation with B10. While the responses of the MB-SP extrinsic neuron appeared as a clear excitation, the responses of the MB-LP extrinsic neuron were typically complex (**Figure 6B** and **6C** respectively). The MB-LP neuron showed a weak response to control and a slightly stronger excitation to stimulation with the mixture B10 (B12 not tested) than with the single odorant 3Z-hexenyl acetate, eliciting a slightly stronger inhibitory than excitatory phase (neuron number 21 in **Figure 3A-G**). The temporal response pattern clearly differed for the blend and the single odorant (**Figure 6C**). The excitatory phase of the first response to B10 was clearly stronger and longer lasting than of the repeated response. The opposite pattern appeared for the single odorant. The maximum frequency was also different between the responses to the blend (100Hz and 80Hz) than to the single odorant (80Hz and 60Hz). This neuron did not respond to stimulation with tastants, which were applied after odor stimulation in order to avoid influence on odor responses. In the LP-SP neuron the responses to stimulation with the single odorants and the blends showed different strength, clearly strongest to the blends B10 and B12, weaker to 3Z-hexenyl acetate, weakest to 2-phenyl ethanol and no response to control. The difference between the B10 and B12 responses was too small to be considered as different. Like the MB-LP neuron, the MB-SP neuron displayed the same difference between the first and the repeated responses, by a stronger response to the first than to the repeated stimulation with the blends and the opposite pattern with 3Z-hexenyl acetate (**Figure 6B,** neuron number 5 in **Figure 3A-G**). The measured latency in the two MB extrinsic neurons was between 150-200ms.

Lateral protocerebral neurons

The two reconstructed and transformed lateral protocerebral neurons differed in respect to dendritic arborisation and axonal projections (**Figure 9A-D**). Both neurons had their dendrites in the lateral protocerebrum but different axonal projections, one in the SP (LP-SP neuron), and the other projecting in the ipsilateral connective (LP-descending neuron). The dendritic arborisations also differed between the two neurons. The LP-SP showed a sparse arborisation in the LP with a few branches extending towards the central complex, terminating proximate but outside the complex (**Figure 9A and C-D**, orange reconstruction). The dendrites of the LP-descending neuron showed a dense and more confined pattern located ventrally in the LP with the terminals arranged in an anterior-posterior direction (**Figure 9B and C-D**, yellow reconstruction). The dendritic arborisations were close but not directly overlapping with the LP-SP dendrites (**Figure 9C-D**) or with the axonal projections of the Type 1 ml-APT PNs (**Figure 11A-C**). After registration of the neurons into the standard atlas it became evident that the dendrites of the LP-descending neuron were positioned anterior-ventrally to the OA of the LP (**Figure 11A-C**, m-APT PNs from Løfaldli et al., (2010)). Comparison of the confocal images of the LP-descending neuron and the mass stained APTs (**Figure 1A**) indicated that the descending neuron dendrites might have a direct overlap with some of the most ventral APT PN projections of the ml-APT or the l-APT. The LP-descending neuron, having a large soma in the SOG, appeared with two major dendritic branches extending from the SOG and giving off a few small branches in the SOG before the axon was leaving the brain via the ipsilateral connective. Unfortunately, the connectives and the thoracic ganglion were not dissected out for further investigations of the axonal projections (**Figure 9B-D**). Axon of the LP-SP neuron projected dorso-medially from the LP into the SP. Here it ramified relatively densely posterior and medial to the α, α′ and γ lobe (vertical lobes) with a few branches projecting slightly more ventrally. The cell soma was located laterally on the posterior side of the brain (**Figure 9A** and **C-D**). Some of the axonal projections of the LP-SP neuron showed partly overlap with axonal projections of both ml-APT PN types and of the MB-SP extrinsic neuron (**Figure 10A-F**).
The LP-SP neuron and the LP-descending neuron both responded to B10, but differently, as shown by the raster plot and the response profile curves in **Figure 6D** and **E**, respectively. The LP-SP neuron showed a long lasting excitation consisting of two peaks, as seen in the response to the first stimulation with the blend (**Figure 6D**). No response was obtained to stimulation with 3Z-hexenyl acetate and the control (neuron number 16 in **Figure 3A-G**). Unfortunately, other odorants were not tested. The LP-descending neuron responded with a long lasting inhibition, the longest to the first stimulation with B10 (raster plot **Figure 6E**). A considerably weaker inhibition was recorded to stimulation with other blends (PB2, PB3 and PB4) and to the first stimulations with linalool and germacrene D (neuron number 19 in **Figure 3A-G**). The other tested odorants (3Z-hexenyl acetate, E-verbenol, farnesenes and control) did not elicit any response. Measured latency for the LP-SP neuron was around 250ms and around 300ms for the LP-output neuron.

The putative circuit

The two MB extrinsic neurons receiving information in the medial lobe and projecting in the superior and lateral protocerebrum, respectively, had partly overlapping axonal projections with the ml-APT neurons, as shown after transformation into the standard

atlas (**Figure 10A-F**). In the lateral protocerebrum the axonal projections of the ml-APT-neurons and the MB-LP neuron overlapped with the dendritic arborisations of one lateral protocerebral neuron, LP-SP, having axonal projections in the superior protocerebrum. In the SP the axonal projections of the LP-SP neuron overlapped with the projections of the other axonal branch of the ml-APT-neurons as well as with the axonal projection of one of the MB extrinsic neurons. Thus, these neurons might form a circuit where the superior protcerebrum directly received information from the AL via the multiglomerular ml-APT neurons and indirectly via the MB extrinsic neuron, as well as from the LP. The input to the lateral protocerebrum in the dorso-medal part is originating in the AL, via all three APTs, as well as in the MB. Output from protocerebrum was only found by the LP-descending neuron.

Discussion

Based on intracellular recordings from superior and lateral protocerebrum, we have described neurons involved in a circuit processing plant odour information in the brain of *H. virescens* females, 28 neurons presented in this study. We have stimulated with primary odorants, each identified as the best odorant for a particular ORN. Thus, we know that the responses obtained in the central neurons to stimulation with the single primary odorants and mixtures of them contain relevant information that can be ascribed to particular ORN types. The response profiles, classified as pure excitation, pure inhibition as well as mixed excitation-inhibition, are similar to responses described for other central olfactory neurons, like the antennal lobe projection neurons of several insect species, including heliothine moths (Christensen et al., 1991 and 1995; Vickers et al., 1998; Heinbockel et al., 1999; Barrozo et al., 2011; Kuebler et al., 2011). Compared to the sparsely obtained responses to plant odorants in previous recordings from the AL of *H. virescens* (unpublished), we obtained more frequently responses when recording from the lateral and superior protocerebrum. Most olfactory neurons responded to several of the primary odorants and the blends and only a few showed more specific responses to one or two odorants. This implies that the information about different primary odorants to a large extend is integrated in these higher order protocerebral neurons. In contrast, most of the medial tract AL PNs, most of them innervating a single and fewer two-three closely located glomeruli, as shown in *H. virescens* and *Bombyx mori* may get excitatory input from one or two-three types of ORNs (Løfaldli et al., 2010; Namiki and Kanzaki, 2011). Thus, when recording from the AL in contrast to protocerebrum, there is a lower probability to stimulate with the particular primary odorant, which explains the sparse responses obtained in *H. virescens*. Furthermore, sparse responses to single odorants may also apply to multiglomerular PNs as shown in this study for the Type 1 ml-APT PN, exclusively responding to the B10 blend. Local excitatory interneurons have not been found in this or in other moth species, in contrast to *Drosophila* where interglomerular excitation is shown (Olsen et al., 2007; Shang et al., 2007), which may contribute to a broader response profile of the PNs (Wilson et al., 2004).

To understand how odour information is integrated in the central neurons of *H. virescens*, we have compared the responses elicited by single primary odorants and two complex mixtures containing the single odorants. In these comparisons we have used the MDS which quantifies response strength (firing rate) in different temporal phases of

the response window. We are aware of the limitation of the results. Due to the relative short duration of this kind of intracellular recordings each neuron was not tested for all odorants in the protocol. However, from the data on the 28 selected neurons tested for the most effective odorants and mixture, several integration principles appeared, like hypoadditivity in eight neurons, suppression in six neurons and best mixture effect in thirteen neurons. Because hypoadditivity and best mixture effect would require tests with all single constituents we cannot conclude whether the responses were exclusively due to a mixture effect and not to another untested single constituent. In spite of these limitations, the results show that the integration is more intricate than just hypoadditivity and suppression, as exemplified in the results (**Figures 2A-C** and **Figure 4**). Thus, a neuron might show similar response strength to a mixture (B10) and to one of the single odorants, but the addition of two other excitatory odorants to the same mixture (B12) elicited a weaker response. Most likely the integrating neurons are activated by an array of input channels which might contribute with different strengths to the evoked post synaptic responses when activated alone by single odorants or in concert by mixtures. In addition to the complex integration in some neurons, others showed more specific responses to stimulation with one or two of the tested odorants.

Putative circuit

Based on the physiology and morphology of the successfully stained neurons presented in this study, we consider them as part of a putative circuit receiving input from the AL and connecting the three protocerebral areas, the SP, the LP and the MB. Anatomical overlap does not automatically indicate functional connectivity. However the responses by all of them to stimulation with the ten component mixture indicate that they are part of a putative circuit handling combinatorial information given by this blend. Like in other insect species, the calyces of the MB and the LP in *H. virescens* are the targets of the m- and l-APT neurons, but in the opposite order (Rø et al., 2007; Galizia and Rössler, 2010). The protocerebral olfactory areas, the calyces, the superior protocerebrum (SP) and the LP in *H. virescens* are visualised by the mass stained APTs (**Figure 1A**), the calyces and the LP covering the projection area of the three m-APT neurons, as shown in **Figure 11A-C** (m-APT PNs from Løfaldli et al., (2010)). The typical five axonal branches of the m-APT neurons innervating the calyces appear before the axon run anterior-laterally into the OA of the LP, as previously shown in Rø et al., (2007) and Løfaldli et al., (2010).

The ml-APT neurons

The clearly mass stained ml-APT in fig – with the distinct pathways and projections in the superior and the lateral protocerebrum of *H. virescens*, show slightly different axonal branching pattern than ml-APTs described in other insect species, like in the honeybee (Kirchener et al., 2006; Galizia and Rössler 2010). For instance, whereas SP is the target area of some ml-ACT neurons in *H. virescens*, the ring neuropil around the α-lobe of the MB seems to be a corresponding area in the honeybee (Abel et al., 2001; Kirschner et al., 2006). Previous studies in moths and the honeybee have reported that the ml-APT contains multiglomerular PNs (Abel et al., 2001; Jefferis et al., 2007; Rø et al., 2007; Galizia and Rössler, 2010; Namiki and Kanzaki, 2011), that have been found to be GABAergic (Hoskins et al., 1986; Schäfer and Bicker, 1986; Berg et al., 2009). In this study the two identified types of ml-APT PNs that follow the pathway of the mass-

stained ml-ACT and exhibit different projection patterns share similarities with the ml-APT neuron types previously described in this species by Rø et al., (2007). The type 2 ml-APT neurons have the distinct axonal bifurcation, one branch projecting in the LP olfactory axis and the other turning dorso-medially into the SP, both showing extensive and wide projection patterns. Since the morphology of this neuron fits with the GABA-immuno-stained ml-APT of this species (Berg et al., 2009), it is possible that this neurone is GABA-ergic. The Type 1 ml-APT neurons, lacking the distinct axonal bifurcation and having a much more condensed arborisation in both the LP and the SP, follow the same pathway to the LP. Another difference between these two neurone types appears in the glomerular innervation; the Type 2 innervating many if not all glomeruli and Type 1 fewer glomeruli located laterally in the AL. Both types show sparse intervention of each glomerulus, Type 1 even sparser than Type 2. Similar morphological patterns of two ml-APT neurons have previously been described in the honeybee (Abel et al., 2001).

The physiological responses recorded in the Type 1 ml-APT neuron in this study seem to reflect the sparse dendritic arborisation in each glomerulus. Since the neuron responded with strong excitation and long latency exclusively to the complex mixture of ten primary odorants and showed no responses to the single odorants in this mixture or to other blends, it implies that the neuron needs input from multiple glomeruli in concert to become activated. This is in contrast to uniglomerular neurons responding to single odorants and having dense innervation in one glomerulus. The correlation between innervation pattern and physiology of multiglomerular neurons has been a matter of speculations in earlier morphological studies by Kirschner et al., (2006) *citation*: "Due to the rather sparse dendritic innervation within glomeruli these neurons probably have a high activation threshold". The functional implication of the ml-APT neuron in *H. virescens* might be to transfer a combinatorial activity pattern from the AL to the target regions in SP and LP. However, different multiglomerular ml-APT neurons might display functional heterogeneity, since in the honeybee responses to single odorants by ml-APT neurons have been shown (Abel et al., 2001). We may further speculate that some GABAergic ml-APT neurons form an inhibitory channel from the AL to protocerebrum in parallel to the excitatory pathways formed by the m- and the l-APT PNs. This together with the functional differentiation between the m-APT and the l-APT described in the honeybee (Krofczik et al., 2009; Yamagata et al., 2009) might imply that third order LP neurons integrate both inhibitory and excitatory information about blends and single odorants from the AL. One possible role for an inhibitory multiglomerular APT channel might be to reset odour elicited activity of third order neurons in the LP network. Other possible functions is the involvement in regulating and synchronising the activity of odour triggered third order LP neurons, similar to the function suggested for other GABAergic protocerebral neurons (Honeybee: Grünewald, 1999; Ganeshina and Menzel, 2001; Szyszka et al., 2005. Locusts: Perez-Orive et al., 2004).

The protocerebral neurons

The two MB extrinsic neurons receiving information in the medial-lobe of the MB had axonal projections in the superior and the lateral protocerebrum, respectively that partly overlapped with the projections of the ml-APT neurons. A variety of MB extrinsic neurons have previously been described in several insect species like the honeybee, the

fruit fly and the cockroach (Honeybee: Homberg, 1984; Mauelshagen, 1993; Rybak and Menzel, 1998; Strausfeld, 2002. Fruit fly: Ito et al., 1998; Tanaka et al., 2008. Cockroach: Li and Strausfeld, 1997). Although we did not find a complete morphological resemblance, the two stained extrinsic neurons in this study make similar connections between the lobes of the MB and the LP and SP as neurons described in the honeybee (Strausfeld 2002) and in *Drosophila* (Ito et al., 1998). For instance, efferent MB extrinsic neurons in *Drosophila* connects mainly the head of the α lobe with the SP and the LP (Ito et al., 1998), whereas the stained MB extrinsic neurons in this study projected exclusively from the swellings of the medial lobes (β and β') to the SP and the LP. Dendritic arborisations confined to the swellings of the lobes seem to be in line with findings in *Drosophila* (Ito et al., 1998).

MB extrinsic neurons, including the PE1 neuron in the honeybee, have been shown as multi modal as well as responding to a variety of odour stimuli (Homberg, 1984; Mauelshagen, 1993; Rybak and Menzel, 1998; Li and Strausfeld, 1999; Okada et al., 2007). Our recordings in *H. virescens* showed that only one of the two MB extrinsic neurons responded to the mechanical stimulation (air puff) but not to stimulation with tastants. However, since stimulation with tastants was only tested for the MB-LP neuron, we can not conclude whether other medial lobe extrinsic neuron respond to this modality. In respect to odour stimuli both MB extrinsic neurons responded to all applied odorants but with a different response profiles. A clear difference in response strength to stimulation with the single odorants and the blends appeared in the MB-SP neuron. This implies an odour specific response to the primary odorants when presented in a novel non-associative situation. More recordings are obviously necessarily to generalise this as a principle for the medial lobe extrinsic neurons in *H. virescens*. However, in other insect species odour specific responses among cells of the MB, including extrinsic neurons has previously been reported (Honeybee: Szyszka et al., 2005. Locust: MacLeod and Laurent, 1996; Perez-Orive et al., 2002; Stopfer et al., 2003; Cassenaer and Laurent, 2007. Fruit fly: Turner et al., 2008). Since MB extrinsic neurons probably are involved in mediating conditioned olfactory information, it would be interesting in future experiments to test MB extrinsic neuron responses to the primary odorants before and after conditioning in *H. virescens*.

Another interesting question is whether the olfactory specificity or the odour code is preserved through the neural network of the olfactory system from the receptor neuron input to specific glomeruli in the AL and further to the descending neurons in the pre-motor area ventrally of the LP. In this study we have shown that the information about a plant odour blend is being processed in parallel through multiple pathways. Thus the SP receives information about the complex B10 blend both directly from the AL and indirectly from the MB and the LP, whereas the LP receives the same information directly from the AL via all three APTs and indirectly from the MB. Whether other parallel routs exist in *H. virescens* is not known. However, in other insects additional pathways to the MB have been described (Ganeshina and Menzel, 2001; Perez-Orive et al., 2002; Keene and Waddell, 2007). One implication of parallel olfactory pathways might be to process information in a context dependent manner in the different areas. Based on many studies it is previously suggested that whereas the MB function as a

coincidence detector for associative olfactory memories, the AL-LP pathway represent a novel or an inexperience independent pathway for olfactory dependent behaviour (Heimbeck et al., 2001; Tanaka et al., 2004; Keene and Waddell, 2007). In *Drosophila* it is speculated whether LP is also involved in olfactory associative memories (Wang et al., 2003b).

In this study the mass and the single cell staining indicates some overlap of the most anterior-ventrally projections from PNs in the l- and the ml-APT and the dendritic arborisation of the LP-descending neuron. This suggests that the output area of the LP is located anterior-ventrally of the OA. Axonal projections of a taste responding neuron have previously been shown to project in this area implying a possible integration of the two chemosensory modalities (Kvello et al., 2009). Integration of multimodal information in the output areas of LP has also been suggested in flies, indicated by visual and olfactory projections to this area (Strausfeld, 1976; Tanaka et al., 2004). Unfortunately, the descending neuron in this study was only tested for olfactory (inhibitory) and mechanical (no response) input and not with gustatory or other modalities. The strong inhibitory responses particularly to the blend might be mediated directly from PNs in the ml-APT like the neuron in this study, from third order LP neurons, as described in the *Drosophila* (Tanaka et al., 2004; Jefferis et al., 2007), or from the MB-LP rout. Although the axonal projections of the presented MB-LP neuron in this study did not overlap with the dendritic arborisations of the descending neuron, other MB-LP neurons might overlap. The inhibitory response of the descending neuron is interesting in connection with the speculation by Okada et al., (2007) regarding inhibition mediated to descending neurons, directly or indirectly from MB extrinsic neuron. It is suggested that MB extrinsic neurons, like the PE1 in the honeybee mediate inhibition to descending neurons in naïve individuals and that olfactory learning reduces inhibition. The challenge of further studies would be to test responses to primary odorants and mixtures before and after learning to find out whether and how the inhibitory responses change in descending neurons. The result that only mixtures, especially the B10, elicited strong inhibitory responses in the descending neuron is interesting in comparison with behavioural results in the *M. sexta*, showing that complex mixtures derived from host plants and not the single constituents elicit feeding behaviour (Riffell et al., 2009a; Riffell et al., 2009b). This implies that odour responses in the descending neuron are elicited upon co-activation of multiple inputs from parallel pathways in the direct AL-LP stream (inexperienced) and/or from the integrative experienced AL-MB-LP stream.

Acknowledgements

The project was financed by the Royal Norwegian Society of Sciences and Letters. We also acknowledge Prof. Erich Buchner (Universität Würzburg, Germany) for providing antibodies and the Insect Rearing Team of Syngenta (Basel, Switzerland) for providing insect materials.

References

Abel, R., Rybak, J., and Menzel, R. (2001). Structure and response patterns of olfactory interneurons in the honeybee, *Apis mellifera*. *J. Comp. Neurol.* 437**,** 363-383.

886 Anton, S., and Hansson, B.S. (1994). Central processing of sex pheromone, host odour,
887 and oviposition deterrent information by interneurons in the antennal lobe of
888 female *Spodoptera littoralis* (Lepidoptera: Noctuidae). *J. Comp. Neurol.* 350**,**
889 199-214.
890 Barrozo, R.B., Jarriault, D., Deisig, N., Gemeno, C., Monsempes, C., Lucas, P., Gadenne,
891 C., and Anton, S. (2011). Mating-induced differential coding of plant odour and
892 sex pheromone in a male moth. *EJN.* 33**,** 1841-1850.
893 Berg, B., Schachtner, J., and Homberg, U. (2009). γ-Aminobutyric acid immunostaining
894 in the antennal lobe of the moth *Heliothis virescens* and its colocalization with
895 neuropeptides. *Cell Tissue Res*. 335**,** 593-605.
896 Berg, B.G., Almaas, T.J., Bjaalie, J.G., and Mustaparta, H. (1998). The macroglomerular
897 complex of the antennal lobe in the tobacco budworm moth *Heliothis virescens*:
898 specified subdivision in four compartments according to information about
899 biologically significant compounds. *J. Comp. Physiol. A.* 183**,** 669-682.
900 Berg, B.G., Galizia, C.G., Brandt, R., and Mustaparta, H. (2002). Digital atlases of the
901 antennal lobe in two species of tobacco budworm moths, the oriental *Helicoverpa*
902 *assulta* (male) and the American *Heliothis virescens* (male and female). *J. Comp.*
903 *Neurol.* 446**,** 123-134.
904 Brant, R., Rohlfing, T., Rybak, J., Krofczik, S., Maye, A., Westerhoff, M., Hege, H. C.,
905 and Menzel, R. (2005). Three-dimensional average shaped atlas of the honeybee
906 brain and its applications. *J. Comp. Neurol*. 492, 1-19.
907 Cassenaer, S., and Laurent, G. (2007). Hebbian STDP in mushroom bodies facilitates the
908 synchronous flow of olfactory information in locusts. *Nature* 448**,** 709-713.
909 Christensen, T.A., Mustaparta H., and Hildebrand J.G. (1991). Chemical Communication
910 in Heliothine Moths. II. Central processing of intra- and interspecific olfactory
911 messages in the male corn earworm moth *Helicoverpa zea*. *J. Comp. Physiol. A*.
912 169, 259-274.
913 Christensen, T.A., Mustaparta H., and Hildebrand J.G. (1995). Chemical Communication
914 in Heliothine Moth. Parallel Pathways for Information Processing in the
915 Macroglomerular Complex of the Male Moth *Heliothis virescens*. *J. Comp.*
916 *Physiol. A*. 177, 545-557.
917 Christensen, T.A., and Hildebrand, J.G. (2002). Pheromonal and host-odor
918 processing in the insect antennal lobe: how different? *Curr. Opin. Neurobiol.* 12**,**
919 393-399.
920 Deisig, N., Giurfa, M., Lachnit, H., and Sandoz, J.-C. (2006). Neural representation of
921 olfactory mixtures in the honeybee antennal lobe. *EJN.* 24**,** 1161-1174.
922 Deisig, N., Giurfa, M., and Sandoz, J.C. (2010). Antennal Lobe Processing Increases
923 Separability of Odor Mixture Representations in the Honeybee. *J. Neurophysiol.*
924 103**,** 2185-2194.
925 Evers, J. F., Schmitt, S., Sibila, M., and Duch, C. (2005). Progress in functional neuro-
926 anatomy: precise automatic geometric reconstruction of neuronal morphology
927 from confocal image stacks. *J. Neurophysiol*. 93, 2331-2342.
928 Flanagan, D., and Mercer, A.R. (1989). An atlas and 3-D reconstruction of the antennal
929 lobes in the worker honey bee, *Apis mellifera* L. (Hymenoptera: Apidae). *Int. J.*
930 *Insect Morphol. Embryol.* 18**,** 145-159.

931 Fukushima, R., and Kanzaki, R. (2009). Modular subdivision of mushroom bodies by
932 kenyon cells in the silkmoth. *J. Comp. Neurol.* 513**,** 315-330.
933 Galizia, C.G., and Menzel, R. (2000). Odour perception in honeybees: coding
934 information in glomerular patterns. *Curr. Opin. Neurobiol.* 10**,** 504-510.
935 Galizia, C.G., and Rössler, W. (2010). Parallel Olfactory Systems in Insects: Anatomy
936 and Function. *Annu. Rev. Entomol.* 55**,** 399-420.
937 Galizia, C.G., and Szyszka, P. (2008). Olfactory coding in the insect brain:
938 molecular receptive ranges, spatial and temporal coding. *Entomol. Exp. Appl*. 128:
939 81-92.
940 Ganeshina, O., and Menzel, R. (2001). GABA-immunoreactive neurons in the mushroom
941 bodies of the honeybee: An electron microscopic study. *J. Comp. Neurol*. 437**,**
942 335-349.
943 Gerber, B., Tanimoto, H., and Heisenberg, M. (2004). An engram found? Evaluating the
944 evidence from fruit flies. *Nature Neurosci.* 14**,** 737-744.
945 Grünewald, B. (1999). Physiological properties and response modulations of mushroom
946 body feedback neurons during olfactory learning in the honeybee, *Apis mellifera*.
947 *J. Comp. Physiol. A*. 185**,** 565-576.
948 Heimbeck, G., Bugnon, V., Gendre, N., Keller, A., and Stocker, R.F. (2001). A central
949 neural circuit for experience-independent olfactory and courtship behavior in
950 *Drosophila melanogaster*. *PNAS.* 98**,** 15336-15341.
951 Heinbockel, T., Christensen, T.A., and Hildebrand, J.G. (1999). Temporal tuning of odor
952 responses in pheromone-responsive projection neurons in the brain of the sphinx
953 moth *Manduca sexta*. *J. Comp. Neurol*. 409, 1-12.
954 Heisenberg, M. (2003). Mushroom body memoir: from maps to models. *Nat. Rev.*
955 *Neurosci.* 4**,** 266-275.
956 Heisenberg, M., Borst, A., Wagner, S., and Byers, D. (1985). *Drosophila* mushroom
957 body mutants are deficient in olfactory learning. *J. Neurogenet.* 2**,** 1-30.
958 Homberg, U. (1984). Processing of antennal information in extrinsic mushroom body
959 neurons of the bee brain. *J. Comp. Physiol. A.* 154**,** 825-836.
960 Homberg, U., Montague, R.A., and Hildebrand, J.G. (1988). Anatomy of antenno-
961 cerebral pathways in the brain of the sphinx moth *Manduca sexta*. *Cell Tissue*
962 *Res.* 254**,** 255-281.
963 Hoskins, S.G., Homberg, U., Kingan, T.G., Christensen, T.A., and Hildebrand, J.G.
964 (1986). Immunocytochemistry of GABA in the antennal lobes of the sphinx moth
965 *Manduca sexta*. *Cell Tissue Res.* 244**,** 243-252.
966 Ito, K., Suzuki, K., Estes, P., Ramaswami, M., Yamamoto, D., and Strausfeld, N.J.
967 (1998). The Organization of Extrinsic Neurons and Their Implications in the
968 Functional Roles of the Mushroom Bodies in *Drosophila melanogaster* Meigen.
969 *Learn. Mem.* 5**,** 52-77.
970 Jefferis, G.S.X.E., Potter, C.J., Chan, A.I., Marin, E.C., Rohlfing, T., Maurer, C.R., and
971 Luo, L.Q. (2007). Comprehensive maps of *Drosophila* higher offactory centers:
972 Spatially segregated fruit and pheromone representation. *Cell* 128**,** 1187-1203.
973 Joerges, J., Kuttner, A., Galizia, C.G., and Menzel, R. (1997). Representations of odours
974 and odour mixtures visualized in the honeybee brain. *Nature* 387**,** 285-288.

975 Kanzaki, R., Arbas, E.A., and Hildebrand, J.G. (1991). Physiology and morphology of
976 descending neurons in pheromone-processing olfactory pathways in the male
977 moth *Manduca sexta*. *J. Comp. Physiol. A.* 169**,** 1-14.
978 Kanzaki, R., Ikeda, A., and Shibuya, T. (1994). Morphological and physiological
979 properties of pheromone-triggered flipflopping descending interneurons of the
980 male silkworm moth, *Bombyx mori*. *J. Comp. Physiol. A.* 175**,** 1-14.
981 Keene, A.C., and Waddell, S. (2007). *Drosophila* olfactory memory: single genes to
982 complex neural circuits. *Nat. Rev. Neurosci.* 8**,** 341-354.
983 Kirschner, S., Kleineidam, C.J., Zube, C., Rybak, J., Grünewald, B., and Rössler, W.
984 (2006). Dual olfactory pathway in the honeybee, *Apis mellifera*. *J. Comp. Neurol.*
985 499**,** 933-952.
986 Krofczik, S., Menzel, R., and Nawrot, M.P. (2009). Rapid odor processing in the
987 honeybee antennal lobe network. *Front.* Comput. Neurosci. (2009)
988 **2**:9. doi: 10.3389/neuro.10.009.2008
989 Kuebler, L.S., Olsson, S.B., Weniger, R., and Hansson, B.S. (2011). Neuronal
990 processing of complex mixtures establishes a unique odor representation
991 in the moth antennal lobe. *Front. Neural Circuits*. **5**:7.
992 doi: 10.3389/fncir.2011.00007
993 Kvello, P.L., Løfaldli, B.B., Rybak, J.R., Menzel, R., and Mustaparta, H. (2009). Digital,
994 three-dimensional average shaped atlas of the heliothis virescens brain with
995 integrated gustatory and olfactory neurons. *Front. Syst. Neurosci*. 3:14. doi:
996 10.3389/neuro.06.014.2009.
997 Laurent, G., Wehr, M., and Davidowitz, H. (1996). Temporal Representations of Odors
998 in an Olfactory Network. *J. Neurosci.*16**,** 3837-3847.
999 Lei, H., Christensen, T.A., and Hildebrand, J.G. (2004). Spatial and Temporal
1000 Organization of Ensemble Representations for Different Odor Classes in the Moth
1001 Antennal Lobe. *J. Neurosci.*24**,** 11108-11119.
1002 Li, Y., and Strausfeld, N.J. (1997). Morphology and sensory modality of mushroom body
1003 extrinsic neurons in the brain of the cockroach, *Periplaneta americana*. *J. Comp.*
1004 *Neurol*. 387**,** 631-650.
1005 Li, Y., and Strausfeld, N.J. (1999). Multimodal efferent and recurrent neurons in the
1006 medial lobes of cockroach mushroom bodies. *J. Comp. Neurol*. 409**,** 647-663.
1007 Løfaldli, B.B., Kvello, P., and Mustaparta, H. (2010). Integration of the antennal lobe
1008 glomeruli and three projection neurons in the standard brain atlas of the moth
1009 *Heliothis virescens*. *Front. Syst. Neurosci*. 4:5. doi: 10.3389/neuro.06.005.2010.
1010 Macleod, K., and Laurent, G. (1996). Distinct mechanisms for synchronization and
1011 temporal patterning of odor-encoding neural assemblies. *Science* 274**,** 976-979.
1012 Marin, E.C., Jefferis, G.S.X.E., Komiyama, T., Zhu, H., and Luo, L. (2002).
1013 Representation of the Glomerular Olfactory Map in the *Drosophila* Brain. *Cell*
1014 109**,** 243-255.
1015 Mauelshagen, J. (1993). Neural correlates of olfactory learning paradigms in an identified
1016 neuron in the honeybee brain. *J. Neurophysiol*. 69**,** 609-625.
1017 Menzel, R. (2001). Searching for the memory trace in a mini-brain, the honeybee. *Learn.*
1018 *Mem.* 8**,** 53-62.

1019 Müller, D.M., Abel, R.A., Brandt, R.B., Zöckler, M.Z., and Menzel, R.M. (2002).
1020 Differential parallel processing of olfactory information in the honeybee, *Apis*
1021 *mellifera* L. *J. Comp. Physiol. A.* 188**,** 359-370.
1022 Namiki, S., and Kanzaki, R. (2011). Heterogeneity in dendritic morphology of moth
1023 antennal lobe projection neurons. *J. Comp. Neurol*. 519, 17, 3367-3386.
1024 Okada, R., Rybak, J., Manz, G., and Menzel, R. (2007). Learning-Related Plasticity in
1025 PE1 and Other Mushroom Body-Extrinsic Neurons in the Honeybee Brain. *J.*
1026 *Neurosci.* 27**,** 11736-11747.
1027 Olsen, S., Bhandawat, V., and Wilson, R. (2007). Excitatory Interactions between
1028 Olfactory Processing Channels in the *Drosophila* Antennal Lobe. *Neuron* 54**,** 89-
1029 103.
1030 Perez-Orive, J., Bazhenov, M., and Laurent, G. (2004). Intrinsic and Circuit Properties
1031 Favor Coincidence Detection for Decoding Oscillatory Input. *J. Neurosci.* 24**,**
1032 6037-6047.
1033 Perez-Orive, J., Mazor, O., Turner, G.C., Cassenaer, S., Wilson, R.I., and Laurent, G.
1034 (2002). Oscillations and sparsening of odor representations in the mushroom
1035 body. *Science* 297**,** 359-365.
1036 Røstelien, T., Stranden, M., Borg-Karlson, A.K., and Mustaparta, H. (2005). Olfactory
1037 receptor neurones in two heliothine moth species responding selectively to
1038 aliphatic green leaf volatiles, aromatics, monoterpenes and sesquiterpenes of plant
1039 origin. *Chem. Senses* 30**,** 443-461.
1040 Reisenman, C.E., Christensen, T.A., and Hildebrand, J.G. (2005). Chemosensory
1041 Selectivity of Output Neurons Innervating an Identified, Sexually Isomorphic
1042 Olfactory Glomerulus. *J. Neurosci.* 25**,** 8017-8026.
1043 Riffell, J.A., Lei, H., Christensen, T.A., and Hildebrand, J.G. (2009a). Characterization
1044 and Coding of Behaviorally Significant Odor Mixtures. *Curr. Biol.* 19**,** 335-340.
1045 Riffell, J.A., Lei, H., and Hildebrand, J.G. (2009b). Neural correlates of behavior in the
1046 moth Manduca sexta in response to complex odors. *PNAS.* 106**,** 19219-19226.
1047 Ruta, V., Datta, S.R., Vasconcelos, M.L., Freeland, J., Looger, L.L., and Axel, R. (2010).
1048 A dimorphic pheromone circuit in *Drosophila* from sensory input to descending
1049 output. *Nature* 468**,** 686-690.
1050 Rybak, J., and Menzel, R. (1998). Integrative Properties of the Pe1 Neuron, a Unique
1051 Mushroom Body Output Neuron. *Learn. Mem.* 5**,** 133-145.
1052 Rø, H., Muller, D., and Mustaparta, H. (2007). Anatomical organization of antennal lobe
1053 projection neurons in the moth *Heliothis virescens*. *J. Comp. Neurol.* 500**,** 658-
1054 675.
1055 Sadek, M.M., Hansson, B.S., Rospars, J.P., and Anton, S. (2002). Glomerular
1056 representation of plant volatiles and sex pheromone components in the antennal
1057 lobe of the female *Spodoptera littoralis*. *J. Exp. Biology* 205**,** 1363-1376.
1058 Schäfer, S., and Bicker, G. (1986). Distribution of GABA-like immunoreactivity in the
1059 brain of the honeybee. *J. Comp. Neurol.* 246**,** 287-300.
1060 Schmitt, S., Evers, J.F., Duch, C., Scholz, M., and Obermayer, K. (2004). New methods
1061 for the computer-assisted 3-D reconstruction of neurons from confocal image
1062 stacks. *Neuroimage* 23, 1283-1298.

1063 Shang, Y., Claridge-Chang, A., Sjulson, L., Pypaert, M., and Miesenböck, G. (2007).
1064 Excitatory Local Circuits and Their Implications for Olfactory Processing in the
1065 Fly Antennal Lobe. *Cell* 128**,** 601-612.
1066 Skiri, H.T., Galizia, C.G., and Mustaparta, H. (2004). Representation of primary plant
1067 odorants in the antennal lobe of the moth *Heliothis virescens*, using calcium
1068 imaging. *Chem. Senses* 29**,** 253-267.
1069 Stocker, R.F., Lienhard, M.C., Borst, A., and Fischbach, K.F. (1990). Neuronal
1070 architecture of the antennal lobe in *Drosophila melanogaster*.
1071 *Cell Tissue Res.* 262**,** 9-34.
1072 Stopfer, M., Jayaraman, V., and Laurent, G. (2003). Intensity versus identitiy coding in
1073 an olfactory system. *Neuron* 39**,** 991-1004.
1074 Strausfeld, N.J. (1976). Atlas of an Insect Brain. New York: Springer-Verlag.
1075 Strausfeld, N.J. (2002). Organization of the honey bee mushroom body: Representation
1076 of the calyx within the vertical and gamma lobes. *J. Comp. Neurol.* 450**,** 4-33.
1077 Szyszka, P., Ditzen, M., Galkin, A., Galizia, C.G., and Menzel, R. (2005). Sparsening
1078 and temporal sharpening of olfactory representations in the honeybee
1079 mushroom bodies. *J. Neurophysiol*. 94, 3303-3313.
1080 Tanaka, N.K., Awasaki, T., Shimada, T., and Ito, K. (2004). Integration of chemosensory
1081 pathways in the *Drosophila* second-order olfactory centers. *Curr. Biol.* 14**,** 449-
1082 457.
1083 Tanaka, N.K., Tanimoto, H., and Ito, K. (2008). Neuronal assemblies of the *Drosophila*
1084 mushroom body. *J. Comp. Neurol*. 508**,** 711-755.
1085 Turner, G.C., Bazhenov, M., and Laurent, G. (2008). Olfactory Representations by
1086 *Drosophila* Mushroom Body Neurons. *J. Neurophysiol.* 99**,** 734-746.
1087 Vickers, N., Christensen, T., and Hildebrand, J. (1998). Combinatorial odor
1088 discrimination in the brain: Attractive and antagonist odor blends are represented
1089 in distinct combinations of uniquely identifiable glomeruli. *J. Comp. Neurol.* 400**,**
1090 35-56.
1091 Vosshall, L.B., Amrein, H., Morozov, P.S., Rzhetsky, A., and Axel, R. (1999). A Spatial
1092 Map of Olfactory Receptor Expression in the *Drosophila* Antenna. *Cell* 96**,** 725-
1093 736.
1094 Vosshall, L.B., and Stocker, R.F. (2007). Molecular Architecture of Smell and Taste in
1095 *Drosophila*. *Annu. Rev. Neurosci.* 30**,** 505-533.
1096 Wang, J.W., Wong, A.M., Flores, J., Vosshall, L.B., and Axel, R. (2003a). Two-photon
1097 calcium imaging reveals an odor-evoked map of activity in the fly brain. *Cell* 112**,**
1098 271-282.
1099 Wang, Y., Chiang, A.S., Xia, S., Kitamoto, T., Tully, T., and Zhung, Y. (2003b).
1100 Blockade of Neurotransmission in *Drosophila* Mushroom Bodies Impairs Odor
1101 Attraction, but Not Repulsion. *Curr. Biol.* 13**,** 1900-1904.
1102 Wilson, R.I., Turner, G.C., and Laurent, G. (2004). Transformation of Olfactory
1103 Representations in the *Drosophila* Antennal Lobe. *Science* 303**,** 366-370.
1104 Wong, A.M., Wang, J.W., and Axel, R. (2002). Spatial representation of the glomerular
1105 map in the *Drosophila* protocerebrum. *Cell* 109**,** 229-241.
1106 Yamagata, N., Schmuker, M., Szyszka, P., Mizunami, M., and Menzel, R. (2009).
1107 Differential odor processing in two olfactory pathways in the honeybee. *Front.*
1108 *Syst. Neurosci.* 3:16. doi: 10.3389/neuro.06.016.2009.

Figure legend

Figure 1: Projection view from stacks of confocal images showing mass stained APTs, spontaneous frequency distribution and response modes among the 28 recorded neurons. (A) Projection view from confocal images of mass staining in the AL revealing the three main APTs. The m- and the l-APTs projecting in the calyces of the MB and the OA of the LP, but in opposite order, and the ml-APT directly in the LP with some branches turning anterior-dorsally terminating in the SP. At this depth most m-APT projections in the LP are not visible. Dorsal view. CB; central body, MBC; mushroom body calyces, AL; antennal lobe, LP: lateral protocerebrum. (B) Graph showing the frequency distribution of the spontaneous activity among recorded neurons in two target areas of APTs, the SP and the LP. (C) Intracellular recording showing the three response modes, excitation (upper trace), inhibition (middle trace) and complex (lower trace), elicited by stimulation with B10 in three different neurons. All responses clearly outlasting the stimulation period (300ms).

Figure 2: Responses of selected neurons presented as MDS, MRF and maximum frequency graphs with the response curves, exemplifying excitatory, inhibitory and complex response modes. (A-C) Average MDS plot for control, four single odorants and the two blends, B10 and B12 of (A) an excitatory, (B) an inhibitory and (C) a complex responding neuron. In A only the response in the excitatory phase is significant (black bars) and in B only in the inhibitory phase (grey bars). (D-F) The response curves for all response modes clearly reflect the corresponding MDS plot. (D) Response curves for three short excitatory, (E) for two short inhibitory and (F) for three complex responding neurons. (G-I) Responses presented as maximum frequency (the two black bars representing repeated responses) and MRF (striped bars) for the same neurons as in A-C. Evidently the MRF and the maximum frequency for the inhibitory (H) and the complex (I) responding neurons do not reflect the response curve.

Figure 3: Response chart shows the response modes of all 28 neurons to the selected stimuli. Neurons represented in each layer (A-G) is sorted according to response modes, neurons 1-16 as excitatory (1-14 short excitatory), 17-20 as inhibitory and 21-27 as complex, whereas 28 is unassigned. For the complex responding neurons the strongest response phase is indicated. Green: excitation, red: inhibition, grey: no response and white: not tested. (A) Response modes to control, (B-D) to the four selected single odorants and (E-F) to the two blends.

Figure 4: Responses of an excitatory neuron presented as MDS histogram for an excitatory responding neuron revealing an intricate response pattern to the single odorants and the blends. The response to B10 showing hypoadditivity as compared to 2-phenyl ethanol. However addition of two components (B12) showed a weaker response (suppression) as well as hypoadditivity compared to 3Z-hexenyl acetate and germacrene D. Pooled SD is indicated.

Figure 5: All significant responses of excitatory (left), inhibitory (middle) and complex responding neurons (right) selected and represented in box plots. The circles indicate the calculated MDS values (Hz) for the individual responses to the control, single odorants,

and the complex blends. For the excitatory neurons only the positive deviation (excitatory MDS) was considered, for the inhibitory neurons only the negative deviation (inhibitory MDS) and for the complex responding neurons the absolute deviation. Wilcoxon rank-sum tests were used to compare the observed values between the three stimuli groups (control, the four single odorants and the two blends selected for analysis). Asterisks indicate significance levels of the tests (* → $p < 0.05$, ** → $p < 0.01$, *** → $p < 0.001$). Since only one inhibitory neuron responded to control, this was not included in the statistical analysis.

Figure 6: Raster plots and response curves of stained neurons responding to stimulation with the B10 blend. (A-E) Left: The raster plots include responses to the same stimuli (control, 3Z-hexenyl acetate and B10) for the six stained neurons, (A) the Type 1 ml-APT PN, (B) the MB-SP neuron, (C) the MB-LP neuron, (D) the LP-SP neuron and (E) the LP-descending neuron. Right: Corresponding response curves showing the average temporal response pattern. 3Z-H.ac.; 3Z-Hexenyl acetate, Cont; Control.

Figure 7: Projection view from stacks of confocal images of two types of ml-APT neurons, 3D reconstructions and transformations into the SBA. (A) Confocal images of the two simultaneously stained Type 1 ml-APT PN showing the dendritic arborisation in the AL with spars innervation in many glomeruli. (B) The axonal branches projecting in the two protocerebral areas, the SP (sparsely) and the LP. (C) Confocal images of the stained Type 2 ml-APT PN showing loose dendritic arborisation in most or all glomeruli. (D) Axonal projections of the same neuron showing extensive and wide branching patterns in the SP and the LP. One axon branch off before reaching the LP and making the characteristic dorso-anterior turn before entering the SP. (E-H) 3D reconstructions of the ml-APT PNs (Type 1; blue and Type 2; yellow) transformed into the SBA showing extensive overlap in the OA of the LP, both axons branching in a dorsal and ventral direction. In the SP some axonal projections are proximate to the MB lobes. Both neurons had soma ventrally in the lateral cell cluster of the AL. (E) frontal view, (F) Close-up frontal view, (G) lateral view and (H) dorsal view. AN; antennal nerve, PED; pedunculus, CB; central body, LP; lateral protocerebrum, SP; superior protocerebrum.

Figure 8: Projection view from stacks of confocal images and 3D reconstruction of two stained efferent MB extrinsic neurons transformed into the SBA. (A) Projection view of the MB-SP neuron showing the dense dendritic arborisation in the medial lobe and (B) the relatively wide axonal projections in the SP proximate to the vertical lobe. (C) Confocal images of the MB-LP extrinsic neuron showing the weak dendritic innervation in the lateral part of the medial lobe and (D) the axonal projection in parts of the OA of the LP. (E-G) 3D reconstruction of the MB-SP (white) and the MB-LP (dark blue) transformed into the SBA visualize the different axonal projections in the SP and LP. (E) Frontal view, (F) lateral view and (G) dorsal view. SP: superior protocerebrum, LP: lateral protocerebrum, MB: mushroom bodies.

Figure 9: Projection view from stacks of confocal images of the LP-SP and the LP-descending neuron reconstructed and transformed into the SBA. (A) Projection view of the LP-SP neuron showing dendritic arborisations in the LP and axonal projections in the

SP. (B) Projection view of the LP-descending neuron having two dendritic branches originating in the SOG and terminating in dense arborisations in the ventro-anterior area of the LP. (C-D) 3D reconstructions of the two neurons transformed into the SBA visualizing the dendritic arborisations and the axonal projections of the LP-descending neuron (yellow), the axon leaving the brain through the ipsilateral connective. The large cell soma is located medio-ventrally in the SOG. The LP-SP neuron (orange) has a few dendritic branches in the OA of the LP and in the medio-inferior parts of the protocerebrum. The dense axonal projections are medially in the SP and some branches terminate around the lobes. No overlap was found between the LP-SP and the LP-descending neuron. (C) Frontal view and (D) lateral view. CB; central body, PED; pedunculus; SP; superior protocerebrum, LP; lateral protocerebrum.

Figure 10: 3D reconstructions of the ml-APT PNs, the MB extrinsic neurons and the LP-SP neuron transformed into the SBA. (A-C) Type 2 ml-APT PN (yellow) shows overlap in the OA of the LP with both the dendrites of the LP-SP (orange) neuron and the axonal projections from the MB-LP neuron (dark blue). Three neurons, the ml-APT, the MB-SP (white) and the LP-SP, having partly overlapping axonal terminals in the SP, indicate input from multiple brain areas. The MB-SP neuron has most terminals in a more dorsal part of the SP than the two other neurons. (A) Frontal view, (B) lateral view and (C) posterior view. (D-F) The Type 1 ml-APT (blue) neurons (two simultaneously stained) transformed into the SBA together with the MB extrinsic neurons and the LP-SP neuron. Due to the sparser projection pattern of the Type 1 ml-APT PN a less extensive overlap with MB-LP axonal terminals and the LP-SP dendrites appeared. (D) Frontal view, (E) lateral view and (F) posterior view.

Figure 11: 3D reconstructions of two PN types and the LP-descending neuron visualized in the SBA. (A-C) The projections of the three m-APT PNs (white) are most dorsal in the LP, clearly separated from the more ventral dendrites of the descending neuron (yellow). The wide projections of the ml-APT neurons (blue) partly overlaps with the m-APT PN projections and extend close to the area of the descending neuron dendrites. (A) Frontal view, (B) lateral view and (C) posterior view.

Doctoral theses in Biology
Norwegian University of Science and Technology
Department of Biology

Year	Name	Degree	Title
1974	Tor-Henning Iversen	Dr. philos Botany	The roles of statholiths, auxin transport, and auxin metabolism in root gravitropism
1978	Tore Slagsvold	Dr. philos Zoology	Breeding events of birds in relation to spring temperature and environmental phenology
1978	Egil Sakshaug	Dr.philos Botany	"The influence of environmental factors on the chemical composition of cultivated and natural populations of marine phytoplankton"
1980	Arnfinn Langeland	Dr. philos Zoology	Interaction between fish and zooplankton populations and their effects on the material utilization in a freshwater lake
1980	Helge Reinertsen	Dr. philos Botany	The effect of lake fertilization on the dynamics and stability of a limnetic ecosystem with special reference to the phytoplankton
1982	Gunn Mari Olsen	Dr. scient Botany	Gravitropism in roots of *Pisum sativum* and *Arabidopsis thaliana*
1982	Dag Dolmen	Dr. philos Zoology	Life aspects of two sympartic species of newts (*Triturus, Amphibia*) in Norway, with special emphasis on their ecological niche segregation
1984	Eivin Røskaft	Dr. philos Zoology	Sociobiological studies of the rook *Corvus frugilegus*
1984	Anne Margrethe Cameron	Dr. scient Botany	Effects of alcohol inhalation on levels of circulating testosterone, follicle stimulating hormone and luteinzing hormone in male mature rats
1984	Asbjørn Magne Nilsen	Dr. scient Botany	Alveolar macrophages from expectorates – Biological monitoring of workers exosed to occupational air pollution. An evaluation of the AM-test
1985	Jarle Mork	Dr. philos Zoology	Biochemical genetic studies in fish
1985	John Solem	Dr. philos Zoology	Taxonomy, distribution and ecology of caddisflies (*Trichoptera*) in the Dovrefjell mountains
1985	Randi E. Reinertsen	Dr. philos Zoology	Energy strategies in the cold: Metabolic and thermoregulatory adaptations in small northern birds
1986	Bernt-Erik Sæther	Dr. philos Zoology	Ecological and evolutionary basis for variation in reproductive traits of some vertebrates: A comparative approach
1986	Torleif Holthe	Dr. philos Zoology	Evolution, systematics, nomenclature, and zoogeography in the polychaete orders *Oweniimorpha* and *Terebellomorpha*, with special reference to the Arctic and Scandinavian fauna
1987	Helene Lampe	Dr. scient Zoology	The function of bird song in mate attraction and territorial defence, and the importance of song repertoires
1987	Olav Hogstad	Dr. philos Zoology	Winter survival strategies of the Willow tit *Parus montanus*
1987	Jarle Inge Holten	Dr. philos Botany	Autecological investigations along a coust-inland transect at Nord-Møre, Central Norway

1987	Rita Kumar	Dr. scient Botany	Somaclonal variation in plants regenerated from cell cultures of *Nicotiana sanderae* and *Chrysanthemum morifolium*
1987	Bjørn Åge Tømmerås	Dr. scient. Zoolog	Olfaction in bark beetle communities: Interspecific interactions in regulation of colonization density, predator - prey relationship and host attraction
1988	Hans Christian Pedersen	Dr. philos Zoology	Reproductive behaviour in willow ptarmigan with special emphasis on territoriality and parental care
1988	Tor G. Heggberget	Dr. philos Zoology	Reproduction in Atlantic Salmon (*Salmo salar*): Aspects of spawning, incubation, early life history and population structure
1988	Marianne V. Nielsen	Dr. scient Zoology	The effects of selected environmental factors on carbon allocation/growth of larval and juvenile mussels (*Mytilus edulis*)
1988	Ole Kristian Berg	Dr. scient Zoology	The formation of landlocked Atlantic salmon (*Salmo salar* L.)
1989	John W. Jensen	Dr. philos Zoology	Crustacean plankton and fish during the first decade of the manmade Nesjø reservoir, with special emphasis on the effects of gill nets and salmonid growth
1989	Helga J. Vivås	Dr. scient Zoology	Theoretical models of activity pattern and optimal foraging: Predictions for the Moose *Alces alces*
1989	Reidar Andersen	Dr. scient Zoology	Interactions between a generalist herbivore, the moose *Alces alces*, and its winter food resources: a study of behavioural variation
1989	Kurt Ingar Draget	Dr. scient Botany	Alginate gel media for plant tissue culture
1990	Bengt Finstad	Dr. scient Zoology	Osmotic and ionic regulation in Atlantic salmon, rainbow trout and Arctic charr: Effect of temperature, salinity and season
1990	Hege Johannesen	Dr. scient Zoology	Respiration and temperature regulation in birds with special emphasis on the oxygen extraction by the lung
1990	Åse Krøkje	Dr. scient Botany	The mutagenic load from air pollution at two work-places with PAH-exposure measured with Ames Salmonella/microsome test
1990	Arne Johan Jensen	Dr. philos Zoology	Effects of water temperature on early life history, juvenile growth and prespawning migrations of Atlantic salmion (*Salmo salar*) and brown trout (*Salmo trutta*): A summary of studies in Norwegian streams
1990	Tor Jørgen Almaas	Dr. scient Zoology	Pheromone reception in moths: Response characteristics of olfactory receptor neurons to intra- and interspecific chemical cues
1990	Magne Husby	Dr. scient Zoology	Breeding strategies in birds: Experiments with the Magpie *Pica pica*
1991	Tor Kvam	Dr. scient Zoology	Population biology of the European lynx (*Lynx lynx*) in Norway
1991	Jan Henning L'Abêe Lund	Dr. philos Zoology	Reproductive biology in freshwater fish, brown trout *Salmo trutta* and roach *Rutilus rutilus* in particular
1991	Asbjørn Moen	Dr. philos Botany	The plant cover of the boreal uplands of Central Norway. I. Vegetation ecology of Sølendet nature reserve; haymaking fens and birch woodlands
1991	Else Marie Løbersli	Dr. scient Botany	Soil acidification and metal uptake in plants
1991	Trond Nordtug	Dr. scient Zoology	Reflctometric studies of photomechanical adaptation in superposition eyes of arthropods
1991	Thyra Solem	Dr. scient Botany	Age, origin and development of blanket mires in Central Norway

1991	Odd Terje Sandlund	Dr. philos Zoology	The dynamics of habitat use in the salmonid genera *Coregonus* and *Salvelinus*: Ontogenic niche shifts and polymorphism
1991	Nina Jonsson	Dr. philos	Aspects of migration and spawning in salmonids
1991	Atle Bones	Dr. scient Botany	Compartmentation and molecular properties of thioglucoside glucohydrolase (myrosinase)
1992	Torgrim Breiehagen	Dr. scient Zoology	Mating behaviour and evolutionary aspects of the breeding system of two bird species: the Temminck's stint and the Pied flycatcher
1992	Anne Kjersti Bakken	Dr. scient Botany	The influence of photoperiod on nitrate assimilation and nitrogen status in timothy (*Phleum pratense* L.)
1992	Tycho Anker-Nilssen	Dr. scient Zoology	Food supply as a determinant of reproduction and population development in Norwegian Puffins *Fratercula arctica*
1992	Bjørn Munro Jenssen	Dr. philos Zoology	Thermoregulation in aquatic birds in air and water: With special emphasis on the effects of crude oil, chemically treated oil and cleaning on the thermal balance of ducks
1992	Arne Vollan Aarset	Dr. philos Zoology	The ecophysiology of under-ice fauna: Osmotic regulation, low temperature tolerance and metabolism in polar crustaceans.
1993	Geir Slupphaug	Dr. scient Botany	Regulation and expression of uracil-DNA glycosylase and O^6-methylguanine-DNA methyltransferase in mammalian cells
1993	Tor Fredrik Næsje	Dr. scient Zoology	Habitat shifts in coregonids.
1993	Yngvar Asbjørn Olsen	Dr. scient Zoology	Cortisol dynamics in Atlantic salmon, *Salmo salar* L.: Basal and stressor-induced variations in plasma levels ans some secondary effects.
1993	Bård Pedersen	Dr. scient Botany	Theoretical studies of life history evolution in modular and clonal organisms
1993	Ole Petter Thangstad	Dr. scient Botany	Molecular studies of myrosinase in Brassicaceae
1993	Thrine L. M. Heggberget	Dr. scient Zoology	Reproductive strategy and feeding ecology of the Eurasian otter *Lutra lutra*.
1993	Kjetil Bevanger	Dr. scient. Zoology	Avian interactions with utility structures, a biological approach.
1993	Kåre Haugan	Dr. scient Bothany	Mutations in the replication control gene trfA of the broad host-range plasmid RK2
1994	Peder Fiske	Dr. scient. Zoology	Sexual selection in the lekking great snipe (*Gallinago media*): Male mating success and female behaviour at the lek
1994	Kjell Inge Reitan	Dr. scient Botany	Nutritional effects of algae in first-feeding of marine fish larvae
1994	Nils Røv	Dr. scient Zoology	Breeding distribution, population status and regulation of breeding numbers in the northeast-Atlantic Great Cormorant *Phalacrocorax carbo carbo*
1994	Annette-Susanne Hoepfner	Dr. scient Botany	Tissue culture techniques in propagation and breeding of Red Raspberry (*Rubus idaeus* L.)
1994	Inga Elise Bruteig	Dr. scient Bothany	Distribution, ecology and biomonitoring studies of epiphytic lichens on conifers
1994	Geir Johnsen	Dr. scient Botany	Light harvesting and utilization in marine phytoplankton: Species-specific and photoadaptive responses
1994	Morten Bakken	Dr. scient Zoology	Infanticidal behaviour and reproductive performance in relation to competition capacity among farmed silver fox vixens, *Vulpes vulpes*

1994	Arne Moksnes	Dr. philos Zoology	Host adaptations towards brood parasitism by the Cockoo
1994	Solveig Bakken	Dr. scient Bothany	Growth and nitrogen status in the moss *Dicranum majus* Sm. as influenced by nitrogen supply
1994	Torbjørn Forseth	Dr. scient Zoology	Bioenergetics in ecological and life history studies of fishes.
1995	Olav Vadstein	Dr. philos Botany	The role of heterotrophic planktonic bacteria in the cycling of phosphorus in lakes: Phosphorus requirement, competitive ability and food web interactions
1995	Hanne Christensen	Dr. scient Zoology	Determinants of Otter *Lutra lutra* distribution in Norway: Effects of harvest, polychlorinated biphenyls (PCBs), human population density and competition with mink *Mustela vision*
1995	Svein Håkon Lorentsen	Dr. scient Zoology	Reproductive effort in the Antarctic Petrel *Thalassoica antarctica*; the effect of parental body size and condition
1995	Chris Jørgen Jensen	Dr. scient Zoology	The surface electromyographic (EMG) amplitude as an estimate of upper trapezius muscle activity
1995	Martha Kold Bakkevig	Dr. scient Zoology	The impact of clothing textiles and construction in a clothing system on thermoregulatory responses, sweat accumulation and heat transport
1995	Vidar Moen	Dr. scient Zoology	Distribution patterns and adaptations to light in newly introduced populations of *Mysis relicta* and constraints on Cladoceran and Char populations
1995	Hans Haavardsholm Blom	Dr. philos Bothany	A revision of the *Schistidium apocarpum* complex in Norway and Sweden
1996	Jorun Skjærmo	Dr. scient Botany	Microbial ecology of early stages of cultivated marine fish; inpact fish-bacterial interactions on growth and survival of larvae
1996	Ola Ugedal	Dr. scient Zoology	Radiocesium turnover in freshwater fishes
1996	Ingibjørg Einarsdottir	Dr. scient Zoology	Production of Atlantic salmon (*Salmo salar*) and Arctic charr (*Salvelinus alpinus*): A study of some physiological and immunological responses to rearing routines
1996	Christina M. S. Pereira	Dr. scient Zoology	Glucose metabolism in salmonids: Dietary effects and hormonal regulation
1996	Jan Fredrik Børseth	Dr. scient Zoology	The sodium energy gradients in muscle cells of *Mytilus edulis* and the effects of organic xenobiotics
1996	Gunnar Henriksen	Dr. scient Zoology	Status of Grey seal *Halichoerus grypus* and Harbour seal *Phoca vitulina* in the Barents sea region
1997	Gunvor Øie	Dr. scient Bothany	Eevalution of rotifer *Brachionus plicatilis* quality in early first feeding of turbot *Scophtalmus maximus* L. larvae
1997	Håkon Holien	Dr. scient Botany	Studies of lichens in spurce forest of Central Norway. Diversity, old growth species and the relationship to site and stand parameters
1997	Ole Reitan	Dr. scient. Zoology	Responses of birds to habitat disturbance due to damming
1997	Jon Arne Grøttum	Dr. scient. Zoology	Physiological effects of reduced water quality on fish in aquaculture
1997	Per Gustav Thingstad	Dr. scient. Zoology	Birds as indicators for studying natural and human-induced variations in the environment, with special emphasis on the suitability of the Pied Flycatcher
1997	Torgeir Nygård	Dr. scient Zoology	Temporal and spatial trends of pollutants in birds in Norway: Birds of prey and Willow Grouse used as Biomonitors

1997 Signe Nybø	Dr. scient. Zoology	Impacts of long-range transported air pollution on birds with particular reference to the dipper *Cinclus cinclus* in southern Norway
1997 Atle Wibe	Dr. scient. Zoology	Identification of conifer volatiles detected by receptor neurons in the pine weevil (*Hylobius abietis*), analysed by gas chromatography linked to electrophysiology and to mass spectrometry
1997 Rolv Lundheim	Dr. scient Zoology	Adaptive and incidental biological ice nucleators
1997 Arild Magne Landa	Dr. scient Zoology	Wolverines in Scandinavia: ecology, sheep depredation and conservation
1997 Kåre Magne Nielsen	Dr. scient Botany	An evolution of possible horizontal gene transfer from plants to sail bacteria by studies of natural transformation in *Acinetobacter calcoacetius*
1997 Jarle Tufto	Dr. scient Zoology	Gene flow and genetic drift in geographically structured populations: Ecological, population genetic, and statistical models
1997 Trygve Hesthagen	Dr. philos Zoology	Population responces of Arctic charr (*Salvelinus alpinus* (L.)) and brown trout (*Salmo trutta* L.) to acidification in Norwegian inland waters
1997 Trygve Sigholt	Dr. philos Zoology	Control of Parr-smolt transformation and seawater tolerance in farmed Atlantic Salmon (*Salmo salar*) Effects of photoperiod, temperature, gradual seawater acclimation, NaCl and betaine in the diet
1997 Jan Østnes	Dr. scient Zoology	Cold sensation in adult and neonate birds
1998 Seethaledsumy Visvalingam	Dr. scient Botany	Influence of environmental factors on myrosinases and myrosinase-binding proteins
1998 Thor Harald Ringsby	Dr. scient Zoology	Variation in space and time: The biology of a House sparrow metapopulation
1998 Erling Johan Solberg	Dr. scient. Zoology	Variation in population dynamics and life history in a Norwegian moose (*Alces alces*) population: consequences of harvesting in a variable environment
1998 Sigurd Mjøen Saastad	Dr. scient Botany	Species delimitation and phylogenetic relationships between the Sphagnum recurvum complex (Bryophyta): genetic variation and phenotypic plasticity
1998 Bjarte Mortensen	Dr. scient Botany	Metabolism of volatile organic chemicals (VOCs) in a head liver S9 vial equilibration system in vitro
1998 Gunnar Austrheim	Dr. scient Botany	Plant biodiversity and land use in subalpine grasslands. – A conservtaion biological approach
1998 Bente Gunnveig Berg	Dr. scient Zoology	Encoding of pheromone information in two related moth species
1999 Kristian Overskaug	Dr. scient Zoology	Behavioural and morphological characteristics in Northern Tawny Owls *Strix aluco*: An intra- and interspecific comparative approach
1999 Hans Kristen Stenøien	Dr. scient Bothany	Genetic studies of evolutionary processes in various populations of nonvascular plants (mosses, liverworts and hornworts)
1999 Trond Arnesen	Dr. scient Botany	Vegetation dynamics following trampling and burning in the outlying haylands at Sølendet, Central Norway
1999 Ingvar Stenberg	Dr. scient Zoology	Habitat selection, reproduction and survival in the White-backed Woodpecker *Dendrocopos leucotos*
1999 Stein Olle Johansen	Dr. scient Botany	A study of driftwood dispersal to the Nordic Seas by dendrochronology and wood anatomical analysis

1999	Trina Falck Galloway	Dr. scient Zoology	Muscle development and growth in early life stages of the Atlantic cod (*Gadus morhua* L.) and Halibut (*Hippoglossus hippoglossus* L.)
1999	Marianne Giæver	Dr. scient Zoology	Population genetic studies in three gadoid species: blue whiting (*Micromisistius poutassou*), haddock (*Melanogrammus aeglefinus*) and cod (*Gradus morhua*) in the North-East Atlantic
1999	Hans Martin Hanslin	Dr. scient Botany	The impact of environmental conditions of density dependent performance in the boreal forest bryophytes *Dicranum majus*, *Hylocomium splendens*, *Plagiochila asplenigides*, *Ptilium crista-castrensis* and *Rhytidiadelphus lokeus*
1999	Ingrid Bysveen Mjølnerød	Dr. scient Zoology	Aspects of population genetics, behaviour and performance of wild and farmed Atlantic salmon (*Salmo salar*) revealed by molecular genetic techniques
1999	Else Berit Skagen	Dr. scient Botany	The early regeneration process in protoplasts from *Brassica napus* hypocotyls cultivated under various g-forces
1999	Stein-Are Sæther	Dr. philos Zoology	Mate choice, competition for mates, and conflicts of interest in the Lekking Great Snipe
1999	Katrine Wangen Rustad	Dr. scient Zoology	Modulation of glutamatergic neurotransmission related to cognitive dysfunctions and Alzheimer's disease
1999	Per Terje Smiseth	Dr. scient Zoology	Social evolution in monogamous families: mate choice and conflicts over parental care in the Bluethroat (*Luscinia s. svecica*)
1999	Gunnbjørn Bremset	Dr. scient Zoology	Young Atlantic salmon (*Salmo salar* L.) and Brown trout (*Salmo trutta* L.) inhabiting the deep pool habitat, with special reference to their habitat use, habitat preferences and competitive interactions
1999	Frode Ødegaard	Dr. scient Zoology	Host spesificity as parameter in estimates of arhrophod species richness
1999	Sonja Andersen	Dr. scient Bothany	Expressional and functional analyses of human, secretory phospholipase A2
2000	Ingrid Salvesen	Dr. scient Botany	Microbial ecology in early stages of marine fish: Development and evaluation of methods for microbial management in intensive larviculture
2000	Ingar Jostein Øien	Dr. scient Zoology	The Cuckoo (*Cuculus canorus*) and its host: adaptions and counteradaptions in a coevolutionary arms race
2000	Pavlos Makridis	Dr. scient Botany	Methods for the microbial econtrol of live food used for the rearing of marine fish larvae
2000	Sigbjørn Stokke	Dr. scient Zoology	Sexual segregation in the African elephant (*Loxodonta africana*)
2000	Odd A. Gulseth	Dr. philos Zoology	Seawater tolerance, migratory behaviour and growth of Charr, (*Salvelinus alpinus*), with emphasis on the high Arctic Dieset charr on Spitsbergen, Svalbard
2000	Pål A. Olsvik	Dr. scient Zoology	Biochemical impacts of Cd, Cu and Zn on brown trout (*Salmo trutta*) in two mining-contaminated rivers in Central Norway
2000	Sigurd Einum	Dr. scient Zoology	Maternal effects in fish: Implications for the evolution of breeding time and egg size
2001	Jan Ove Evjemo	Dr. scient Zoology	Production and nutritional adaptation of the brine shrimp *Artemia* sp. as live food organism for larvae of marine cold water fish species
2001	Olga Hilmo	Dr. scient Botany	Lichen response to environmental changes in the managed boreal forset systems

2001	Ingebrigt Uglem	Dr. scient Zoology	Male dimorphism and reproductive biology in corkwing wrasse (*Symphodus melops* L.)
2001	Bård Gunnar Stokke	Dr. scient Zoology	Coevolutionary adaptations in avian brood parasites and their hosts
2002	Ronny Aanes	Dr. scient	Spatio-temporal dynamics in Svalbard reindeer (*Rangifer tarandus platyrhynchus*)
2002	Mariann Sandsund	Dr. scient Zoology	Exercise- and cold-induced asthma. Respiratory and thermoregulatory responses
2002	Dag-Inge Øien	Dr. scient Botany	Dynamics of plant communities and populations in boreal vegetation influenced by scything at Sølendet, Central Norway
2002	Frank Rosell	Dr. scient Zoology	The function of scent marking in beaver (*Castor fiber*)
2002	Janne Østvang	Dr. scient Botany	The Role and Regulation of Phospholipase A_2 in Monocytes During Atherosclerosis Development
2002	Terje Thun	Dr.philos Biology	Dendrochronological constructions of Norwegian conifer chronologies providing dating of historical material
2002	Birgit Hafjeld Borgen	Dr. scient Biology	Functional analysis of plant idioblasts (Myrosin cells) and their role in defense, development and growth
2002	Bård Øyvind Solberg	Dr. scient Biology	Effects of climatic change on the growth of dominating tree species along major environmental gradients
2002	Per Winge	Dr. scient Biology	The evolution of small GTP binding proteins in cellular organisms. Studies of RAC GTPases in *Arabidopsis thaliana* and the Ral GTPase from *Drosophila melanogaster*
2002	Henrik Jensen	Dr. scient Biology	Causes and consequenses of individual variation in fitness-related traits in house sparrows
2003	Jens Rohloff	Dr. philos Biology	Cultivation of herbs and medicinal plants in Norway – Essential oil production and quality control
2003	Åsa Maria O. Espmark Wibe	Dr. scient Biology	Behavioural effects of environmental pollution in threespine stickleback *Gasterosteus aculeatur* L.
2003	Dagmar Hagen	Dr. scient Biology	Assisted recovery of disturbed arctic and alpine vegetation – an integrated approach
2003	Bjørn Dahle	Dr. scient Biology	Reproductive strategies in Scandinavian brown bears
2003	Cyril Lebogang Taolo	Dr. scient Biology	Population ecology, seasonal movement and habitat use of the African buffalo (*Syncerus caffer*) in Chobe National Park, Botswana
2003	Marit Stranden	Dr.scient Biology	Olfactory receptor neurones specified for the same odorants in three related Heliothine species (*Helicoverpa armigera, Helicoverpa assulta* and *Heliothis virescens*)
2003	Kristian Hassel	Dr.scient Biology	Life history characteristics and genetic variation in an expanding species, *Pogonatum dentatum*
2003	David Alexander Rae	Dr.scient Biology	Plant- and invertebrate-community responses to species interaction and microclimatic gradients in alpine and Artic environments
2003	Åsa A Borg	Dr.scient Biology	Sex roles and reproductive behaviour in gobies and guppies: a female perspective
2003	Eldar Åsgard Bendiksen	Dr.scient Biology	Environmental effects on lipid nutrition of farmed Atlantic salmon (*Salmo Salar* L.) parr and smolt
2004	Torkild Bakken	Dr.scient Biology	A revision of Nereidinae (Polychaeta, Nereididae)
2004	Ingar Pareliussen	Dr.scient Biology	Natural and Experimental Tree Establishment in a Fragmented Forest, Ambohitantely Forest Reserve, Madagascar

2004	Tore Brembu	Dr.scient Biology	Genetic, molecular and functional studies of RAC GTPases and the WAVE-like regulatory protein complex in *Arabidopsis thaliana*
2004	Liv S. Nilsen	Dr.scient Biology	Coastal heath vegetation on central Norway; recent past, present state and future possibilities
2004	Hanne T. Skiri	Dr.scient Biology	Olfactory coding and olfactory learning of plant odours in heliothine moths. An anatomical, physiological and behavioural study of three related species (*Heliothis virescens, Helicoverpa armigera* and *Helicoverpa assulta*)
2004	Lene Østby	Dr.scient Biology	Cytochrome P4501A (CYP1A) induction and DNA adducts as biomarkers for organic pollution in the natural environment
2004	Emmanuel J. Gerreta	Dr. philos Biology	The Importance of Water Quality and Quantity in the Tropical Ecosystems, Tanzania
2004	Linda Dalen	Dr.scient Biology	Dynamics of Mountain Birch Treelines in the Scandes Mountain Chain, and Effects of Climate Warming
2004	Lisbeth Mehli	Dr.scient Biology	Polygalacturonase-inhibiting protein (PGIP) in cultivated strawberry (*Fragaria* x *ananassa*): characterisation and induction of the gene following fruit infection by *Botrytis cinerea*
2004	Børge Moe	Dr.scient Biology	Energy-Allocation in Avian Nestlings Facing Short-Term Food Shortage
2005	Matilde Skogen Chauton	Dr.scient Biology	Metabolic profiling and species discrimination from High-Resolution Magic Angle Spinning NMR analysis of whole-cell samples
2005	Sten Karlsson	Dr.scient Biology	Dynamics of Genetic Polymorphisms
2005	Terje Bongard	Dr.scient Biology	Life History strategies, mate choice, and parental investment among Norwegians over a 300-year period
2005	Tonette Røstelien	ph.d Biology	Functional characterisation of olfactory receptor neurone types in heliothine moths
2005	Erlend Kristiansen	Dr.scient Biology	Studies on antifreeze proteins
2005	Eugen G. Sørmo	Dr.scient Biology	Organochlorine pollutants in grey seal (*Halichoerus grypus*) pups and their impact on plasma thyrid hormone and vitamin A concentrations
2005	Christian Westad	Dr.scient Biology	Motor control of the upper trapezius
2005	Lasse Mork Olsen	ph.d Biology	Interactions between marine osmo- and phagotrophs in different physicochemical environments
2005	Åslaug Viken	ph.d Biology	Implications of mate choice for the management of small populations
2005	Ariaya Hymete Sahle Dingle	ph.d Biology	Investigation of the biological activities and chemical constituents of selected *Echinops* spp. growing in Ethiopia
2005	Anders Gravbrøt Finstad	ph.d Biology	Salmonid fishes in a changing climate: The winter challenge
2005	Shimane Washington Makabu	ph.d Biology	Interactions between woody plants, elephants and other browsers in the Chobe Riverfront, Botswana
2005	Kjartan Østbye	Dr.scient Biology	The European whitefish *Coregonus lavaretus* (L.) species complex: historical contingency and adaptive radiation

2006	Kari Mette Murvoll	ph.d Biology	Levels and effects of persistent organic pollutans (POPs) in seabirds Retinoids and α-tocopherol – potential biomakers of POPs in birds?
2006	Ivar Herfindal	Dr.scient Biology	Life history consequences of environmental variation along ecological gradients in northern ungulates
2006	Nils Egil Tokle	ph.d Biology	Are the ubiquitous marine copepods limited by food or predation? Experimental and field-based studies with main focus on *Calanus finmarchicus*
2006	Jan Ove Gjershaug	Dr.philos Biology	Taxonomy and conservation status of some booted eagles in south-east Asia
2006	Jon Kristian Skei	Dr.scient Biology	Conservation biology and acidification problems in the breeding habitat of amphibians in Norway
2006	Johanna Järnegren	ph.d Biology	Acesta Oophaga and Acesta Excavata – a study of hidden biodiversity
2006	Bjørn Henrik Hansen	ph.d Biology	Metal-mediated oxidative stress responses in brown trout (*Salmo trutta*) from mining contaminated rivers in Central Norway
2006	Vidar Grøtan	ph.d Biology	Temporal and spatial effects of climate fluctuations on population dynamics of vertebrates
2006	Jafari R Kideghesho	ph.d Biology	Wildlife conservation and local land use conflicts in western Serengeti, Corridor Tanzania
2006	Anna Maria Billing	ph.d Biology	Reproductive decisions in the sex role reversed pipefish *Syngnathus typhle*: when and how to invest in reproduction
2006	Henrik Pärn	ph.d Biology	Female ornaments and reproductive biology in the bluethroat
2006	Anders J. Fjellheim	ph.d Biology	Selection and administration of probiotic bacteria to marine fish larvae
2006	P. Andreas Svensson	ph.d Biology	Female coloration, egg carotenoids and reproductive success: gobies as a model system
2007	Sindre A. Pedersen	ph.d Biology	Metal binding proteins and antifreeze proteins in the beetle *Tenebrio molitor* - a study on possible competition for the semi-essential amino acid cysteine
2007	Kasper Hancke	ph.d Biology	Photosynthetic responses as a function of light and temperature: Field and laboratory studies on marine microalgae
2007	Tomas Holmern	ph.d Biology	Bushmeat hunting in the western Serengeti: Implications for community-based conservation
2007	Kari Jørgensen	ph.d Biology	Functional tracing of gustatory receptor neurons in the CNS and chemosensory learning in the moth *Heliothis virescens*
2007	Stig Ulland	ph.d Biology	Functional Characterisation of Olfactory Receptor Neurons in the Cabbage Moth, (*Mamestra brassicae* L.) (Lepidoptera, Noctuidae). Gas Chromatography Linked to Single Cell Recordings and Mass Spectrometry
2007	Snorre Henriksen	ph.d Biology	Spatial and temporal variation in herbivore resources at northern latitudes
2007	Roelof Frans May	ph.d Biology	Spatial Ecology of Wolverines in Scandinavia
2007	Vedasto Gabriel Ndibalema	ph.d Biology	Demographic variation, distribution and habitat use between wildebeest sub-populations in the Serengeti National Park, Tanzania

2007	Julius William Nyahongo	ph.d Biology	Depredation of Livestock by wild Carnivores and Illegal Utilization of Natural Resources by Humans in the Western Serengeti, Tanzania
2007	Shombe Ntaraluka Hassan	ph.d Biology	Effects of fire on large herbivores and their forage resources in Serengeti, Tanzania
2007	Per-Arvid Wold	ph.d Biology	Functional development and response to dietary treatment in larval Atlantic cod *(Gadus morhua* L.) Focus on formulated diets and early weaning
2007	Anne Skjetne Mortensen	ph.d Biology	Toxicogenomics of Aryl Hydrocarbon- and Estrogen Receptor Interactions in Fish: Mechanisms and Profiling of Gene Expression Patterns in Chemical Mixture Exposure Scenarios
2008	Brage Bremset Hansen	ph.d Biology	The Svalbard reindeer (*Rangifer tarandus platyrhynchus*) and its food base: plant-herbivore interactions in a high-arctic ecosystem
2008	Jiska van Dijk	ph.d Biology	Wolverine foraging strategies in a multiple-use landscape
2008	Flora John Magige	ph.d Biology	The ecology and behaviour of the Masai Ostrich (Struthio camelus massaicus) in the Serengeti Ecosystem, Tanzania
2008	Bernt Rønning	ph.d Biology	Sources of inter- and intra-individual variation in basal metabolic rate in the zebra finch, (*Taeniopygia guttata*)
2008	Sølvi Wehn	ph.d Biology	Biodiversity dynamics in semi-natural mountain landscapes. - A study of consequences of changed agricultural practices in Eastern Jotunheimen
2008	Trond Moxness Kortner	ph.d Biology	"The Role of Androgens on previtellogenic oocyte growth in Atlantic cod (*Gadus morhua*): Identification and patterns of differentially expressed genes in relation to Stereological Evaluations"
2008	Katarina Mariann Jørgensen	Dr.Scient Biology	The role of platelet activating factor in activation of growth arrested keratinocytes and re-epithelialisation
2008	Tommy Jørstad	ph.d Biology	Statistical Modelling of Gene Expression Data
2008	Anna Kusnierczyk	ph.d Bilogy	*Arabidopsis thaliana* Responses to Aphid Infestation
2008	Jussi Evertsen	ph.d Biology	Herbivore sacoglossans with photosynthetic chloroplasts
2008	John Eilif Hermansen	ph.d Biology	Mediating ecological interests between locals and globals by means of indicators. A study attributed to the asymmetry between stakeholders of tropical forest at Mt. Kilimanjaro, Tanzania
2008	Ragnhild Lyngved	ph.d Biology	Somatic embryogenesis in *Cyclamen persicum.* Biological investigations and educational aspects of cloning
2008	Line Elisabeth Sundt-Hansen	ph.d Biology	Cost of rapid growth in salmonid fishes
2008	Line Johansen	ph.d Biology	Exploring factors underlying fluctuations in white clover populations – clonal growth, population structure and spatial distribution
2009	Astrid Jullumstrø Feuerherm	ph.d Biology	Elucidation of molecular mechanisms for pro-inflammatory phospholipase A2 in chronic disease

2009	Pål Kvello	ph.d Biology	Neurons forming the network involved in gustatory coding and learning in the moth *Heliothis virescens:* Physiological and morphological characterisation, and integration into a standard brain atlas
2009	Trygve Devold Kjellsen	ph.d Biology	Extreme Frost Tolerance in Boreal Conifers
2009	Johan Reinert Vikan	ph.d Biology	Coevolutionary interactions between common cuckoos *Cuculus canorus* and *Fringilla* finches
2009	Zsolt Volent	ph.d Biology	Remote sensing of marine environment: Applied surveillance with focus on optical properties of phytoplankton, coloured organic matter and suspended matter
2009	Lester Rocha	ph.d Biology	Functional responses of perennial grasses to simulated grazing and resource availability
2009	Dennis Ikanda	ph.d Biology	Dimensions of a Human-lion conflict: Ecology of human predation and persecution of African lions (*Panthera leo*) in Tanzania
2010	Huy Quang Nguyen	ph.d Biology	Egg characteristics and development of larval digestive function of cobia (*Rachycentron canadum*) in response to dietary treatments -Focus on formulated diets
2010	Eli Kvingedal	ph.d Biology	Intraspecific competition in stream salmonids: the impact of environment and phenotype
2010	Sverre Lundemo	ph.d Biology	Molecular studies of genetic structuring and demography in *Arabidopsis* from Northern Europe
2010	Iddi Mihijai Mfunda	ph.d Biology	Wildlife Conservation and People's livelihoods: Lessons Learnt and Considerations for Improvements. Tha Case of Serengeti Ecosystem, Tanzania
2010	Anton Tinchov Antonov	ph.d Biology	Why do cuckoos lay strong-shelled eggs? Tests of the puncture resistance hypothesis
2010	Anders Lyngstad	ph.d Biology	Population Ecology of *Eriophorum latifolium*, a Clonal Species in Rich Fen Vegetation
2010	Hilde Færevik	ph.d Biology	Impact of protective clothing on thermal and cognitive responses
2010	Ingerid Brænne Arbo	ph.d Medical technology	Nutritional lifestyle changes – effects of dietary carbohydrate restriction in healthy obese and overweight humans
2010	Yngvild Vindenes	ph.d Biology	Stochastic modeling of finite populations with individual heterogeneity in vital parameters
2010	Hans-Richard Brattbakk	ph.d Medical technology	The effect of macronutrient composition, insulin stimulation, and genetic variation on leukocyte gene expression and possible health benefits
2011	Geir Hysing Bolstad	ph.d Biology	Evolution of Signals: Genetic Architecture, Natural Selection and Adaptive Accuracy
2011	Karen de Jong	ph.d Biology	Operational sex ratio and reproductive behaviour in the two-spotted goby (*Gobiusculus flavescens*)
2011	Ann-Iren Kittang	ph.d Biology	*Arabidopsis thaliana* L. adaptation mechanisms to microgravity through the EMCS MULTIGEN-2 experiment on the ISS:– The science of space experiment integration and adaptation to simulated microgravity
2011	Aline Magdalena Lee	ph.d Biology	Stochastic modeling of mating systems and their effect on population dynamics and genetics
2011	Christopher Gravningen Sørmo	ph.d Biology	Rho GTPases in Plants: Structural analysis of ROP GTPases; genetic and functional studies of MIRO GTPases in *Arabidopsis thaliana*

2011	Grethe Robertsen	ph.d Biology	Relative performance of salmonid phenotypes across environments and competitive intensities
2011	Line-Kristin Larsen	ph.d Biology	Life-history trait dynamics in experimental populations of guppy (*Poecilia reticulata*): the role of breeding regime and captive environment
2011	Maxim A. K. Teichert	ph.d Biology	Regulation in Atlantic salmon (*Salmo salar*): The interaction between habitat and density
2011	Torunn Beate Hancke	ph.d Biology	Use of Pulse Amplitude Modulated (PAM) Fluorescence and Bio-optics for Assessing Microalgal Photosynthesis and Physiology
2011	Sajeda Begum	ph.d Biology	Brood Parasitism in Asian Cuckoos: Different Aspects of Interactions between Cuckoos and their Hosts in Bangladesh
2011	Kari J. K. Attramadal	ph.d Biology	Water treatment as an approach to increase microbial control in the culture of cold water marine larvae
2011	Camilla Kalvatn Egset	ph.d Biology	The Evolvability of Static Allometry: A Case Study
2011	AHM Raihan Sarker	ph.d Biology	Conflict over the conservation of the Asian elephant (*Elephas maximus*) in Bangladesh
2011	Gro Dehli Villanger	ph.d Biology	Effects of complex organohalogen contaminant mixtures on thyroid hormone homeostasis in selected arctic marine mammals
2011	Kari Bjørneraas	ph.d Biology	Spatiotemporal variation in resource utilisation by a large herbivore, the moose
2011	John Odden	ph.d Biology	The ecology of a conflict: Eurasian lynx depredation on domestic sheep
2011	Simen Pedersen	ph.d Biology	Effects of native and introduced cervids on small mammals and birds
2011	Mohsen Falahati-Anbaran	ph.d Biology	Evolutionary consequences of seed banks and seed dispersal in *Arabidopsis*
2012	Jakob Hønborg Hansen	ph.d Biology	Shift work in the offshore vessel fleet: circadian rhythms and cognitive performance
2012	Elin Noreen	ph.d Biology	Consequences of diet quality and age on life-history traits in a small passerine bird
2012	Irja Ida Ratikainen	ph.d Biology	Theoretical and empirical approaches to studying foraging decisions: the past and future of behavioural ecology
2012	Aleksander Handå	ph.d Biology	Cultivation of mussels (*Mytilus edulis):*Feed requirements, storage and integration with salmon (*Salmo salar*) farming
2012	Morten Kraabøl	ph.d Biology	Reproductive and migratory challenges inflicted on migrant brown trour (*Salmo trutta* L) in a heavily modified river
2012	Jisca Huisman	ph.d Biology	Gene flow and natural selection in Atlantic salmon
2012	Maria Bergvik	ph.d Biology	Lipid and astaxanthin contents and biochemical post-harvest stability in *Calanus finmarchicus*
2012	Bjarte Bye Løfaldli	ph.d Biology	Functional and morphological characterization of central olfactory neurons in the model insect *Heliothis virescens*.